A Thesis

FOR THE DEGREE OF MASTER OF SCIENCE

Molecular Characterization of seven
Glutathione-s-transferases from Disk Abalone
(*Haliotis discus discus*), Potential Biomarkers of
Endocrine-disrupting Chemicals

Qiang Wan

Department of Marine Biotechnology

GRADUATE SCHOOL

CHEJU NATIONAL UNIVERSITY

2007. 12

Molecular characterization of seven glutathione-s-transferases from disk abalone (*Haliotis discus discus*), potential biomarkers of endocrine-disrupting chemicals

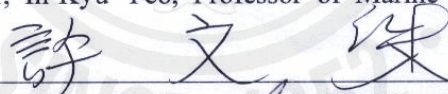Qiang Wan

(Supervised by Professor Jehee Lee)

A thesis submitted in partial fulfillment of the requirement for the degree of Master of Science

2007 . 12 .

This thesis has been examined and approved

_____
Thesis director, In-Kyu Yeo, Professor of Marine Biotechnology

_____
Moon-Soo Heo, Professor of Marine Biotechnology

_____
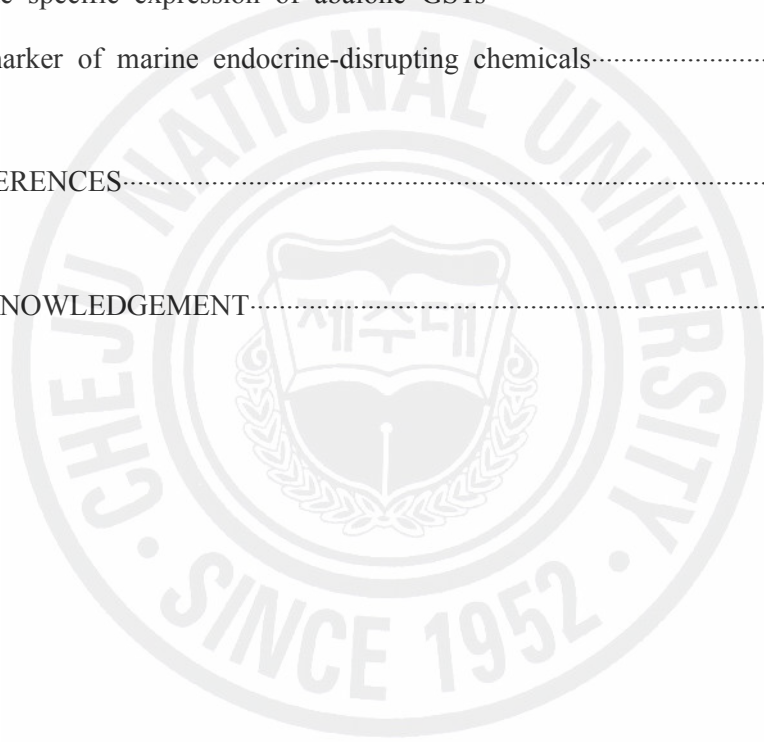Jehee Lee, Professor of Marine Biotechnology

Dec. 27th. 2007
Date

Department of Marine Biotechnology

GRADUATE SCHOOL

CHEJU NATIONAL UNIVERSITY

CONTENTS

요 약 문

Glutathione s-transferase (GST)는 GSH 항산화 시스템에 중요한 성분이며, 환경오염물질, 살충제, 항생제, 그리고 세포질내 산화 성분등을 포함하는 electrophile의 phase II detoxification에 중요한 역할을 한다. 수년간, GSTs 활성과 전사 수준은 환경오염 진단을 위한 바이오마커처럼 넓게 측정되어져 왔다. 이 연구에서, 우리는 까막전복의 cDNA library로부터 기존에 GSTs로 알려진 염기서열과 40% 이상 유사성을 나타내는 7개의 GST cDNA 클론을 선택하였다. 7개의 cDNA 클론들은 전체 염기 서열 분석과multiple alignment, phylogenetic 연구를 통해 분석되었으며, 하나의 mu class GST (HdGSTM1), 두 개의 omega class GSTs (HdGSTO1 and HdGSTO2), 세 개의 sigma class GST (HdGSTS1, HdGSTS2 and HdGSTS3), 그리고 한 개의 novel rho class GST (HdGSTR1)로 확인되어졌다. 그 후, 이들 7 개의 GST를 코딩하는 ORF 서열을 pMAL vector 안으로 클로닝하고, *E. coli* K12 (Tb1)을 이용하여 과잉 발현을 유도하였다.

7개의 재조합 GST들의 효소적 특성은 5가지 전형적인 GST 기질인 1-Chloro-2, 4-dinitrobenzenel (CDNB) 1, 2-Dichloro-4-nitrobenzene (DCNB), ethacrynic acid (ECA), 4-nitrobenzyl chloride (4-NBC)와4-Nitrophenethyl bromide (4-NPB)을 사용하여 분석되어졌다. 부가적으로, Omega GST를 위해 DHA reductase 활성과 thioltrasferase 활성 측정이 수행되었다. HdGSTS3를 제외한 모든 전복 GST들은 특이 기질에 대한 활성을 나타냈다. Rho class GST HdGSTR1는 2.73±0.05 μmol/min/mg, CDNB는 0.35±0.03 μm/min/mg로 ECA에 대해 가장 높은 활성을 나타냈다. 하지만 mu class GST HdGSTM1는 높은 활성을 나타냈지만 CDNB와 ECA에 대해 1U/mg 보다 낮은 catalytic 능력을 보였다. 두 omega GST들에서, HdGSTO1는 DHA reductase와 thioltransferase활성이 높았지만, 전형적인 GST 기질에 대한 활성은 없었다. 모든 전복 GST들은25 ~ 35 ℃ 온도 범위에서 최적 온도를 나타내었고, 최적 pH는 7.5 ~ 9.0 사이에서 보여졌다.

부가적으로, mu class GST역시 넓은 범위의 온도와 pH에서 안정적으로 나타났다.

　전복 GST들의 초기 구조와 그들의 효소활성들 사이의 관계를 설명하기 위해 homology modeling이 수행되어졌다. 전복 GST들을 다른 활성 GST 유전자들과 비교하여 주된 활성 부위에 있는 여러 개의 잔기들이 확인되었고, 서열에 차이를 보였으며 이러한 서열의 차이로 인해 기질과 GST가 결합하는 catalitic 활성이 기존에 GST 활성보다 낮은 것으로 생각된다.

　7개의 전복 GST들에 대해 다섯 개의 기관들(아가미, 맨틀, 근육, 소화관, 생식선)에서 조직적 분포를 조사하였다. 다양한 수생 오염물질에 노출된 초기 호흡기관처럼, 음식물의 모든 성분을 흡수하는 그 기관과 생식모세포 발달 장소, 아가미, 소화관, 생식선은 전복 GST들의 발현되는 주된 기관들이었다.

전복의 챌린져 테스트를 위해 세 종류의 endocrine-disrupting chemicals (EDCs), PAH−type chemical β−naphthoflavone, PCB−type chemical aroclor−1254와 한 종류의 TBT-type chemical tributyltin chloride를 저농도와 고농도하에서 사용하였다. 모든 처리구에서 노출 48시간 후, HdGSTM1와 HdGSTO1는 아가미와 소화관에서 의미있게 유도되었다. Rho class GST는 PCB와 TBT 처리구에서만 두 배 이상 유도되어졌다. HdGSTS1는 소화관에서 주로 유도되어졌다. Sigma class에서 가장 높은 활성을 가지는 HdGSTS2는 어떤 처리구에서도 낮게 나타났다. 비활성 isoform HdGSTS3의 발현은 처리구들에서 주로 억제됐다. 요약하자면, HdGSTM1 와 HdGSTO1은 다양한 스트레스 인자들에 대한 바이오마커 유전자로 사용할 수 있고, HdGSTR1는 PCB와 TBT에 특이적인 바이오마커로 사용할 수 있을 것으로 기대한다.

ABSTRACT

GSTs (glutathione s-transferases) are a large gene family of detoxification enzyme, whichcontribute to biotransformation of a wide variety of xenobiotics and endogenous oxidative product. In this present study, we identified seven GST genes including one mu class GST (HdGSTM1), two omega class GSTs (HdGSTO1 and HdGSTO2dH), one rho class GST (HdGDTR1) and three sigma class GSTs (HdGSTS1, HdGSTS2 and HdGSTS3), from disk abalone (*Haliotis discus discus)*cDNA library. The full-length sequence of seven GSTs have been determined, showing over 40% protein sequence similarity with other known GST genes. The modeling structure result also revealed that they shared coincident three-dimentional structures with specific GST subfamily members. The recombinant protein of seven GSTs fused with maltose binding protein tag was overexpressed in *E. coli* K12 (Tb1) cells. All the GSTs except for HdGSTS3 displayed detectable activity in enzyme assay. Mu class, rho class and sigma GSTs have specific activity towards two typical GST substrates 1-Chloro-2, 4-dinitrobenzenel (CDNB) and ethacrynic acid (ECA). On the contrary, Two omgea GSTs showed activity of DHA reductase and thioltransferase. The homology modeling revealed that the improper active site and catalytic structures resulted in the low activities of abalone GSTs. Gill, digestive tract and gonad appeared to be the major tissue where abalone GSTs distribute. After waterborne exposure of three endocrine-disrupting chemicals (EDCs) for 48 hrs, HdGSTM1 and HdGSTO1 were significantly induced in both gill and digestive tract by all treatments, exhibiting as potential biomarkers of marine environmental EDCs.

Key words: Glutathione s-transferase; Abalone; Biomarker; Endocrine-disrupting
chemicals

LIST OF FIGURES AND TABLES

Ⅰ. INTRODUCTION

Every living organism in this world is exposed to a great number of xenobiotics in the course of its lifetime, including a variety of environment toxicants, food components and pharmaceuticals. To detoxify these xenobiotics and survive, organisms have evolved highly complex detoxification systems. The detoxification system generally consists of two enzyme systems (phase I and II) and one group of transporters (phase III). Phase I enzyme system is made up bycytochrome p450 (CYP) and short chain dehydrogenase/reductase (SDR), catalyzing the reactions of adding functional groups, often hydroxyl groups, onto the foreign compounds. The addition of the phase Ifunctional group typically results in a more polar molecule, thus making it more excretible. However, most of the products from phase I detoxification would become more reactive and toxic, which could damage the intracellular protein and nuclear acid without further biotransformation or excretion in time. In contrast, phase II enzyme system catalyzes the actual detoxification reactions, such as acetylation, sulfation, glucuronidation, sulfation, and glutathione and amino acid conjugation, to transfer xenobiotics more water-soluble and less toxic. A number of conjugation enzymes, particularly glutathione S-transferases (GSTs) and UDP-glucuronosyltransferases (UGTs), perform as main enzymatic tools in phase II metabolism. At last, ATP-binding cassette (ABC) transporters in phase III play the role of excreting the final metabolites out of cell.
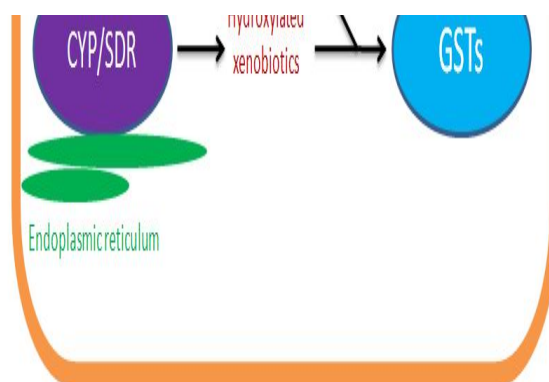
Glutathione s-transferases (GSTs) are a well established gene family, which play key roles in phase-II enzymatic detoxification. GSTs catalyze mainly the nucleophilic addition of reduced glutathione to a wide variety of electrophilic compounds,converting the electrophiles into more hydrophilic and less reactive products to facilitate excretion (Ivarsson, Mackey et al. 2003). These electrophilic compounds include environmental carcinogens, pesticides, antibiotics, and endogenous product of oxidative damage (Hayes JD 1995). In recent studies, GSTs have been also closely linked with cancer diagnosis and therapy, since they are involved in both the regulation of cellular apoptosis (Townsend, Findlay et al. 2005) and the metabolism of antitumor drugs (Beeghly, Katsaros et al. 2006; Czeczot, Scibior et al. 2006; McIlwain, Townsend et al. 2006).

GSTs have been found widely in all eukaryotic and prokaryotic organisms studied, including animals, plant and bacteria (Ivarsson, Mackey et al. 2003). Mammalian GSTs are the first and best characterized GSTs. They have been grouped into at least eight different classes (alpha, kappa, mu, omega, pi, sigma, theta and zeta) on the basis of their primary and tertiary structure, substrate/inhibitor specificity and immunological cross-reactivity. Additionally, many novel GST sequences and their crystal structures from non-mammalian organisms were also identified, such as beta

class found in bacteria; delta and epsilon classes found in insect; lambda, phi and tau classes found in plant (Hayes, Flanagan et al. 2005). It is generally recognized that the identity of amino acid sequence of GSTs from the same class should more than 40%, which is less than 30% among different GST classes (Hayes JD 1995).

In this present study, we identified seven GST genes including one mu class GST, two omega class GSTs, one rho class GST and three sigma class GSTs, from disk abalone (*Haliotis discus discus)*cDNA library. Among them, Omega class GST is a newly named cytosolic GST, which was identified by analyzing the sequence similarity in human expressed sequence tag (ETS) database in 2000 (Board, Coggan et al. 2000). So far omega GSTs have been variously identified in mammalian, fish, ascidian, insect, mollusk, nematode, plant, yeast and bacteria, indicating the crucial role for organisms (Wilson, Ainscough et al. 1994; Ishikawa, Casini et al. 1998; Board, Coggan et al. 2000). Omega class GSTs show novel structure and function compared with other GST classes. The conserved glutathione-binding site of N-terminal domain is cysteine in omega class, in contrast of serine or tyrosine in other GSTs. The three dimensional structure of omega GST is also unique, appearing an additional extending beyond the N-terminus of other class GSTs (Board, Coggan et al. 2000). These unique characteristics of primary and tertiary structure lead to unusual enzyme properties as well. The Omega GSTs have minimal catalytic activity with the typical substrates for members of other GST classes, however, exhibit thiol transferase and dehydroascorbate reductase activities which are generally observed in glutaredoxins (Rouimi, Anglade et al. 2001; Girardini, Amirante et al. 2002; Schmuck, Board et al. 2005; Whitbread, Masoumi et al. 2005). In mammalian brain, the reduction and recycling of dehydroascorbate is modulated by omega class GSTs.They play key roles of scavenging free radicals and reactive oxygen species to protect the brain against damage caused by oxidative stress, hence prevent the

occurrences of several degenerative neurological disease, such as Alzheimer's disease (AD) and Parkinson's disease (PD) (Rice 2000; Mattson 2004). The convergence of genetic linkage, gene expression, and association studies showed that SNPs in two human omega GSTs are associated with age-at-onset in AD and PD (Li, Oliveira et al. 2003). Additionally, omega GSTs also mediate in the biomethylation pathway of inorganic arsenic metabolism, protecting organisms from acute and chronic arsenic toxicosis (Chowdhury, Zakharyan et al. 2006).

Sigma class GST is one of the largest GST subfamilies distributed in both vertebrate and invertebrate animals with multiple functions. It was first identified from cephalopod lens S-crystallins, major lens polypeptide without GST catalytic function, which are considered to evolve from the ancestral GST genes (Tomarev and Zinovieva 1988; Tomarev, Zinovieva et al. 1992; Tomarev, Zinovieva et al. 1993; Zinov'eva, Tomarev et al. 1994). A number of enzymatically active sigma GSTs were identified from the parasitic helminthes, nematodes, and digestive gland of squid as well, showing high catalytic activities toward 1-chloro-2, 4-dinitrobenzene (CDNB) (Harris, Coles et al. 1991; Tomarev, Zinovieva et al. 1993; Liebau, Walter et al. 1994; Meyer, Muimo et al. 1996). In dipteran insects, sigma GST is one of the three distinct insect GST classes, playing both structural and metabolic roles. The recent study on *Drosophila* Sigma GST showed that it was not only astretch sensor that bounded to the heavy subunit of the IFM thin filament troponin complex to enable the indirect flight muscle to perform repeated cycles of contraction (Clayton, Cripps et al. 1998), but also had significant activity in catalyzing the conjugation of GSH with the lipid peroxidation product 4-hydroxynonenal (4-HNE) playing a role of protection against oxidative stress in muscle and central nervous system (Singh, Coronella et al. 2001; Agianian, Tucker et al. 2003).

Cytosolic GSTs are active as dimers of either homogeneous or heterogeneous

subunits whose molecular masses range from 23 to 28 kDa. All cytosolic GSTs share the same two-domain structure. The N-terminal domain adopts a βαβαββα motif, which is a thioredoxin like structure and contains GSH-binding sites (G-sites). In contrast, the C-terminal domain is a large αdomain, containing five to six α-helices and hydrophobic substrate-binding sites (H-sites) (Sun, Kuan et al. 1998). The G-sites are well conserved among different classes of GSTs, whereas the H-sites vary widely in different classes, resulting in different substrate specificities (Ivarsson, Mackey et al. 2003).

For years, GST activities and transcriptional levels have been widely measured in aquatic species as exposure biomarkers of organic or inorganic contaminants (Lee 1988; Sole′ 1996; Willett 1999; Damiens, His et al. 2004; Perez, Blasco et al. 2004; Devier, Augagneur et al. 2005; Hoarau, Damiens et al. 2006), due to its nonsensibility to several abiotic and biotic factors such as temperature, season, sex and age (Kirchin 1992). Additionally, GST biomarkers can provide a more integrated view that how the contaminants influence the health of organisms biologically than the simple measurement of contaminants accumulating in tissues (Van der Oost 1996). Marine bivalves, such as mussel and oyster, have been widely used as indicator species in numerous marine environment assessment projects. Meanwhile, a large number of biomarker genes were also identified and characterized in marine bivalves (Boutet, Meistertzheim et al. 2005; Hoarau, Damiens et al. 2006; Gao, Song et al. 2007). In contrast, there is few related report of abalone (Kuhajek and Schlenk 2003), which is one of the most prized marine gastropods. Compared with bivalves, abalones have a different feeding and habitation style that they are herbivorous and capable to migrate, therefore they could potentially exhibit a distinctive response to the pollutants in marine environment.

Nowadays, there have been increasing concerns about some particular environment

pollutants termed as endocrine-disrupting chemicals (EDCs). These chemicals are structurally similar with endogenous hormones, able to interact with hormone transporter, or able to disrupt hormone metabolism, consequently resulting in reproductive and endocrine disrupting effects in an intact organism or its progeny (Colborn, vom Saal et al. 1993). Due to the persistent and lipophilic properties, most of these chemicals could transfer in food-chain and accumulate in organisms in a high level. The contaminated organisms could exhibit disturbed sex differentiation with abnormal sex organ, changed sexual behavior, altered growth and immune function. Moreover, these abnormalities are usually irreversible. The list of EDCs comprises mainly organochlorines pesticides, phthalates, alkylphenolic compounds, polycyclic aromatic hydrocarbons (PAH), polychlorinated biphenyls (PCBs), hexachlorobenzene (HCB), polychlorinated dibenzo-*p*-dioxins (PCDDs), polychlorinated dibenzofurans (PCDFs), tributyltin (TBT) and several heavy metals (Bondgaard and Bjerregaard 2005). In our study, we sub-cloned and overexpressed seven abalone GSTs in *Escherichia. coli*. Furthermore, the biochemical properties of recombinant GSTs and their inducible expression in the exposure of three model endocrine-disrupting chemicals (beta-naphathoflavone, aroclor-1254 and tributyltin chloride) have been characterized as well.

Ⅱ. MATERIALS AND METHODS

2.1 Materials

The cDNA library of disk abalone *Haliotis discus discus*was constructed using the whole body tissue. Glutathione reduced (GSH), 1-chloro-2,4-dinitrobenzene (CDNB), 1, 2-Dichloro-4-nitrobenzene (DCNB), ethacrynic acid (ECA), 4-nitrobenzyl chloride (4-NBC), 4-Nitrophenethyl bromide (4-NPB), dehydroascorbic acid (DHA), 2-hydroxyethyl disulfide (HED), NADPH, glutathione reductase, β-naphthoflavone, aroclor 1254, tributyltin chloride, and Bradford reagent were purchased from Sigma-Aldrich in Korea. Isopropyl-b-D-thiogalactopyranoside (IPTG) was obtained from Promega. All restriction endonucleases and T4 DNA ligase were obtained from NEB. Protein markers were obtained from Bio-rad. All other chemicals were of analytical grade.

2.2 Animals

Disk abalones (*Haliotis discus discus*) with shell length of 8.5–11.5 cm and weight of 70-100 g, were bought from abalone farm in Jeju island. Abalones were scraped clean of fouling organisms and acclimated to laboratory conditions in filtered seawater (4 litter of seawater per abalone) for 7 days prior to experimentation. The seawater was continuously aerated, and salinity and temperature maintained at 32(±1) ‰ and 20(±1) ℃, respectively. Abalones were fed daily and the seawater was renewed on a daily basis. For the exposure experiments, abalones were separated into 7 different groups, one control group and six challenge groups. Every group had three abalones. Three model EDCs, PAH-type chemical β-naphthoflavone (0.1 and 1 μM), a PCB-type chemical aroclor-1254 (5 and 50 ppb) and a TBT-type chemical tributyltin chloride (0.1 ppb and 1 ppb) were dissolved in DMSO and made up two

different concentrations for each exposure group. In the control group, only DMSO was added. The final waterborne DMSO concentration of all aquaria was 10 ppb. The toxicant-laden seawater was renewed daily, and abalones were not fed during exposure. After 48 hrs exposure, abalones were sacrificed. The tissue of gills, mantle, gonad, foot and digestive tract were dissected and frozen in liquid nitrogen immediately.

2.3 cDNA identification and full-length sequencing

Seven cDNA clones, HdGSTM1, HdGSTO1, HdGSTO2, HdGSTR1, HdGSTS1, HdGSTS2 and HdGSTS3 with putative GST function were isolated from cDNA library of disk abalone after the expressed sequence tag (EST) blast. Plasmid DNA of seven cDNA clones were then transformed into XLI-Blue MRF' cells and purifiedby Accuprep^{TM} plasmid extraction kit (Bioneer Co., Korea). Insert sizes were determined by restricted digestion of miniprep DNA with *Xho*1 followed by analysis on a 1% agarose gel. Complete sequences were determined by totally two or three times of sequencing reactions. The open reading frames (ORFs), deduced amino acid sequences, protein molecular weights and pI values were obtained from DNASIST 2.1 program.

2.4 Phylogenetic analysis

To make a clear classification, the deduced amino acid sequence of seven GSTs were first aligned with 55 known GST sequences from 13 different classes (alpha, kappa, mu, omega, pi, sigma, theta, zeta, rho, tau, phi, delta and beta) using ClustalX software. On the basis of the alignment, one phylogenetic tree was then reconstructed using Neighbour-joining (NJ) with 1000 bootstrap replicates. All the analysis was performed by MEGA v.3.1.

Table.1. Oligo list of present study. From PC-MF1 to PC-SR1 are upstream and downstream cloning primers of HdGSTM1, HdGSTO1, HdGSTO2, HdGSTR1, HdGSTS1, HdGSTS2 and HdGSTS3，respectively. From PR-MF1 to PRSR3 are relative primers for RT-PCR. PR-BAF, PR-BAR, PR-RPF and PR-RPR are primers of beta-actin and ribsome protein in RT-PCR experiment.

Oligo Name	Sequences
PC-MF1	GAGAGAGAATTCATGCCTACTCTTGGATACTGGG
PC-MR1	GAGAGAAAGCTTTCACTTGAACAGTGCACTCTTGT
PC-OF1	GAGAGAGAATTCATGACTGAGAAGTCCTACACAACGAC
PC-OR1	GAGAGACTGCAGTCAAAGGCCAACGTCATAGTCTG
PC-OF2	GAGAGAGAATTCATGTCCCTGAAGTCACACGC
PC-OR2	GAGAGAAAGCTTTCATAAACCATAGTCATAGTCTGGG
PC-RF1	GAGAGAGAATTCATGTCGTCCAACATGTTTCTGTACTGG
PC-RR1	GAGAGACTGCAGTCACACGGGTCCCATGATGG
PC-SF1	GAGAGAGAATTCATGCCTTCCTACAAGCTGATCTACAC
PC-SR1	GAGAGACTGCAGTCAGAATTGTGTGACCGGCC
PC-SF2	GAGAGAGAATTCATGCCTACCTACAAGCTGAGATATTTC
PC-SR2	GAGAGACTGCAGCTAGTTTTCCGTTTGGGGCCTC
PC-SF3	GAGAGAGAATTCATGCCGACATACAGGTTTCGCTA
PC-SR3	GAGAGAAAGCTTTCAGAATGCTGTAACTGGTCGTTTCT
PR-MF1	ATTGTCGGGCTCTGTTACAACCCT
PR-MR1	ATGGGTCTCCTGATGAACTTGGCA
PR-OF1	AGAAGCCATCTTGGTTCTGGGACA
PR-OR1	ACTGGACCAAGAGCATCGTGGAAT
PR-OF2	TTGCTGTCTTCAGGAGGCAGTGAT
PR-OR2	AAACATCGTGGCTTTGACTGCTGG
PR-RF1	GACAAAGGAACGAAACTGCTGCCA
PR-RR1	ACATCCGCCATTGTGAAGTTGCTG
PR-SF1	TGGACGGGAAACAGTATGCACAGA
PR-SR1	AAAGGCAGCGACATCTGCAAATCC
PR-SF2	AACCAAACACTCCACTCGGACAGA
PR-SR2	ACACAGACACGTCAGCAAGGGTAA
PR-SF3	GATGGGAAACCCTTTAGCCAGAGT
PR-SR3	GCCACGTTGTCACAGCATTTCTTG
PR-BAF	AGCACATCCTATGGATCAGCCAGT
PR-BAR	ACCCTTCATAAATGGGCACGGTGT
PR-RPF	GGGAAGTGTGGCGTGTCAAATACA
PR-PRR	TCCCTTCTTGGCGTTCTTCCTCTT

2.5 Construction of expression vector for seven GSTs

The plasmid DNA of seven cDNA clones was used as templates for ORF amplification with specific upstream primers and downstream primers list in table 1. PCR was performed in TAKARA thermal cycler in a final volume of 50μL containing 2.5 units Takara Ex Taq polymerase (Takara Korea Biomedical Inc., Korea), 5 μL 10x Ex Taq buffer, 4 μL of 2.5 mM each dNTP, 50 ng of cDNA template and 50 pmol of each primer. The PCR conditions consisted of an initial denaturation at 94°C for 2 min, followed by 25 cycles of 94°C for 30 s, 51°C for 30 s and 72°C for 30 s, and the final extension was carried out at 72°C for 5 min. The PCR products were purified with AccuPrep^{TM}gel purification kit (Bioneer Co., Korea) and digested with relative restriction enzymes. Thereafter, the digested product was subcloned into the expression plasmid pMAL^{TM}-c2X (New England BioLabs, USA) previously cut with the same restriction enzymes, yielding plasmid pMAL^{TM}-c2X/HdGSTM1, pMAL^{TM}-c2X/HdGSTO1, pMAL^{TM}-c2X/HdGSTO2, pMAL^{TM}-c2X/HdGSTR1, pMAL^{TM}-c2X/HdGSTS1, pMAL^{TM}-c2X/HdGSTS2 and pMAL^{TM}-c2X/HdGSTS3. Abalone GSTs were designed to express as seven maltose-binding protein (MBP) fusion protein (Maina, Riggs et al. 1988).
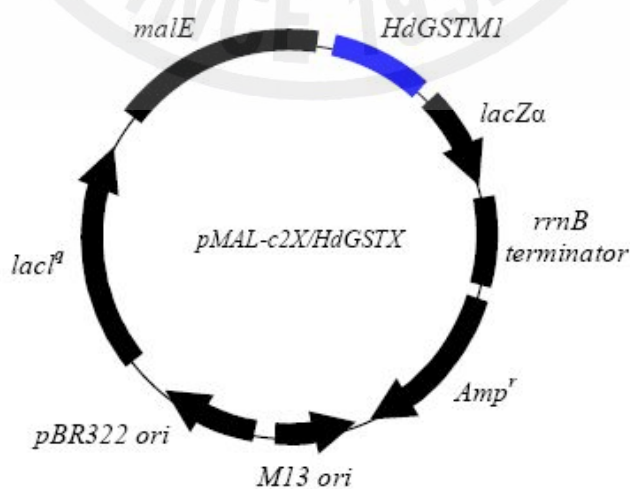
2.6 Recombinant expression and purification

E. coli K12 (Tb1) transformed with seven expression vectors were grown at 37^oC overnight in LB Broth medium plus 100μg/ml ampicillin. The overnight cultures were inoculated into LB Broth medium supplemented 2 g/L glucose and 100μg/ml ampicillin with the dilution of 1: 50. Bacterial cultures were grown until the OD_{600} reached 0.8. Thereafter, isopropyl-b-D-thiogalactoside (IPTG) was added to the medium at a final concentration of 0.2 mM to induce recombinant protein expression. The inductions were carried out with shaking at 25 $^oC$for 5 hrs. The Cells were cooled on ice for 30 min and then harvested by centrifugation at 3500 rpm for 30 min at 4^oC, re-suspended in column buffer (Tris-HCl, PH 7.4, 200 mM NaCl, 0.5 M EDTA), and frozen at -20 ^oC overnight. After thawing, the cells were disrupted by cold sonication and then centrifuged at 9000 x g for 30 min at 4 ^oC. The supernatants were diluted with 1:5 column buffer prior to purification with pMAL^{TM} protein fusion and purification system. Briefly, amylose resin was poured into seven 1 x 5 cm columns and washed with 8 x column volumes of column buffer. The diluted crude extracts were loaded by gravity flow rate. After washed with 12 x column volume of column buffer, seven fusion protein were finally eluted with elution buffer (column buffer + 10 mM maltose). The purity of the each fusion protein preparation was ascertained by SDS polyacrylamide gel electrophoresis (SDS – PAGE).

2.7 Enzyme assay for typical GST substrates

The specific activities of recombinant GSTs were measured as described by Habig et al (Habig, Pabst et al. 1974). Briefly, the reaction was performed in afinal volume of 1 ml containing 100 mM phosphate buffer of pH 6.5; 1 mM GSH reduced; 1.0 mM CDNB and appropriate amount of enzyme. The reaction was initiated by addition of

CDNB, and absorbance at 340 nm was monitored at 25 $^{\circ}$C for 5 min. The activity towards other substrates, DCNB, ECA, 4-NBC and 4-NPB, were measured under the same condition as described above. The changes in absorbance per minute were converted into moles of the substrate conjugated /min/mg protein using the molar extinction coefficient: ε_{340}=mM^{-1} cm^{-1} for CDNB, ε_{340}=mM^{-1} cm^{-1} for DCNB, ε_{270}=mM^{-1} cm^{-1}for EA, andε_{310}=mM^{-1} cm^{-1} for 4-NBC, and ε_{310}=mM^{-1} cm^{-1}for 4-NPB (Habig, Pabst et al. 1974).

2.8 DHA reductase and thioltransferase assay

For two omega GSTs, another two activity tests DHA reductase and thioltransferase assay were carried out as well. Glutathione depended dehydroascorbate reductase activity was measured by the spectrophotometerical method described by William W et al (Wells, Xu et al. 1995).The standard reactions were performed in a final volume of 1 ml containing 0.2 M sodium phosphate buffer; pH 6.85 1.0 mM EDTA; 3.0 mM GSH and 1.5 mM dehydroascorbic acid (DHA) with or without enzyme. Reactions were initiated by addition of DHA. The increase in absorbance at 265 nm, which is due to formation of ascorbic acid, was recorded at 30 $^{\circ}$C for 2 min. The reaction which contained all reagents without enzyme was used as control, and the resulting absorbance change was subtracted from that obtained from reaction with enzyme. The millimolar extinction coefficient of ascorbic acid was reported as 14.7/mM/cm (Daglish 1951). Assays were performed in triplicate. DHA was prepared freshly in ice-cold water saturated by N$_2$and was adjusted to pH 6.85 by cautious addition of 2 M NaOH.

Thioltransferase (TTase) was assayed using 2-hydroxyethyl disulfide (HED) as substrate described by Holmgren A (Holmgren and Aslund 1995). The reaction mixture contained 1 mM GSH, 0.4 mM NADPH, 2 mM EDTA, 0.1 mg/ml BSA, 4

U glutathione reductase in 0.1 M Tris-C1, pH 8.0 and 0.7 mM HED with a final volume of 1 ml. The reaction was initiated by adding enzyme after a preincubation at 25 °C for 2 min, which allowed the formation of a mixed disulfide between GSH and HED. The addition of enzyme gave a decrease of absorption at 340 nm, and the rate of decrease was monitored. The reaction without enzyme was linear up to give the spontaneous background. One unit of TTase activity was defined as 1μmol of NADPH oxidized per min using a molar extinction coefficient of 6.22/mM/cm.

2.9 Optimum pH and temperature and Kinetic analysis

The optimum pH and temperature of HdGSTM1, HdGSTR1, HdGSTS1 and HdGSTS2 were evaluated by standard activity assay using CDNB as substrate at pH range from 4.0 to 9.0 and temperature range from 20 °C to 50 °C. Differently the test of pH and temperature effect of omega GST HdGSTO1 was carried out by standard DHA reductase assay. The reaction condition was variable at pH range from 4.0 to 9.0 and temperature range from 15 °C to 45 °C. The thermostability and pH-stability test was carried out only in HdGSTM1 by measuring the residual activity of recombinant protein incubated at variou temperatures for 30 min and measuring the residual activity of recombinant protein incubated at 4 °C and various pH values for 12 hs, respectively. The apparent kinetic parameters of HdGSTM1 for GSH were determined using a GSH ranging of 0.1-1.0 mM and a fixed CDNB concentration of 1.0 mM; similarly, the apparent K_m and V_{max} values of HdGSTM1 for CDNB were determined using a CDNB ranging from 0.2 to 1.2 mM and a fixed GSH concentration of 1.0 mM. The apparent kinetic parameters of recombinant HdGSTO1 for GSH were determined using a GSH range of 0.2-3.0 mM and a fixed DHA concentration of 1.5 mM; similarly, the apparent K_m and V_{max} values of HdGSTO1 for DHA were determined using a DHA range from 0.2 to 2.0 mM and

a fixed GSH concentration of 3.0 mM. All of the reactions were measured at pH 6.5 and 25 $^{\circ}$C for triplicate. The Michaelis Constants were calculated using Lineweaver-Burk Plot method in the *Hyper* program. Protein concentration was determined by *Bradford*method with bovine serum albumin as a standard (Bradford 1976).

2.10 Homology modeling

To generate the three-dimensional structure models, the protein sequences of seven GSTs were submitted to Swiss-Model (http://swissmodel.expasy.org//SWISS-MODEL.html) and analyzed using the Project (optimise) mode (Schwede, Kopp et al. 2003). The 2.3 angstrom resolution crystal structure of human GSTM1-1 complexed with 1-(s-(glutatahionyl)-2, 4-dinitrobenzene (Protein Data Bank code Nos. 5gstB) was used as a template for HdGSTM1. The X-ray structures of Human GSTO1-1 (Protein Data Bank code Nos. 1eemA) with 40% and 42% sequence simlarity to respective target was chosen as template for two omega GSTs, HdGSTO1 and HdGSTO2. For three sigma GSTs, one 1.75 Åresolution crystal structure of drosophila sigma class glutathione S-transferase (Protein Data Bank code Nos. 1m0uA) was selected from PDB database (http://www.rcsb.org/pdb/home/home.do) as template. Deu to the lack of know crystal structure of rho class GST, two most identical GST structures (Protein Data Bank code Nos. 1jlvA and 1f2eA) were used as template for HdGSTR1. All the three-dimensional images were generated by Swiss-Pdb viewer version 3.7 sp5 and rendered by Pov-Ray 3.6.

2.11 Semi-quantitative reverse transcription (RT)-PCR analysis

To investigate the tissue distribution of seven GST transcripts, total RNA was

isolated from gills, mantle, gonad, foot and digestive tract tissues of disk abalone using TRIzol reagent (Invitrogen). In contrast, in the EDCs challenge experiment, only the RNA from gills and digestive tract was isolated. cDNA was synthesized by SuperScript[TM] III First-Strand Synthesis system for RT-PCR (Invitrogen, USA). 100 ng mRNA isolated from each tissue was used as templates to amplify GST transcripts derived from the abalone. In our study, two housekeeping gene, β-actin and ribosomal proteinS5, were introduced to use as internal control to quantify RNA amount. RT-PCR was conducted in standard procedure with nine sets of specific primers listed in table.1. Amplified products were analyzed by electrophoresis on a 1.5 % agarose gel. The intensities of amplified fragments were measured by Scion Image. The relative expression level of each GST transcript was calculated using intensity value ratio of target gene dividing beta actin or ribosomal protein of the same tissue sample.

Ⅲ. RESULTS

3.1. Primary structure analysis of seven GST cDNA

HdGSTM1 contains a 5′-untranslated region (UTR) of 129 bp and an open reading frame (excluding the stop codon) of 645bp. The nucleotide and deduced amino acid sequences were shown in Fig.1-1. The HdGSTM1 cDNA encodes a polypeptide of 215 amino acids with a predicted molecular mass of 25kDa and an estimated pI of 8.3. The blast search in NCBI GenBank using the deduced amino acid sequence of HdGSTM1 revealed that it had high sequence similarity to mu class GSTs. HdGSTM1 showed a highest sequence identity of 60% to oyster GST (GenBank no. P46409), following 57% and 55% identity to two snail mu GSTs (GenBank no. ABS32297 and ABS32298, respectively). Besides, it showed also more than 50% identity to mouse GST mu 2 (GenBank AAH37068), rabbit GST mu 1 (GenBank CAG07510) and frog GST M1 (GenBank no. CAJ83810). To investigate the homology in mu class GST family, HdGSTM1 was aligned with 16 other identified mu class GSTs (Fig.2-1), followed by an analysis of amino acid sequence identity values. HdGSTM1 showed a high homological N-terminal domain as other mu class GSTs, and there is conserved G-site motif "PNLPY"between residues 57 and 61, which can bind GSH molecules with high specificity. In addition, there exist some conserved hydrophobic residues in the much more variable C-terminal domain, such as Phe-141, Leu-142, Gly-143, Gly-149, Phe-157, Leu-163, Pro-171 and Leu-180. The hydrophobic side chains of these residues form a hydrophobic pocket of H-site, which are potential to bind variety of hydrophobic electrophiles through Van der waal interaction.The identity values of HdGSTM1 with other mu class GSTs were between 36% and 61%, which were within the range of all aligned mu class GSTs

(36% - 97%).

The two omega GSTs, HdGSTO1 and HdGSTO2 contained two open reading frames of 714 and 711 bps lengths, encoding two polypeptides with similar predicted molecular mass of 27.4 and 26.9 kDa, respectively. The full-length nucleotide and deduced amino acid sequences of two cDNA clones were shown in Fig. 1-2 and Fig. 1-3. The protein sequences of HdGSTO1 and HdGSTO2 were aligned with two human omega GSTs (NP_004823 and NP_89962), oyster omega GSTs (CAD89618), silkworm omega GST (ABD36128) and ascidian omega GST (BAD77935) (Fig.2-2). Similar to other GST subfamilies, omega GSTs showed high homology in N-terminal domain and a variable C-terminal domain. It was found that though the aligned sequences were derived from same class, they only showed sequence similarity of around 40% with two abalone omega GSTs. On the contrary, the identities among mammalian omega GST sequences could reach 90% (not shown).

The open reading frames of three sigma GST cDNA clones are 603, 606 and 609 base pairs, encoding three polypeptides with similar predicted molecular mass of 23.0, 23.1 and 23.0 kDa, respectively. The full-length nucleotide and deduced amino acid sequences of three cDNA clones were shown in Fig.1-4~Fig.1-6. HdGSTS2 had much larger untranslated regions (UTR) than HdGSTS1 and HdGSTS3 at 3' and 5' terminus, indicating a possibility of modification or regulation post transcription. three disk abalone GSTs were aligned with another putative sigma GST of disk abalone identified previously (GenBank ABF67507), one sigma GST identified from squid digestive gland (GenBank P46088), and one drosophila sigma GST (GenBank NP_725653) (Fig.2-3). The sequence identities among four disk abalone sigma GSTs ranged between 47.0 and 64.5 %, satisfied with the similarity criterion of GST classification (Hayes JD 1995). However, four GSTs of disk abalone showed weak homologies with squid and drosophila sigma GSTs, which were only 30%

approximately. Additionally, sigma GST of drosophila exhibited a distinct N-terminal terminus, with a proline/alanine-rich extension (46-residues). Consequently, drosophila GST had an approximately 40 residues longer polypeptide chain. Similar structures of N-terminal terminus were also observed in some other insect sigma GSTs and omega class GSTs.

The full-length sequencing of rho GST HdGSTR1 revealed a 1651bp insert containing an open reading frame (ORF) of 675 bp flanked by a 5' untranslated region (UTR) of 113 bp and a significantly longer 3'UTR of 838 bp (Fig.1-7). The polypeptide deduced from the ORF comprises 225 amino acid, with a calculated molecular mass of 25,439 Da and an estimated isoelectric point of 7.86. The BLAST search using deduced amino acid sequence of novel GST revealed that our sequence was most similar with a cluster of fish GSTs withoust clear classification: 53% (116/216) identity with GST of amphioxus (*Branchiostoma belcheri tsingtaunese*, GenBank Accession No. AAQ83893.2), 47% (102/217) identity with GST of Rivulus (*Kryptolebias marmoratus*, GenBank Accession No. ABF70330.1), 46% (100/216) identity with GST of plaice (Pleuronectes platessa, GenBank Accession No.CAA64493.1), and 43% (94/217) identity with GST of Largemouth bass (*Micropterus salmoides*, GenBank Accession No. AAQ91198.1). In addition, two Rho class GSTs (*Pagrus major*, GenBank Accession No. BAD98442.1) and (*Cyprinus carpio*, GenBank Accession No. ABD67511.1) also exhibited high identities of 43% and 47% with our sequence, respectively. A multiple alignment was carried out using deduced amino acid sequence of novel GST and the sequences above (Fig. 2-4). Same as all other GST subfamilies, the N-terminal domain of aligned GSTs are highly conserved. They also shared a similar length of polypeptide chain of 225 a.a and a similar molecular mass of approximate 26 kDa.

A neighbor-joining phylogenetic tree involving 55 GSTs was reconstructed.

HdGSTM1, HdGSTO1, HdGSTO2, HdGSTS1, HdGSTS2, HdGSTS3 and HdGSTR1 were placed in the branch of mu class, omega class, sigma class and rho class with strong bootstrap support, respectively (Fig.3). This NJ tree was rooted with two beta class GST which is the subfamily in bacteria.

Fig.1-1: Nucleotide sequence and deduced amino acid sequence of disk abalone glutathione-s-transferase (GST) HdGSTM1. The ATG start codon is underlined. The TGA translation stop codon and the poly (A+) signal are marked by an asterisk and bold, respectively.

```
                              AAAGCGCAGAT
CGATTAATTGTGCTTATTCATGGTGACAGGCAT
ACTGAGTTGAATTCATTCACACACAACATCGCC
TCTGCCTTCCCGGCGCTCACACCGGGCAAACTA
   S   A   F   P   A   L   T   P   G   K   L    20
TATGCGGAGAGAACGAGACTAGTTCTTGAACAT
   Y   A   E   R   T   R   L   V   L   E   H    40
ACTGACTTGAAACAGAAGCCATCTTGGTTCTGG
   T   D   L   Q   K   P   S   W   F   W    60
ATCTTAGAAAAAGACGACAAGGTGCTCTATGAG
   I   L   E   K   D   D   K   V   L   Y   E    80
GAAGTCTACCCTAACAACAAACTGACACCCTCG
   E   V   Y   P   N   N   K   L   T   P   S    100
CTCATTGTGGAACTGTTTTCAAAGGCAGTGACC
   L   I   V   E   L   F   S   K   A   V   T    120
GATGTTCCAAAGGATGCTATAAAGGGATTCCAC
   D   V   P   K   D   A   I   K   G   F   H    140
CTCGCAGAGAGGGGTACTCCGTTCTTTGGTGGC
   L   A   E   R   G   T   P   F   F   G   G    160
ATTTGGCCTCATGTTGAAAGGTTTGACGCTATG
   I   W   P   H   V   E   R   F   D   A   M    180
ACAGATGATCGGTACCCCAAGCTTACCAAGTGG
   T   D   D   R   Y   P   K   L   T   K   W    200
GTACAGAAATGTCGCTGGGACACAGCGGCACAC
   V   Q   K   C   R   W   D   T   A   A   H    220
GGAAAACCAGACTATGACGTTGGCCTTTGAATC
   G   K   P   D   Y   D   V   G   L   *    240
GATGACAACACAACATAGCTATTGTACCTGCA
CTAAAGATGTTCAGGATAATTTGTTACAAAG
AAATGAGCTAACCTTTGGAATGAAAGTTATCG
TTTGTTTATTTCAAAACTTTGGACTTGCGCAA
GATTTTTGGTCTAGAAGAATATTCATCTTGGG
GTTTGAAGATTGTTATTTTAATTACATATACA
AGGCTCTTGCAGCCAAGATGTCAGTCACATCC
TGGTGCTCCGAGCTAATGTACATTCATTTGCC
ATATGAAATCATACACTTGTAGTGCGTCAATT
AAAAAAAAAAAAAAAAAAAAAAAAAA
```

Fig.1-2: Nucleotide sequence and deduced amino acid sequence of disk abalone glutathione-s-transferase (GST) HdGSTO1.

GCATGAGATTCTGTCCATTCGCCCAGAGGACCCGTCTAGTGCTGGAGCAT
S   M   R   F   C   P   F   A   Q   R   T   R   L   V   L   E   H   40
CGCATGAGACAATCAACGTGGACTTGAAGAAGAAGCCGGACTGGTTCCTG
P   H   E   T   I   N   V   D   L   K   K   K   P   D   W   F   L   60
CGCTGGGTCTGGTGCCAGTGCTGGAAAAGACAGACCAGGTGGTGTACGAG
P   L   G   L   V   P   V   L   E   K   D   D   Q   V   V   Y   E   80
GTGACGACTACCTGGACCAGGTCTACCCAGACTTTCCGCTCTACCCTCAG
C   D   D   Y   L   D   Q   V   Y   P   D   S   P   L   Y   P   Q   100
AGAAGGCTAGAGATGGGATTCTGTTGGAAACCTTCTCACAGGTGACAACT
K   K   A   R   D   G   I   L   L   E   T   F   S   Q   V   T   T   120
AGTTGCTGTCTTCAGGAGGCAGTGATGAAGCAGGGGAGAAGTTCTTCAGT
K   L   L   S   S   G   G   S   D   E   A   G   E   K   F   F   S   140
CGTATGAAACTGCCCTTGGTGATCGAGGGGAGTTCTTTGGAGGTGCCACT
T   Y   E   T   A   L   G   D   R   G   E   F   F   G   G   A   T   160
TGGACTTCACAGCGTGGCCATGGTTTGAAAGAAGTGGAGTCTTGGAGAAG
L   D   F   T   A   W   P   W   F   E   R   S   G   V   L   E   K   180
AGTATGCCATCACTGAAAGCAACTTCCCCAACATTGCAGCCTGGCAGAAG
K   Y   A   I   T   E   S   N   F   P   N   I   A   A   W   Q   K   200
AACTTCCAGCAGTCAAAGCCACGATGTTTGACACAGAGTCCCATCTCAGA
E   L   P   A   V   K   A   T   M   F   D   T   E   S   H   L   R   220
CTTACAAAGCAGGCGCCCCAGACTATGACTATGGTTTATGACTACGCCAA
S   Y   K   A   G   A   P   D   Y   D   Y   G   L   *   240
GAACACTGACTGAACCGACGACCACTGTTGTTTTATTTCTATAAGCTGTG
TGTGGGTCAGTCGGTTCACTGGAGAAGAAATAACTGCTAGATCTTAAACT
ATTATTTGTCAAACAGATTAGTAGGGTTTGTGATTTTATCAAGAACAATC
ATTAATATAGGACTCTTTTTTAGTTTATTTTCTGTTTGCTGCATTTAAAC
CAAAAATGGCATCTTATACATGATAGATTAATGTATAGTCTTTCATGTCA
AATGTGATGGTCCAATTGATGGAAAGATATGAGGAAACAAAAAAAAAAAA
AAAAAAA

Fig.1-3: Nucleotide sequence and deduced amino acid sequence of disk abalone glutathione-s-transferase (GST) HdGSTO2.

```
GGTTTCAGGGAAG
G   F   H   G   K        80
ACGACATCTTCAGT
N   D   I   F   S       100
ACATAATAAAGCAA
D   I   I   K   Q       120
TATTGAAGAACAAT
I   L   K   N   N       140
CTGCCTTTGACACC
A   A   F   D   T       160
TAAAAGCCAATAAG
V   K   A   N   K       180
GGCGGTCACACAA
R   P   V   T   Q       200
AAAGCCAGGGCCCA
                        201
ACAAAATGGGAGTT
CTGTTCCTAGAGGC
TGATCCACGAGCTT
GATAATCATCAATT
ATGTGTTTCCACAC
GAAGCATATTAATC
AAAAAAAAAAAAAA
```

Fig.1-4: Nucleotide sequence and deduced amino acid sequence of disk abalone glutathione-s-transferase (GST) HdGSTS1.
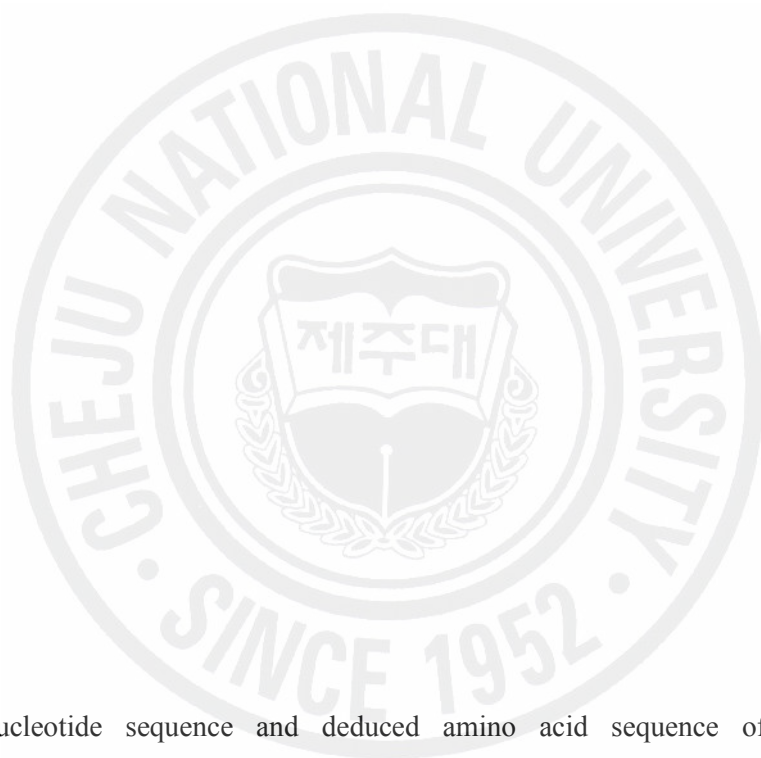
Fig.1-5: Nucleotide sequence and deduced amino acid sequence of disk abalone glutathione-s-transferase (GST) HdGSTS2.

CAGGACGTATTCTACCCGTGCACACATCACAATC
CGACTACAAGGCCGTGGGCGAGCTGTCCCGGCTG
   D   Y   K   A   V   G   E   L   S   R   L   20
CGAGGACGTCAGGATCACTTATGAAACATGGCCC
   E   D   V   R   I   T   Y   E   T   W   P   40
TCAGGTTCCCGTCCTTGAAATTGATGGGAAACCC
   Q   V   P   V   L   E   I   D   G   K   P   60
ATACCTTGCAAGGACATTGGCTTCTATGGTAAC
   Y   L   A   R   T   F   G   F   Y   G   N   80
TCAGGTCCTAGGTGTGGTCCAAGACGTCAACACC
   Q   V   L   G   V   V   Q   D   V   N   T   100
AGACGAAGCCAAGAAGGCTGAGTTGCTGAAGGAG
   D   E   A   K   K   A   E   L   L   K   E   120
TTTCGGGATGTTTGAGAAGCTACTGAAGAAAAT
   F   G   M   F   E   K   L   L   K   N   140
GAAGATTAGTATTGCTGATGTCAGTCTCTTTGAT
   K   I   S   I   A   D   V   S   L   F   D   160
GTTGAAGATAGAAGACTACCCTCTAGTCAAGAAA
   L   K   I   E   D   Y   P   L   V   K   K   180
TAAAATCAAAGCATGGGTTGAGAAACGACCAGTT
   K   I   K   A   W   V   E   K   R   P   V   200
ATATTTCTTCTAAGTACAAGTGGCAAGTACTTGG

                                 203

CAACAGAGGTGTAACTATAATTGTATTCATCACT
CTGCAAGACCTGAAACACCAATTTCAAGGACAGT
TTTTCTAAAAAAAAAAAAAAAAAAAAAAAAAAAA

Fig.1-6: Nucleotide sequence and deduced amino acid sequence of disk abalone glutathione-s-transferase (GST) HdGSTS3.

Fig.1-7: Nucleotide sequence and deduced amino acid sequence of disk abalone glutathione-s-transferase (GST) HdGSTR1.

```
                      1       *        *                                    *      *****        75
HdGSTM1        (1)  ---MPULGYWAIRGLAQPIRLLLKYAGEDFDDVMYEQGDAPEYSRESWUKVKFULGLPIPNLPYYVDGNIKIUQS
B. taurus      (1)  --MPMILGYWDIRGLAHAIRLLLEYTDTNYEERQYSVGDAPDYDRSQWLNEKFKLGLDFPNLPYLIDGTHKLTQS
C. gigas       (1)  ---MSTLGYWNIRGLGQPIRLLLNYVGEEFDDVQYELGDAPDYSREEWLSVKNTLGLAFPNIPYYIDDDIKITQS
C. longicausdatus (1) --MPMILGYWNVRGLTNPIRLLLEYTDSSYEEKKYTMGDAPDSDRSQWLNEKFKLGLDFPNLPYLIDGSHKITQS
D. pteronyssinus (1) -MSQPILGYWDIRGYAQPIRLLLTYSGVDFVDKRYQIGPAPDFDRSEWLNEKFNLGLDFPNLPYYIDGDMKMTQT
D. rerio       (1)  --MAMKLAYWDIRGLAQPIRLLLEYTGTKYEEKFYTCGEAPNYDKSCWFNEKSKLGMDFPNLPYLEDGDRKIVQS
F. hepatica    (1)  --MPAKLGYWKLRGLAQPVRLFLEYLGEEYEEHLYG-----RDDREKWMSEKFNMGLDPNLPYYIDDKCKLTQS
G. callus      (1)  --MVVTLGYWDIRGLAHAIRLLLEYTETPYQERRYKAGPAPDFDPSDWTNEKEKLGLDFPNLPYLIDGDVKLTQS
H. spapiens    (1)  --MPMILGYWDIRGLAHAIRLLLEYTDSSYEEKKYTMGDAPDYDRSQWLNEKFKLGLDFPNLPYLIDGAHKITQS
M. auratus     (1)  --MPVTLGYWDIRGLAHAIRLLLEYTDTSYEEKKYTMGDAPNFDRSQWLNEKFKLGLDFPNLPYLIDGSHKITQS
M. fascicularis (1) --MPMTLGYWNIRGLAHSIRLLLEYTGSSYEEKKYTMGDAPDYDRSQWLNEKFKLGLDFPNLPYLIDGTHKITQS
M. musculus    (1)  --MPVTLGYWDIRGLGHAIRLLLEYTETGYEERRYAMGDAPDYDRSQWLNDKFKLGLDFPNLPYLIDGSHKVTQS
O. cuniculus   (1)  --MPMTLGYWDVRGLALPIRMLLEYTDTSYEEKKYTMGDAPNYDQSKWLSEKFTLGLDFPNLPYLIDGTHKLTQS
P. pygmaeus    (1)  --MPIILGYWNIRGLAHSIRLLLEYTDSSYEEKKYMMGDAPDYDRSQWLNEKFKLGLDFPNLPYLIDGTHKITQS
R. norvegicus  (1)  --MPMTLGYWDIRGLAHAIRLFLEYTDTSYEDKKYSMGDAPDYDRSQWLSEKFKLGLDFPNLPYLIDGSHKITQS
S. hominis     (1)  MSSKPTLGYWNIRGLAQPIRMMLSYAGVDFVDKRYNYGPAPDFDRSEWLNEKFNLGLDFPNLPYYIDGDVKLTQS
X. tropicalis  (1)  ----MILGYWDIRGLAHSIRLLLEYTGTQYEEKKYITGDAPNYDKTQWLDEKEKLGLDFPNLPYLLDGDVKLTQS

                      76                                  *  ##  *                          150
HdGSTM1        (73) NAILLRYIARKHQLLGEKEEEERVKVDVMLDUAMDFRNGIVGLCYNPEFEKKQAAYFEALPAKLEMFKSELGDQQFF
B. taurus      (74) NAILLRYIARKHNLCGETEEEMIRVDILENQVMDVRLAMARICYSPDFEKLKPGFLKEIPEKIKLFSERLGKRPWF
C. gigas       (73) NSILRYIGDKHGLLGKTPRDKVDCDMMVENAMDFRNGVIRLCYDNDYEKLKDDYFANVKDKLRQFDTFLGDKPWF
C. longicausdatus (74) NAILLRYIARKHNLCGETEEERIRVDIVENQAMDTRMQLIMLCYNPDFEKQKPEFLKTIPEKMKMYSEFLGKRPWF
D. pteronyssinus (75) FAILLRYLGRKYKLNGSNDHEEIRISMAEQQTEDMMAAMIRVCYDANCDKLKPDYLKSLPDCLKLMSKFVGEHAFI
D. rerio       (74) NAILMRYIARKHNLCGETEEEQMRVDILENQAMDFRNGFVQLCY-LDFDKNKSSYCEKLSGTLKQFSDFLGDRKWF
F. hepatica    (69) VAILMRYIADKHGMLGTTPEERARISMIEGAAMDLRIGFGRVCYNPKFEEVKEEYVKELPKTLKMWSDFLGDRHYL
G. callus      (74) NAILLRYIARKHNMCGETEVEKQRVDVLENHLMDLRMAFARLCYSPDFEKLKPAYLELLPGKLRQLSRFLGSRSWF
H. spapiens    (74) NAILLCYIARKHNLCGETEEEKIRVDILENQTMDNHMQLGMICYNPEFEKLKPKYLEELPEKLKLYSERLGKRPWF
M. auratus     (74) NAILLRYIARKHDLCGETEEERIQLDILENQAMDTRMQLAMVCYSPDFEKRKPEYLEGLPEKMKLYSERLGKRSWF
M. fascicularis (74) NAILLRYIARKHNLCGETEKEKIREDILENQLMDNRMQLARLCYDPDFEKLKPEYLEGLPEMLKLYSQFLGKQPWF
M. musculus    (74) NAILLRYLGRKHNLCGETEEERIRVDILENRVMDTRIQMGMLCYSADFEKRKPEFLKGLPDQLKLYSERLGKQPWF
O. cuniculus   (74) NAILRYLARKHGLCGETEEERIRVDILENQLMDNRFQLVNVCYSPDFEKLKPEYLKGLPEKLQLYSQFLGSLPWF
P. pygmaeus    (74) NAILLRYIARKHNLCGETEKEKIQEDILENQLMDNRMQLARLCYNPDFEKLKPEYLEGLPEMLKLYSQFLGKQPWF
R. norvegicus  (74) NAILLRYLGRKHNLCGETEEERIRVDVLENQAMDTRLQLAMVCYSPDFERKKPEYLEGLPEKMKLYSERLGKQPWF
S. hominis     (76) LAILRYIARKHKLDGHNEQEWLRIALCEQQIVDLYMAMGRISYDPNFEKLKPDYLEKLPDNLKLFSERLGDHPFV
X. tropicalis  (72) NAILRYIARKHGLCGESEKEKMYVDLIENQTMDFRMGLVVIAYNPQFETLKGPYLEKLPIALKRFSCFLGDRSWF

                      151                                              ##      #  225
HdGSTM1       (148) AGSKVUVCDFPIYELDDQURIMQPGSLDAFPULLAFMGRIEALPAIKUFMSSAKFIRRPINNKSALFK-------
B. taurus     (149) AGDKLTYVDFLVYDVLDMHRIFEPKCLDAFPNLKDFISRFEGLKKISAYMKSSRFLPGPLFMKLAVWGNK-----
C. gigas      (148) AGDGITICDFPLYELDDQHRLMKPGILDYPNLTKFVERFENLPKIKAYMASDKFMARPVNNKFALFK--------
C. longicausdatus (149) AGDKVTLCGFLAYDVLDQYQMFEPKCLDPFFNLKDFLARFEGLKKISAYMKTSRFLRRPIFSKMAQWSNK-----
D. pteronyssinus (150) AGANISYVDFNLYEYLCHVKVMVPEVFGGQFENLKRYVERMESLPRVSDYIKKQQ--PKTFNAPTSKWNASYA---
D. rerio      (148) AGDKITFVDFIMYELDDQHRMFEPACLDFKNLRCFLDHFESLEKIAEYMKSNRFMETPVNNKMAKWGNKKE---
F. hepatica   (144) TGSSVSHVDFMLYETLDSIRYLAPHCLDEFPKLKEFKSRIEALPKIKAYMESKRFIKWPLNGWAASFGAGDAPPS
G. callus     (149) VGDKLTFVDFLAYDVLDQQRMFVPDCPELQGNLSQFLQRFEALEKISAYMRSGRFMKAPIFWYTALWNNKKE---
H. spapiens   (149) AGNKITFVDFLVYDVLDLHRIFEPNCLDAFPNLKDFISRFEGLEKISAYMKSSRFLPRPVFSKMAVWGNK-----
M. auratus    (149) AGDKITYVDFLIYDVLDQHRIFAPKCLDAFPNLKDFLARFEGLKKISDYMKSSRFSCKQIFAKMAVWNSK-----
M. fascicularis (149) LGDKITFVDFIAYDVLERNQVFEPSCLDAFPNLKDFISRFEGLEKISAYMKSSRFLPRPVFTKMAVWGNK-----
M. musculus   (149) AGDKITFADFLVYDVLDQHRMFEPTCLDAFPNLKDFMARFEGLRKISAYMKTSRFLPSPVYLKQATWGNE-----
O. cuniculus  (149) AGDKITFADFLVYDVLDQNRIFVPGCLDAFPNLKDFHVRFEGLPKISAYMKSSRFIRVPVFLKKATWTGI-----
P. pygmaeus   (149) LGDKITFVDFIAYDVLERNQVFEPSCLDAFPNLKDFISRFEGLEKISAYMKSSRFLPRPVFTKMAVWGNK-----
R. norvegicus (149) AGNKITYVDFLVYDVLDQHRIFEPKCLDAFPNLKDFVARFEGLKKISDYMKSGRFLSKPIFAKMAFWNPK-----
S. hominis    (151) AGTNLSYVDFVVYEYLIRLKAMTPEVFAKFQNLGNYVNRFESMPKISAYLKQQQ--PQFFNGLMAKWNMKY----
X. tropicalis (147) AGDKITFVDFVVYDVLDQHRILEPTCLQNFKNLQDFLKRFEALPAIDAYMKSSRFMKTPINNRMASWGNK-----
```

Fig.2-1: Alignment of amino acid sequences of HdGSTM1 and other known mu class GSTs. Sequence of GST from each organism was obtained from NCBI GenBank database: R. *norvegicus* (*Rattus norvegicus*, NP_803175); M. *auratus* (*Mesocricetus auratus*, CAA43368); X. *tropicalis* (*Xenopus tropicalis*, CAJ83810); S. *hominis* (*Sarcoptes scabiei type hominis*, AAX37321); P. *pygmaeus* (*Pongo pygmaeus,* CAH91962); O. *cuniculus* (*Oryctolagus cuniculus,* P46409); M. *musculus* (*Mus musculus,* O35660) M. *fascicularis* (*Macaca fascicularis,* AAF08540); G. *gallus* (*Gallus gallus,* S18464); F. *hepatica* (*Fasciola hepatica,* P31670); D. *rerio* (*Danio rerio,* NP_997841); D. *pteronyssinus* (*Dermatophagoides pteronyssinus,* AAB3224); C. *gigas* (*Crassostrea gigas,* CAD90167); B. *tarus* (*Bos taurus,*CAD90167). The active sites of mu class GST motif was marked with asterisk and key site divergences were marked with pound.

```
YAQRTRLMLALKNVDHEVINIDLKDKPAWFLEKYQAG
YAERTVLTLNAKNIPYDLVFINLDQKPEWIFNFSPKG
YAQRALVLTYKNIPHEVVNINLKNKPEWFLQKNPLG
```

```
LTPSDPYRRARDRLIVELFSKAVTLFYKIAYGKDV--
LYPQDAYKKARDRILLETFSQVTTAWYKLLSSGGS--
LPDDPYEKACQKMILELFSKVPSLVGSFIRSQNK-E
FPYDPYERARQKMLLELFCKVPHLTKECLVALRCGR
GLPTDPYKKAQARLLIYELGKIPSKFYGFARQAEN——
QASDPLRRAQDKILVESFAPAQSAYYTAAFNAQALE
LTPDDPYRQARDKMTVEVFSQFVSDFQKMMSSPPQ--
```

```
QMIDFTIWPHVERFDAMAQLVKEARVTDD-RYPKLTK
SMLDFTAWPWFERSGVLEKVAPKYAITES-NFPNIAA
SMIDYLIWPWFERLEAMKLNEC----VD--HTPKLKL
SMIDYLLWPWFERLDVYGILDC----VS--HTPALRL
SYVDYMIWPWFERIGTWCGELP-----KG-KFPNITR
GWVDYTLWPFLRFEALPLIGKAEFAIDQTKYERLVT
QMLDFLLWPWFERILIFAKVVP-LTFSLE-DYPALCE
```

```
-DYDVGL-------------
-DYDYGL-------------
EACDYGL-------------
NAFDFGLC------------
-VYDLE--------------
YNMLDTSAVCCMRPRKKKE
-DYDVPKTSQS---------
```

Fig.2-2: Alignment of amino acid sequences of two abalone omega GSTs and other five omega class GSTs. The putative glutathione binding sites are marked with asterisks. The putative hydrophobic sites are marked with "§". The homological residues are marked by black background and shadows. All the sequences were obtained from NCBI GenBank database: Human O1 (Homo sapiens, NP_004823); Human O2 (Homo sapiens, NP_899062); Ascidian (Halocynthia roretzi, BAD77935); Silkworm (Bombyx mori, ABD36128); Oyster (Crassostrea gigas, CAD89618).

```
                                      ----------------------------------MPSYKLIYTDNKGRAEVSR
                                      ----------------------------------MPTYKLRYFNARGFGEVSR
                                      ----------------------------------MPTYRFRYFDYKAVGELSR
                                      ----------------------------------MSQYKLIYLDFRGRGELSR
                                      ----------------------------------MPKYTLHYFPLMGRAELCR
              APPAEGEAPPPAEGAEGAVEGGEAAPPAEPAEPIKHSYTLFYFNVKALAEPLR

                                                                       130
       *          **              *
VRWTRETFQTEKQNLLFGQIPVLEVDGKQYAQSMAIAGFLAREFGFHGKTSVE
VRFTQETWPAEKPNTPLGQMPVLDVDGQSFGQSSAISRFLARRFNFYGQGDVQ
VRITYETWPAEKPNTPLGQVPVLEIDGKPFSQSSAISRYLARTFGFYGNGDLE
VRFKREDWPAVKDKYIFGRIPVLEVDGKQYGQSMAIASFLAKRFGFHGSTDVE
RVVEMADWPNLKATMYSNAMPVLDIDGTKMSQSMCIARHLAREFGLDGKTSLE
VRVTRDEWPALKPTMPMGQMPVLEVDGKRVHQSISMARFLAKTVGLCGATPWE

                                                       195
  §    §    §
DIFSALIKQFHEQDEEKKADIIKQNNETTFPKFISFFEKILK-N-NNTGFYVG
DIINALIKAYYEKDEERKAQALKENKEEKMPLYFGMLEKLLERN-GSTGFFVG
DVNTFMRDYHKEQDEAKKAELLKEAKDVKIPLYFGMFEKLLKKN-GSTGLFVG
DIRAALVRAFLERDEGRKAEIVTENKETNIPRFLGFLETVLK-N-NNTGYYVG
DIFNDVVKIKFAPEAAK--EAVQQNYEKSCKRLAPFLEGLLVSNGGDGFFVG
DFRLKIAVVSYEPEDEIKEKKLVTLNAEVIPFYLEKLEQTVK---DNDGHLAL

                                                       252
   §   §                                      §
ILSKI--EAGIN-MDDFPLVKANKEKVASNERVAKVLQDRPVTQF
IYDK---AKPMVDLDKFPLVKKSVDNVASNPKIKTWIEKRPQTEN
ICDKT--TDAMLKIEDYPLVKKCCDNVAANPKIKAVVEKRPVTAF
DLFAA--RIEESLMERFPLVKANSEKVKADEKIAQVLAKRPQTQI
ALEVP-LKHTPELLKDCPKIVALRKRVAECPKIAAYLKKRPVRDF
ITDYMNYMVKRDLLEPYPALRGVVDAVNALEPIKAVIEKRPVTEV
```
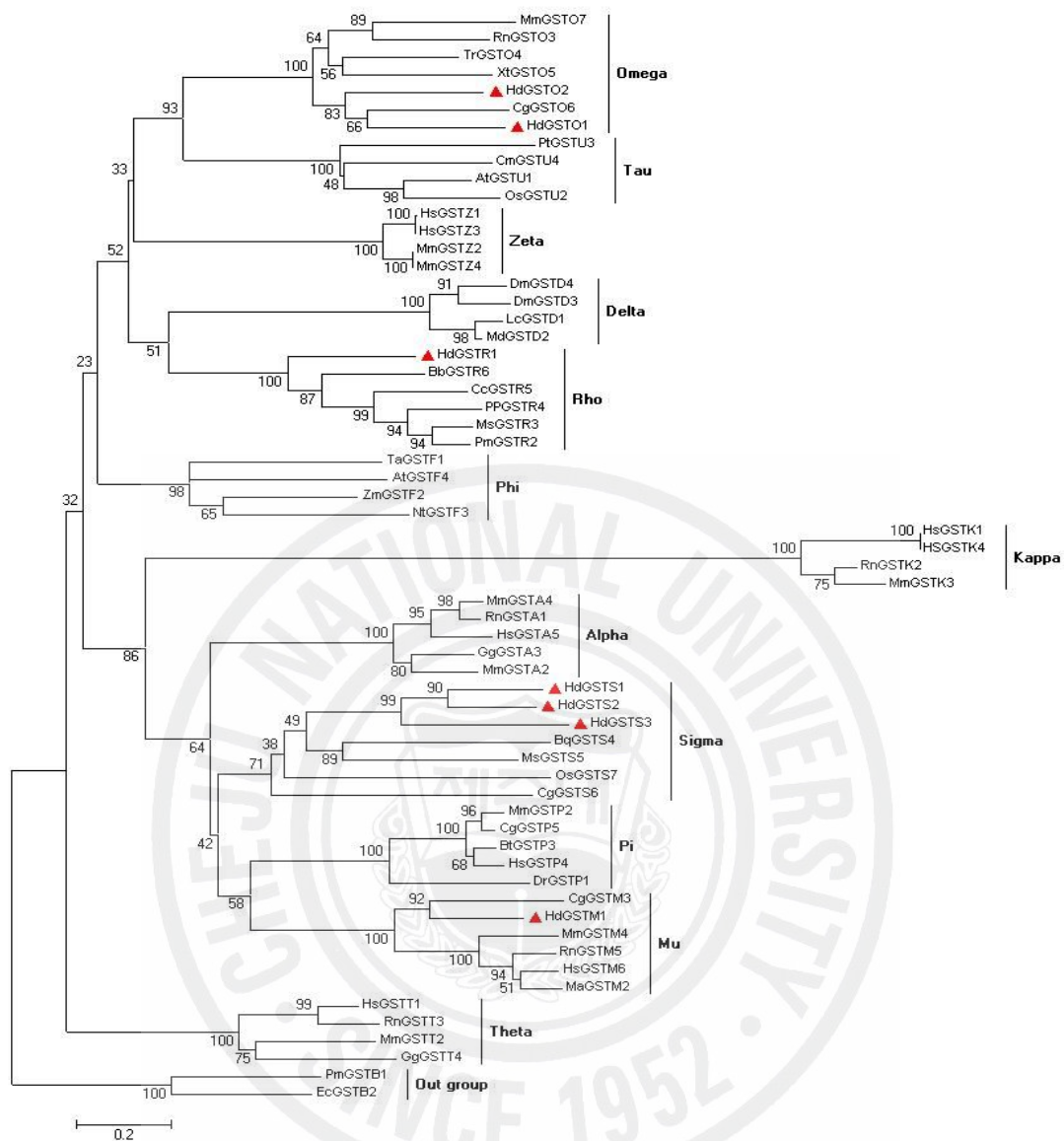
Fig.2-3: Multiple alignment between three previously identified sigma GSTs and three abalone GSTs of our study. Putative G-site and H-site residues are marked with asterisk and "§", respectively. The residue which belongs to both G-site and H-site is marked with "☼".

```
                1               *                                      60
   HdGSTR1    (1) MSSNMFLYWGSGSIPCWKPMLVLEEKGLAGYPNKKISFSDKEHKSEEILKLNPRGQVPUF
 B.belcheri    (1) MASDMTLYWGAGSGPCWRAMICLEEKGLSDYNSKLISFDNKEHKSDEVLKINPRGQMPTF
   C.carpio    (1) MAQNMMLYWGSGSPPCWRVMIALEEKMLQGYKHKFLSFDKNEHKCEEVKALNPRAEVPTF
K.marmoratus   (1) MAKDMTLYWGSGSPPCWRVMIALEEKNLQGYNSKLLSFEKGEHKSKEVMDVNCRGQLPAF
 P.platessa    (1) MAKDMTLLWGSGSPPCWRVMIVLEEKNLQAYNSKLLSFEKGEHKSAEVMSMNPRGQLPSF
M.salmoides    (1) MAKDMTLLWGSGSPPCWRVQIALEEKSLQGYNQKLLRFDKMEHKSQEVMDMNPRGQLPAF
   P.major     (1) MAKDMTLLWGSGSPPCWRVMITLEEKNLKGYNQKLLSFEKMEHKSEEVMKMNPRGQLPAF
                61                                                    120
   HdGSTR1   (61) KDGEIVVNESGAICFYLENKFSDKGUKLLPDDNAERARVLQRVFEVSNVDSSIIUNLLHY
 B.belcheri  (61) KHGNAIVNESFAICLYLENTFKGQGAKLLPDDPVQQALVLQRAVESQNIREKAAFGVLSY
   C.carpio  (61) KHGDIVVNESFAACLYLESAFKSQGTRLIPDDPTEQALVYQRMFETNNLQQK-MYDVAFY
K.marmoratus (61) KDGKIIVNESYGICLYLEDRYKSKGTKLIPDNPDEMALMHQRMFEGLTLFQK-MAQSLFY
 P.platessa  (61) KHGSKVLNESYAACMYLESQFKSQGNKLIPDCPAEQAMMYQRMFEGLTLAQK-MADVIYY
M.salmoides  (61) KHGNNVLNESYAACLYLESEFKSQGNKLIIPDCSAEKALMYQRMFEGLTLNQK-MADVIYY
   P.major   (61) KHGDKVLNESYAACLYLENQFKSQGNKLVPDCPAELAMMYQRMFEGLSLNQK-MADVIYY
                121                                                   180
   HdGSTR1  (121) RFRUPKDKLDEELLKUKYEAVRUELKKWEGHLAAS--QGYVVGSNFUMADVFFFPYVAFG
 B.belcheri (121) FFRTKPEDRTEAMLEEKKKTCHEELQIWEGYLAKLGDGSYIAGKNFTLADACTFPFIATL
   C.carpio (120) EYYVPEGERLESALKRNKESLVAELKLWDGYLEKMGKGSYLAGKSFTMADVVCFPVIAYF
K.marmoratus(120) TRFVPENERHASAEERNRGELREEVQRWENYMKCD----YLAGKHFTMADVIVFPVIAFL
 P.platessa (120) SWKVPEAERHDSAVKRNKENLSTELKLWEEYLQKTS-GSFVAGKSFSLADVSVFPGVAYL
M.salmoides (120) NWKVPEGERHDSAVKRNRDVLSAEVKLWEGYLQKAS-GSFFAGKNFSLADVTVYPSIAYL
   P.major  (120) NWKVPEGERHDSAVKRNRESLTAELKLWEGYLQKTS-GGFLAGKTFSLADVCVYPSICYV
                181                      228   Identity
   HdGSTR1  (179) VRLGLDISKYPAISAYYDKVKDRPSVKAUWPPHWADGP-GDSSIMGPV
 B.belcheri (181) VRMGFNMSRYPHLAKYYDLVKDRPCVKASWPPHWKDTL-NKDVLKDI-       53%
   C.carpio (180) PRLHCPREHCPRLMEYYEMLKDRPSIKASWPLEWLEKPEGPDTLKNL-       47%
K.marmoratus(176) FRFGLCEEKYAKLAAYYKNLKDRPSIKSTWPPSWKDSP-GMDTLKSL-       47%
 P.platessa (179) FRFGLTEERYPQLTAYYNSLKERPSIKASWPPTWLESPQGQDMLKDV-46%
M.salmoides (179) FHFGLCEERYPKLAAYYNSNKDRPSIKATWPPTWLENPQGQDQLKDI-       43%
   P.major  (179) FRFGLCEERYPKLASYYNSLKDRPSIKASYPPTWLENPQGQDVLKDI-       43%
```

Fig.2-4: Sequence alignment of HdGSTR1 and other rho class GSTs obtained from GenBank on NCBI. The predicted catalytic G-site was marked with asterisk. M.salmoides (*Micropterus salmoides*, AAQ91198.1); P.major (*Pagrus major*, BAD98442.1); P.platessa (Pleuronectes platessa, CAA64493.1); K.marmoratus (*Kryptolebias marmoratus*, ABF70330.1); C.carpio (*Cyprinus carpio*, ABD67511.1); B.belcheri (*Branchiostoma belcheri tsingtaunese*, AAQ83893.2)

Fig.3: Neighbor-joining phylogenetic tree including 13 GST classes. Bootstrap values from a sample of 1000 replicates are shown on each branch. All the sequences were obtained from GenBank on NCBI: MsGSTS5 (*Manduca sexta,* P46429) CgGSTS6 (*Crassostrea gigas,* CAE11863); BgGSTS4 (*Blattella germanica,* O18598; OsGSTS7 (*Ommastrephes sloani,* P46008); RnGSTA1 (*Rattus norvegicus,* AAF33739); MmGSTA2 (*Mus musculus,* NP_034487); GgGSTA3 (*Gallus gallus,* P26697); MmGSTA4 (*Mus musculus,* P30115); HsGSTA5 (*Homo sapiens,*

Q7RTV2); HsGSTM6 (*Homo sapiens*, NP_000839); MaGSTM2 (*Mesocricetus auratus*, CAA43368); CgGSTM3 (*Crassostrea gigas*, CAD90167); MmGSTM4 (*Mus musculus*, NP_034490); RnGSTM5 (*Rattus norvegicus*, NP_058710); DrGSTP1 (*Danio rerio*, AAG35785); MmGSTP2 (*Mus musculus*, NP_038569); BtGSTP3 (*Bos taurus*, NP_803482); HsGSTP4 (*Homo sapiens*, P09211); CgGSTP5 (*Cricetulus griseus*, S71959); HsGSTK1 (*Homo sapiens,* NP_057001);RnGSTK2 (*Rattus norvegicus,* P24473); MmGSTK3 (*Mus musculus,* Q9DCM2); HsGSTK4 (*Homo sapiens,* Q9Y2Q3); HsGSTZ1 (*Homo sapiens,* AAH01453); MmGSTZ2 (*Mus mulculus,* AAH31777); HsGSTZ3 (*Homo sapiens,* AAC33591); MmGSTZ4 (*Mus mulculus,* NP_034493); PtGSTU3 (*Pinus tabuliformis,* AAT69969); OsGSTU2 (*Oryza sativa*, AAQ02687); CmGSTU4 (*Cucurbita maxima*, BAC21263); AtGSTU1 (*Aegilops tauschii*, 1GWC_A); CgGSTO6 (*Crassostrea gigas,* CAD89618); MmGSTO7 (*Mus musculus,* NP_080895); RnGSTO3 (*Rattus norvegicus,* AAH79363); TrGSTO4 (*Takifugu rubripes,* AAL08414); XtGSTO5 (*Xenopus tropicalis,* AAH87558); LcGSTD1 (*Lucilia cuprina*, AAA29287); MdGSTD2 (*Musca domestica,* CAA43599); DmGSTD3 (*Drosophila melanogaster*, NP_524912); DmGSTD4 (*Drosophila melanogaster*, NP_524912); HsGSTT1 (*Homo sapiens,* NP_000845); MmGSTT2 (*Mus musculus,* NP_032211); RnGSTT3 (*Rattus norvegicus,* NP_036928); GgGSTT4 (*Gallus gallus,* P20135); LcGSTT5 (*Lucilia cuprina,* P42860); TaGSTF1 (*Triticum aestivum,* CAD29476); ZmGSTF2 (*Zea mays*, P04907); NtGSTF3 (*Nicotiana tabacum*, P46440); AtGSTF4 (*Arabidopsis thaliana*, P42761); PmGSTB1 (*Proteus mirabilis,* P15214); EcGSTB2 (*Escherichia coli,* BAA15396) MsGSTR3 (*Micropterus salmoides*, AAQ91198.1); PmGSTR2 (*Pagrus major*, BAD98442.1); PpGSTR4 (Pleuronectes platessa, CAA64493.1); KmGSTR (*Kryptolebias marmoratus*, ABF70330.1); CcGSTR5 (*Cyprinus carpio*, ABD67511.1); BbGSTR6 (*Branchiostoma belcheri tsingtaunese*, AAQ83893.2).
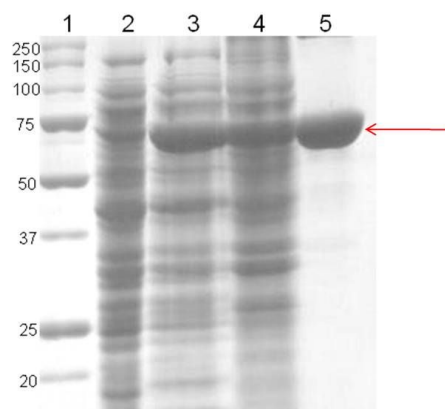
Fig.4-1: SDS–PAGE analysis of the recombinant HdGSTM1. Lane 1, molecular mass markers with the sizes shown on the left in kilodaltons; lane 2, total cellular extract from *E. coli* K12; lanes 3, total cellular extracts from induced bacteria containing pMALTM-c2X / HdGSTM1; lanes 4, supernatant after ultrasonication and centrifugation of cells expressing recombinant HdGSTM1; lanes 5, the purified recombinant HdGSTM1. In the N-terminal of recombinant GSTs is a maltose binding protein tag with a molecular weight of 42.5 kDa.

Fig.4-2: SDS–PAGE analysis of the recombinant HdGSTO1 and HdGSTO2. Lane 1, molecular mass markers with the sizes shown on the left in kilodaltons; lane 2, total cellular extract from uninduced *E. coli* K12; lanes 3 and 4, total cellular extracts from induced bacteria containing pMAL^TM-c2X / HdGSTO1 and pMAL^TM-c2X / HdGSTO2, respectively; lanes 5 and 6, the purified recombinant HdGSTO1 and HdGSTO2 respectively.
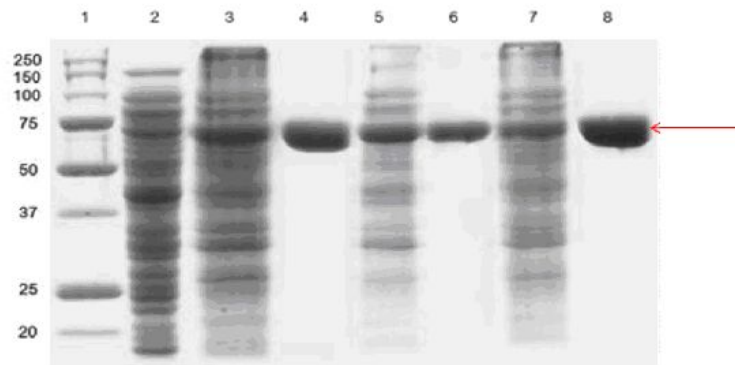
Fig.4-3: SDS–PAGE analysis of the recombinant HdGSTS1, HdGSTS2 and HdGSTS3. Lane 1, molecular mass markers with the sizes shown on the left in kilodaltons; lane 2, total cellular extract from *E. coli* K12-Tb1; lanes 3, 5 and 7, total cellular extracts from induced bacteria containing pMALTM-c2X/HdGSTS1, HdGSTS2 and HdGSTS3, respectively; lanes 4, 6 and 8, the purified recombinant HdGSTS1, HdGSTS2 and HdGSTS3 respectively.
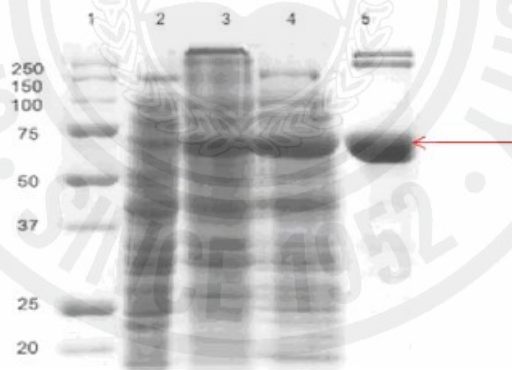
Fig.4-4: SDS–PAGE analysis of the recombinant HdGSTR1. Lane 1, molecular mass markers with the sizes shown on the left in kilodaltons; lane 2, total cellular extract from uninduced *E. coli* K12-Tb1; lanes 3, total cellular extracts from induced bacteria containing pMALTM-c2X/HdGSTR1; Lane 4, the soluble protein from induced bacteria; lanes 5, the purified recombinant HdGSTR1.

2.2. Recombinant expression

Seven expression vectors encoding the recombinant GSTs fused with a maltose binding protein tag, were constructed and used for protein over-expression o in the *E. coli*K12 (Tb1) strain. To determine the optimal condition to express abundant soluble protein, a ladder of temperature, cell concentration, IPTG concentration and induction time was tried for induction. Thereafter, the cell lysates were separated into insoluble

(inclusion bodies and cell debris) and soluble fractions, and analyzed by 10% SDS–PAGE (data not shown). Optimal expression was obtained 5after induction with 0.2IPTG at 25°C. The expressed protein band was enriched in the soluble fraction, which contained more than 80% of the expressed protein. The recombinant GST protein was purified from the soluble fraction by affinity chromatography on a 1 cm maltose-affinity amylose column. The apparent molecular mass of the over-expressed protein was about consistent with the predicted value (Fig.4-1~4-4).

2.3 Biochemical characterization of recombinant GSTs

The specific activity measurement result of the recombinant GST towards various substrates is listed in table 2. Generally, the abalone mu class GST, sigma class GST and rho class GST have specific activies only towards CDNB and ECA. Whereas, omega GSTs have only two omega class specific activities of DHA reductase and thioltransferase.

The catalytic activity of HdGSTM1 was highest for CDNB as 0.172±0.010 μmol/min/mg. In addition, it also catalyzed the conjugation of ECA (0.114 ± 0.003 μmol/min/mg), a specific substrate for mammalian pi and alpha classes GSTs. However, there was no detectable activity toward DNCB, which is proposed to be catalyzed by mu class GSTs specifically. The activity of recombinant HdGSTM1 was

broadly optimal between pH 6.5 and 9.0, at which it showed over 70% of maximum activity towards CDNB (Fig.5-1). In contrast, the rage of optimal temperature of recombinant HdGSTM1 was narrow, which was only between 30 $^{\circ}$C and 40 $^{\circ}$C (Fig. 5-1). The recombinant HdGSTM1 was relatively stable during incubation at temperatures below 30 $^{\circ}$C and a pH between 5.0 and 9.0 (Fig. 5-3). The enzyme kinetics assays was done at various concentrations of GSH and CDNB. At fixed CDNB concentrations, the K_m and V_{max} values for GSH were 0.734 ± 0.053 mM and 0.276±0.002 µmol/min per mg protein, respectively. At fixed GSH concentrations, the K_m and V_{max} values for CDNB were 2.721 ± 0.236 mM and 0.365±0.021 µmol/min per mg protein, respectively (Table. 3).

Four typical GST substratesof CDNB, DCNB, ECA, 4-NBC and 4-NPB was used in the reaction of two omgea GSTs at their appropriate conditions, however, neither enzyme showed detectable activity (Table.2). In contrast, the dehydroascorbate reductase (DHAR) and thioltransferase (TTase) activities were observed in HdGSTO1 and HdGSTO2. The reaction containing all reagents without glutathione was also carried out and no catalytic activity had been detected, indicating these non-typical GST activity was glutathione dependent. This enzymatic property was similar to three yeast omega GSTs (Garcera, Barreto et al. 2006). Between two abalone omega GSTs, the catalytic capabilityas DHAR and TTase showed a big difference that the activity of HdGSTO1 was much higher, suggesting that HdGSTO1 might play a more important role in abalone antioxidant system. In most cases, omega GSTs showed little or no GSH-conjugating activity towards standard GST substrates. Instead, they catalyze the GSH dependent reduction of protein disulfides and dehydroascorbate which are more characteristic of glutaredoxins. Additionally, the comparison of crystal structure of glutaredoxin and omega GST revealed a high similarity of their manners to bound glutathione molecular, which was supposed to be the main reason for

similar activity property. Although there are overlappings of both structure and function, it is not difficult to discriminate omega GST from glutaredoxin and some DHAR, since omega GSTs have significantly higher molecular weights and longer peptide sequences than DHAR. It is clear that these two abalone cDNA clone should be classified into omega GST family. Due to lack of activity to common GST substrates, the assays associated with enzymatic optimum pH, optimum temperature, and kinetic parameters were determined by DHAR assay. Only HdGSTO1 obtained satisfied result. It showed a maximum DHAR activity at pH 8.0 and an optimum temperature of 25 ^{o}C (Fig. 5-2). Both abalone omega GSTs were sensitive to high temperature and low pH, appearing lots of precipitate when temperature reached to 50 ^{o}C or pH reduced to 2. The kinetics assay was done at various concentrations of GSH and DHA. At fixed DHA concentrations, the K_m and V_{max} values for GSH were 1.028 ± 0.05 mM and 1.23 ± 0.13 μmol/min per mg protein, respectively. At fixed GSH concentrations, the K_m and V_{max} values for DHA were 0.509 ± 0.02 mM and 1.62 ± 0.11 μmol/min per mg protein, respectively (Table.4), exhibiting high specificity toward DHA.

The specific activities of three recombinant sigma GSTs towards vary substrates were measured (Table.2). Both HdGSTS1 and HdGSTS2 displayed detectable activities towards 1-Chloro-2, 4-dinitrobenzenel (CDNB) and ethacrynic acid (ECA). In contrast, HdGSTS3 failed to show catalytic ability towards any substrates in our test. Thereafter, the test of pH and temperature effect was carried out only in HdGSTS1 and HdGSTS2 using CDNB as substrate (Fig.5-1). Two abalone sigma GSTs exhibited narrow optimum pH between 8.0 and 9.0. Compared to HdGSTS1, HdGSTS2 had a more broad optimum temperatures of between 20 ^{o}C and 45 ^{o}C, in which maintaining more than 60% maximum activity towards CDNB.Two abalone GSTs shared a similar optimum catalytic condition of 30 ^{o}C and pH 8.0

approximately.

Rho class GST HdGSTR1 exibited similar enzymatic features with mu and sigma class GST in spite of the different classcifications. It showed the highest activy toward CDNB and ECA in all abalone GSTs (Table.2). Compared to other GSTs, the optimal temperature and pH of HdGSTR1 is a litter more necessary, same as the other rho class GST from red sea bream (Konishi, Kato et al. 2005). It showed highest catalytic ability at 25 $^{\circ}$C and pH of 8.0, beyond which, the activity was reduced dramatically (Fig.5-1).

Table.2: Specific activity of abalone GSTs towards different substrates. ND, not detectable.

Substrate	Class	Specific activity (μmol/min/mg protein)						
		HdGSTM1	HdGSTR1	HdGSTO1	HdGSTO2	HdGSTS1	HdGSTS2	HdGSTS3
CDNB	Over all class	0.172 ± 0.01	2.73 ± 005	ND	ND	0.17 ± 0.01	1.06 ± 0.02	ND
DCNB	Mu	ND	ND	ND	ND	ND	ND	ND
ECA	Alpha & Pi	0.114 ± 0.01	0.35 ± 0.03	ND	ND	0.18	0.25	ND
4-NBC	Mu & Theta	ND	ND	ND	ND	ND	ND	ND
4-NPB	Theta	ND	ND	ND	ND	ND	ND	ND
DHA reductase	Omega	ND	ND	1.18 ± 0.01	0.05 ± 0.005	ND	ND	ND
Thiol transferase	Omega	ND	ND	2.59 ± 0.01	0.19 ± 0.01	ND	ND	ND

Table.3. Kinetic constant values for the recombinant HdGSTM1 using CDNB and GSH.

Substrate	K_m(mM)	V_{max} (μmol/min per mg)	K_{cat} (min^{-1})	k_{cat}/K_m (mM/min)
GSH	0.734±0.053	0.276±0.020	18.63	25.38
CDNB	2.721 ±0.236	0.365 ±0.031	24.64	9.05

Table.4: Kinetic parameters of the recombinant HdGSTO1 using GSH and DHA as substrates.

Substrate	K_m(mM)	V_{max} (μmol/min per mg)	K_{cat}(min^{-1})	k_{cat}/K_m (mM/min)
GSH	1.028 ± 0.05	1.23 ± 0.13	85.8	83.5
DHA	0.509 ± 0.02	1.62 ± 0.11	109.8	215.8
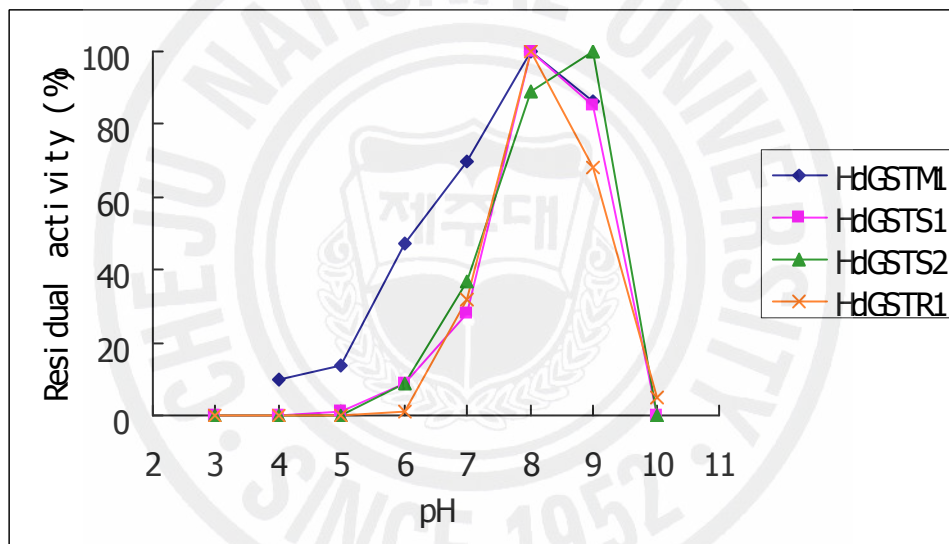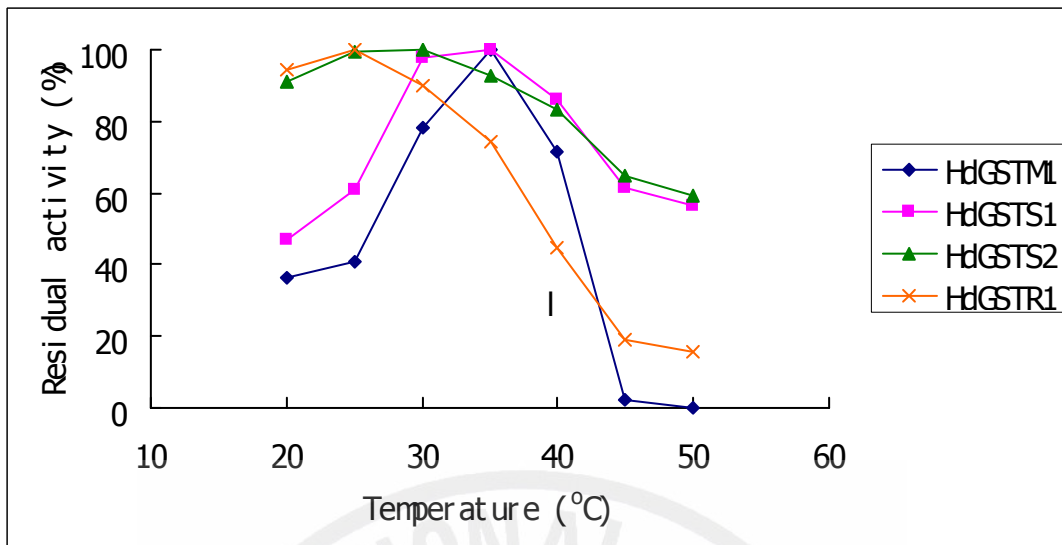
Fig.5-1: Temperature and pH effect on recombinant GSTs activity using CDNB as substrate.
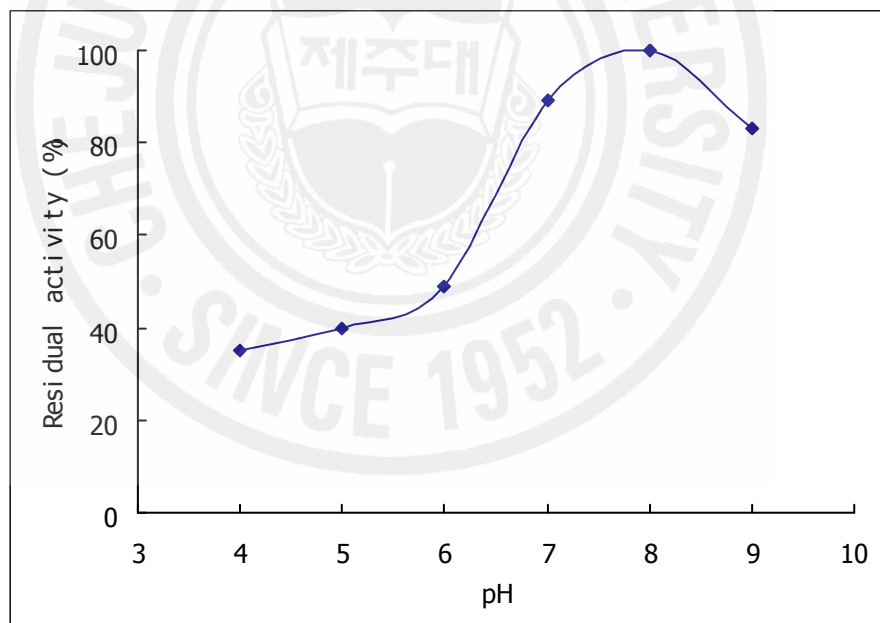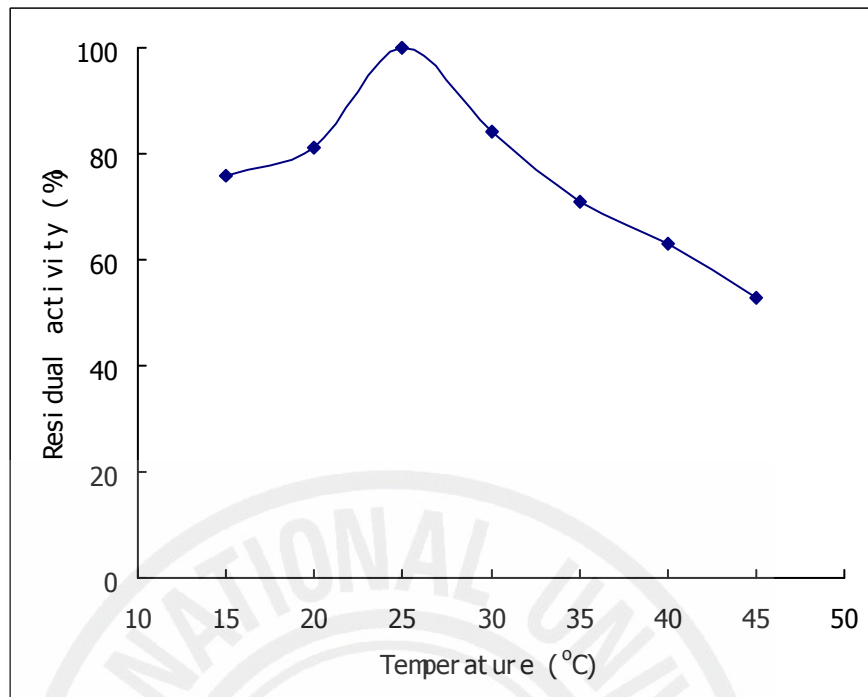
Fig.5-2: Temperature and pH effect on catalytic activity of HdGSTO1 using DHA as substrate.
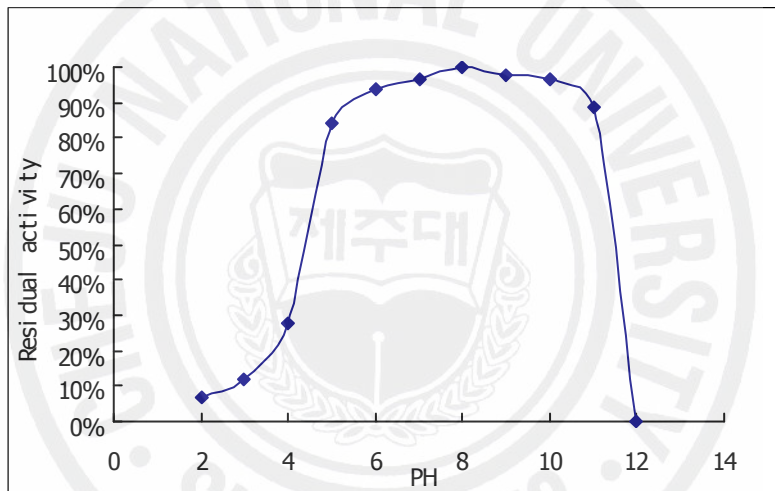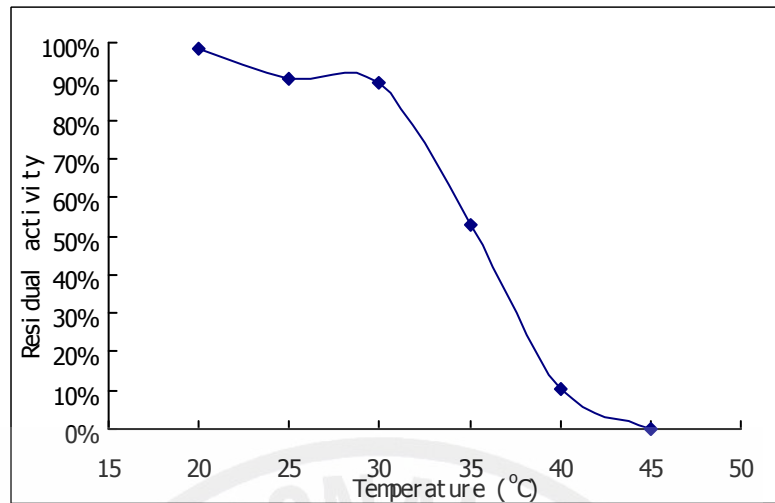
Fig.5-3: Heat and pH stability of recombinant HdGSTM1.

2.4. Molecular modeling and active sites analysis

The three-dimensional structure of HdGSTM1 complexed with glutathionyl-s-dinitrobenzene (GS-DNB) was generated on the basis of the X-ray structure of human GSTM1-1 complexed with GS-DNB (Fig.6-1). HdGSTM1 shares 49% identity with the template GST sequence. A Ramachandran plot statistic showed that 88% of residues were in the most favored regions and 97% of residues were in the allowed regions; and superimposition of alpha carbon backbones gave a root-mean-square-deviation (RMSD) of 0.10 for N-terminal domain and 0.11 for C-terminal domain. These values ensured the high quality of this structure model and a practicability of further structural analysis. The monomer of HdGSTM1 showed a typical GST folding pattern, appearing to consist of two spatially distinct domains: a small thioredoxin-like N-terminal domain and a larger helices rich C-terminal domain. The N-terminal domain (residues 1 to 82) comprises a $\beta\alpha\beta$ motif (β_1, α_1 and β_2), a $\beta\beta\alpha$ (β_3, β_4 and α_3) motif and a small α helix linker (α_2) between them. The residue Tyr-6 on β_1 is considered as an important catalytic site which conserves in N-terminus of most class GSTs, though with a little variation in positions (Reinemer, Dirr et al. 1991). Fig.6-1 also showed the schematical localization of seven conserved residues (Tyr-6, Trp-45, Pro-57, Asn-58, Leu-59, Pro-60 and Gln-71) around the GSH molecule in the G-site of HdGSTM1. It revealed that the distance between phenolic hydroxyl group of Tyr6 and the sulphydryl group on GSH was only 3.59 angstrom, appearing a hydrogen bond forming. The tyrosine can play a role as hydrogen bond acceptor (S-H$^{...}$O-Tyrosine) to remove the proton of sulphydryl and increase nucleophilicity of sulfur atom (Reinemer, Dirr et al. 1991). Consequently, the covalent addition between S atom and the electrophilic site on xenobiotic substrate will be accelerated greatly. On the contrary, a replacement of tyrosine would result in at least 10 folds decreasing of enzyme efficiency (Liu, Zhang et al. 1992).

Besides, the residues Trp-45, Pro-57, Asn-58, Leu-59, Pro-60 and Gln-71 also showed interactions with the carboxylate group of the glutamyl and glycine moiety of glutathione molecule, appearing to contribute significantly to binding the GSH molecule onto GST. In the C-terminal domain (residues 90 to 215) there were seven right-hand spiral helices (α_4 – α_{10}), with a number of hydrophobic residues forming a hydrophobic pocket to bind xenobiotic compound. The main contacts between the enzyme and the ligands are Van der waals force. According to the structure model, it revealed that only Met-104 and Val-111 in C-terminal domain and Leu-12 in N-terminal domain contributing the interactions between HdGSTM1 and the dinitrobenzene ring of CDNB. Thus, these three residues were supposed to be the important components of H-site. In addition, it is noteworthy that the residues Arg-11, Leu-19, Leu-20, Pro-60, Gln-71, Ile-75, Asp-97, Asp-105, Tyr-115, Gly-149, Leu-163 and Arg-186, which were conserved within mu class GST, were proposed to determine dimmer conformation, structure stability and stereoselectivity of GST. Replacing these residues will diminish enzyme activity or enhance sensitivity to inhibitor, though they were not the direct binding sites (Ji, Zhang et al. 1992; Dirr, Reinemer et al. 1994).

The three-dimensional structures of HdGSTO1 and HdGSTO2 were predicted on the basis of the X-ray structure of human omega GSTO1-1 (PDB 1eeMA) (Fig.6-2). HdGSTO1 and HdGSTO2 shared sequence identity of 42% and 40% with the template, respectively. To determine the accuracy of modeling structures, a Ramachandran plot statistic was assayed and showed that 97.0% and 94.4% of residues were in the allowed regions, 89.8% and 83.7% of residues were in the most favored regions, ensuring the high quality of the structure models. The superimposition of alpha carbon backbones gave root-mean-square-deviation (RMSD) of 3.17 for full-length sequence of HdGSTO1, however, aRMSD of 5.92 for

HdGSTO2, showing a little high divarication between the HdGSTO2 and template. Whereas the conservation of major active-sites, it was still practicable to do further structural analysis on the basis of this modeling structure. Both of the monomers of HdGSTO1 and HdGSTO2 consisted of two spatially distinct domains: a small thioredoxin-like N-terminal domain and a larger helices rich C-terminal domain. The N-terminal domain (residues 1 to 91) comprises four stranded β sheets and three α helices. In N-terminus of each structure model, an extending coil structure formed by the first 19 residues, which is the distinct structure of omega GSTs, was identified. Omega GSTs therefore showed approximately 20 residues longer polypeptide chains than other classes. C-terminal domain of HdGSTO1 consisted of seven helices, similar to the template, whenas HdGSTO2 lacked of the last helix α_{10}. Among the known GST classes, mu class and pi class GSTsshowed a prevalence of six helices in C-terminal domain (Ji, Tordova et al. 1997; Sun, Kuan et al. 1998). Nevertheless, the helix α_9 and C-terminal tail of HdGSTO2 folds back over the top of the N-terminal domain, appearing a structure apart from other class GSTs but similar to human omega GSTs (Whitbread, Tetlow et al. 2003).

Three-dimensional structures ofthree abalone sigma GSTs were generated on the basis of the X-ray structure of drosophilia sigma GST (GenBank NP_725653) complexed with GSH (PDB No.1m0uA) (Fig.6-3).Three target sequences showed less than 40% identity with template. Nevertheless, a Ramachandran plot statistic showed that 89.0 % residues of HdGSTS1, 89.1 % residues of HdGSTS2 and 89.7 % residues of HdGSTS3 were in the most favored regions, and more than 98.0 % of residues in three sequences were in the allowed regions as well. Additionally, the test of alpha carbon backbones superimposition gave three values of root-mean-square-deviation (RMSD)of 0.16, 0.17 and 0.17, respectively for three models. All above analysis ensured the high quality of three structural models and practicability of further

structural analysis. Only monomers were modeled in our study. Similar to other cytosolic GSTs, three sigma class GSTs from disk abalone consisted of a conserved N-terminal domain with βαβαββα structural motif and an all-α helices C-terminal domain. In the N-terminal domain, three abalone GSTs shared the same GSH catalytic site of tyrosine-8 as other sigma GSTs, which plays a role as hydrogen bond acceptor (S-H⋯O-Tyrosine) to remove the proton of sulphydryl and increase nucleophilicity of sulfur atom in glutathione (Habig, Pabst et al. 1974; Ji, Johnson et al. 1994). In addition to tyrosine-8, the x-ray crystallographic data of drosophila GST-2 reveal that there are several other amino acid residues (L60, W85, Q96, M97 and S110) contacting with glutathione molecule closely by hydrogen bonds, to constitute G-site (glutathione binding site). The corresponsive residues in three abalone sigma GSTs are R14, F39, Q50, I51 and S64 in HdGSTS1; F14, Y39, Q50, M51 and S64 in HdGSTS2; and V14, W39, Q50, V51 and S64 in HdGSTS3, showing varietyin three sites: 14, 39 and 51 (Fig.6-3). It is believed that the alteration of F39W in HdGSTS1 would result in the lack of one hydrogen bond formed between residue-14 and carboxylate group in glutathione. Similarly, the alterations of I51M in HdGSTS1 and V51M in HdGSTS3 would influence the formation of hydrogen bond as well. Consequently, two sigma GSTs lack of the capability to bind glutathione and exhibited much lower activity than HdGSTS2 and drosophila GST-2. On the contrary, the alterations in residue-14 among three sigma GSTs have not changed the property of amino acid residues, thus it would not contribute to the different enzymatic features.

In contrast to the highly conserved N-terminal domains with identities range between 55% and 75%, C-terminal domains of three sigma GSTs showed much variable with less than 30% sequence similarity to each other. Therefore, the components of H-site (hydrophobic binding site) of three GSTs are significantly different as well. As

shown in crystal structure, the hydrophobic pocket of drosophila GST-2 was formed by the top sections of helices α4 and α6, the loop connecting β1 and α1 and the C terminus of the protein (Singh, Coronella et al. 2001). The residues of V57, L60, R145, A149, Y153, Y208, Y211 and Y249 performed as putative H-site of drosophila GST-2. The corresponsive residues of three abalone sigma GSTs were shown in Fig.8-B. The variable H-site could be also a crucial factor resulting in different catalytic abilities. Three sigma GSTs showed a deletion of residue corresponsive to Y211 of drosophila GST-2 in multiple alignment and structural models, however, some other residues would take the place in real crystal structures. In addition to the contributions in direct binding to electrophiles, R145 and Y208 in drosophila GST-2 also participates in formation of a water-mediated hydrogen bond to reduce the flexibility of hydrophobic pocket. In three abalone sigma GSTs, it shows a prevalence of lysine in residue-163 instead of tyrosine in residue-208 of drosophila GST-2 which provides hydrogen oxygen to form hydrogen bond. Additionally, three abalone sigma GSTs show deviations in the other hydrogen bond donor residue-99 that phenylalanine, isoleucine and asparagines replace the arginine in drosophila GST-2, respectively, suggesting different stabilities of hydrophobic pocket, hence resulting in different catalytic abilities. Fig. 6-5showed the potential electrostatic surfaces of three abalone sigma GSTs. Both HdGSTS1 and HdGSTS2 form largely open hydrophobic cavities which are essential to bind the hydrophobic moiety of the electrophilic co-substrates. Oppositely, the pocket of HdGSTS3 is more tight and hydrophilic, revealing a weak catalytic capability, by comparison. Whereas, three abalone pockets were significantly different from the one in drosophila GST-2, which processes a much flatter topography. The residues from N-terminal loop and C-terminal tail of three abalone sigma GSTs form a ceiling of each pocket.

Rho class GSTs are a group of newly termed GSTs, which were only found in

several marine fish. Therefore, the information and reference of rho GSTs are relatively few. So far there is no crystal structure of rho class GST has been establised, thus, the predicted three-dimentional structure of HdGSTR1 might be unreliable. Our strucutre model is lack of the N-terminal region which contain the important GSH-binding sites. Consequently, the active site analysis of HdGSTR1 was failed to carried out.
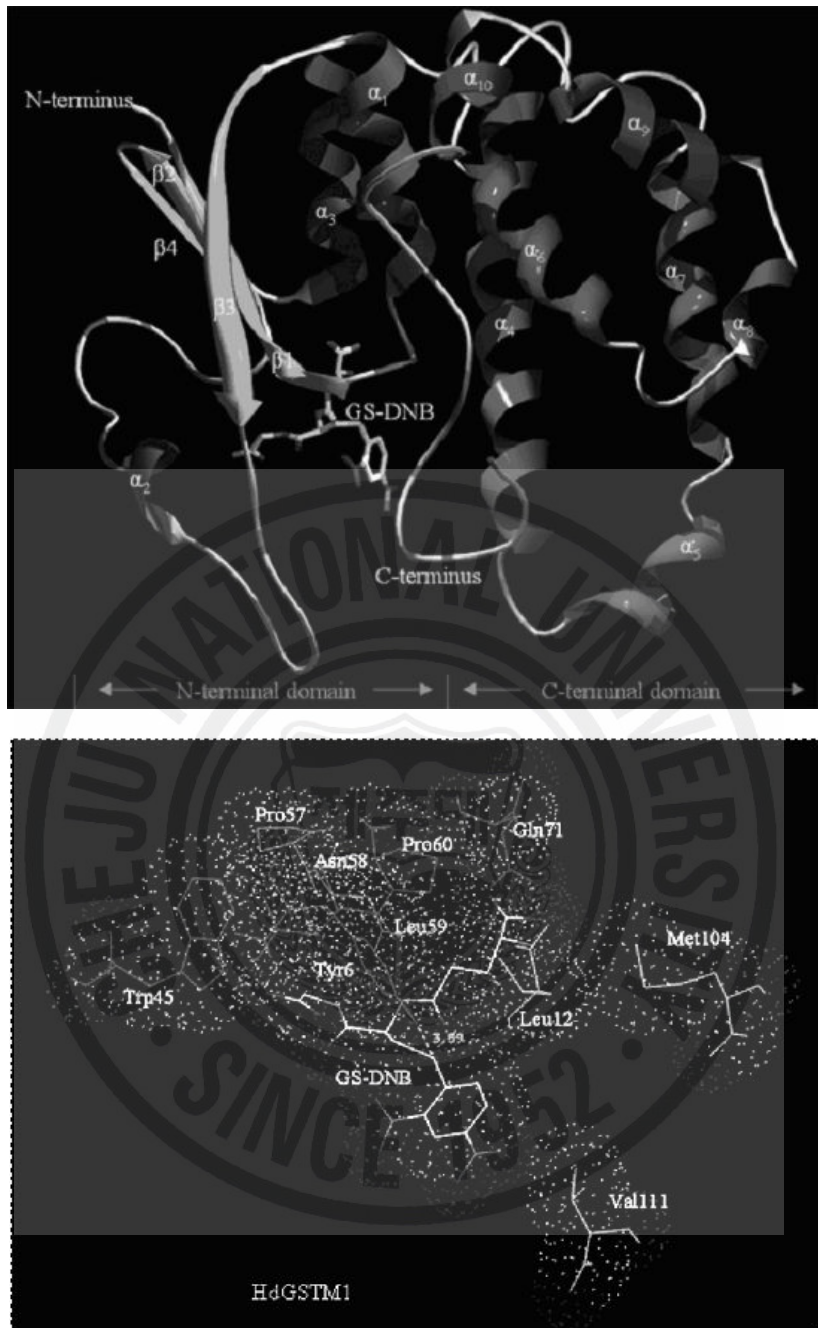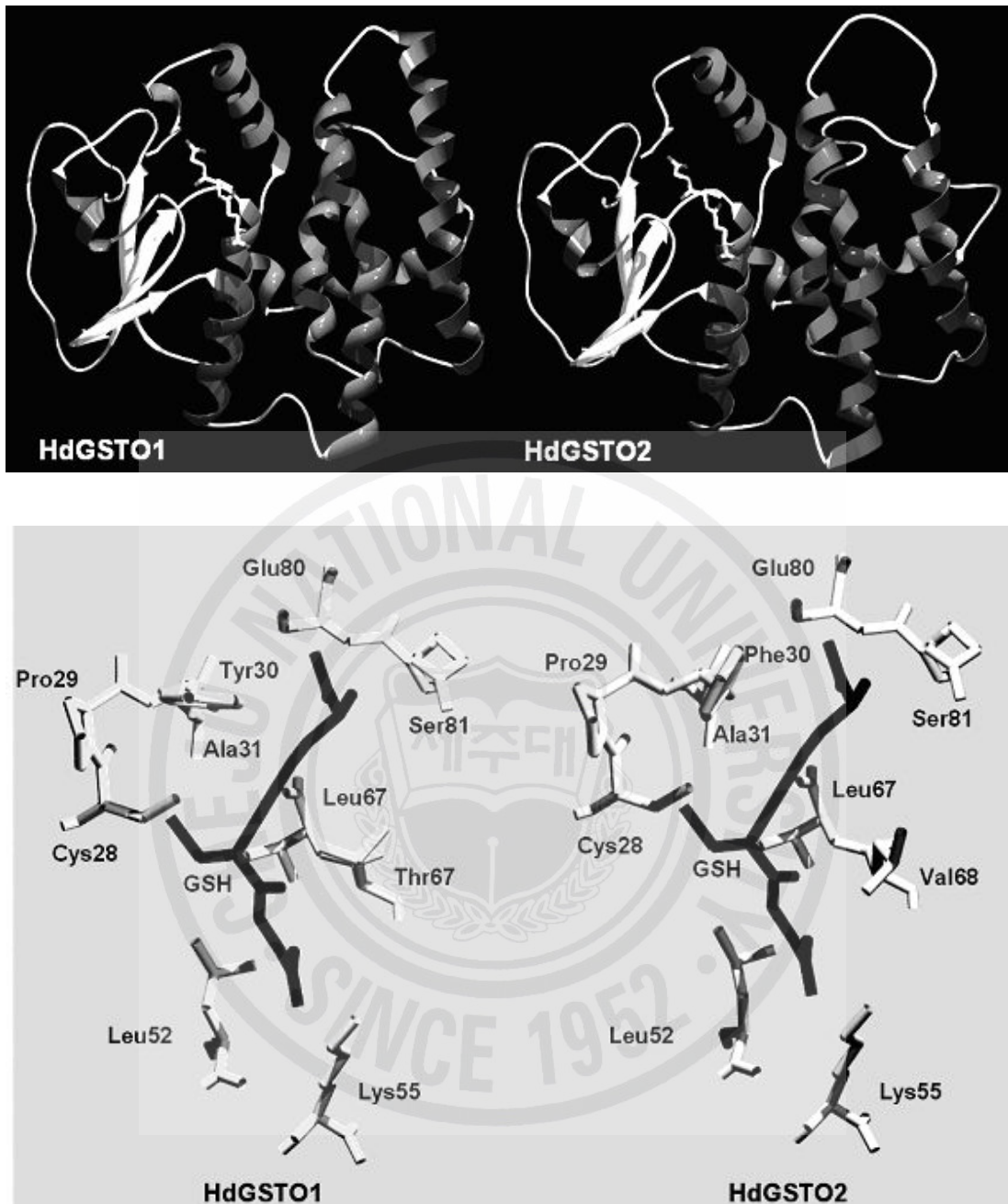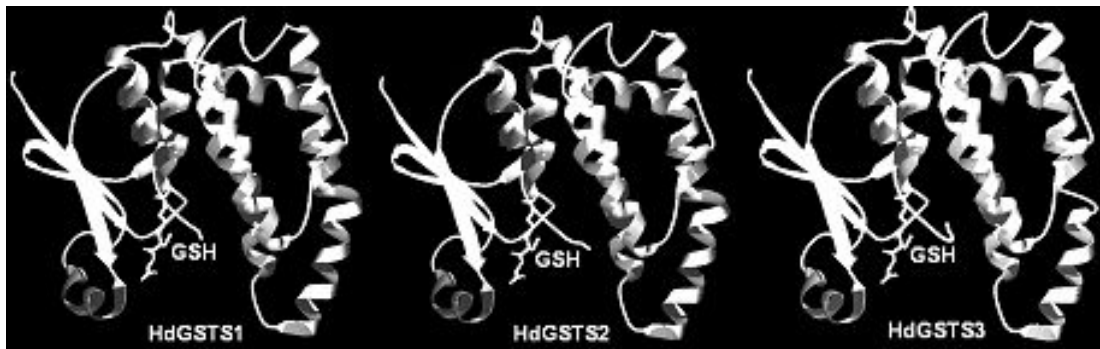
Fig.6-1 Predicted three-dimensional structure and location of glutathione binding sites and hydrophobic binding sites of HdGSTM1.
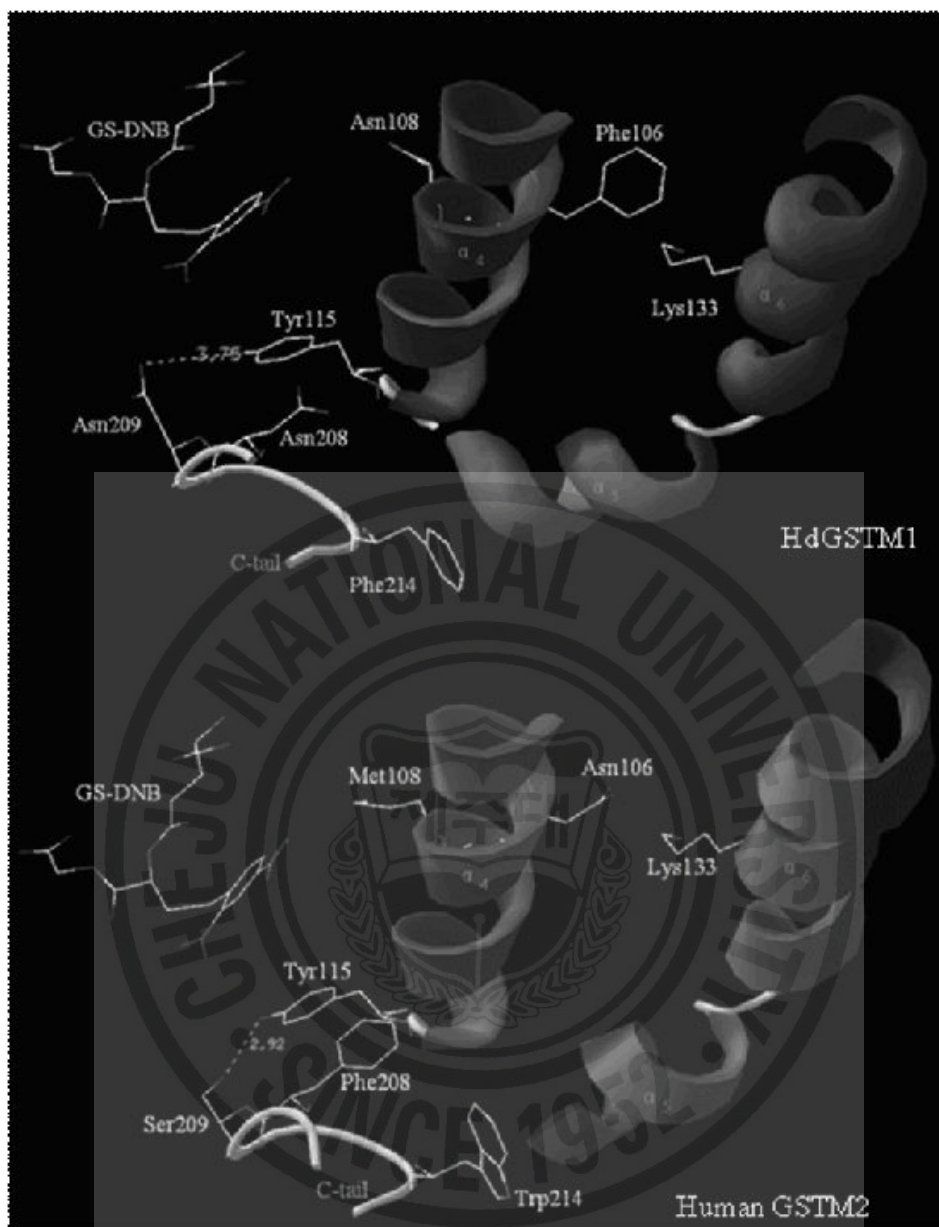
Fig.6-2: Comparison of hydrophobic binding region in HdGSTM1 and Human GSTM2.

Fig.6-3: Homology modeling structures and putative glutathione binding sites (G-sites) of HdGSTO1and HdGSTO2.

Fig.6-4: Homology modeling structures and putative glutathione binding sites (G-sites) of HdGSTS1, HdGSTS2 and HdGSTS3.
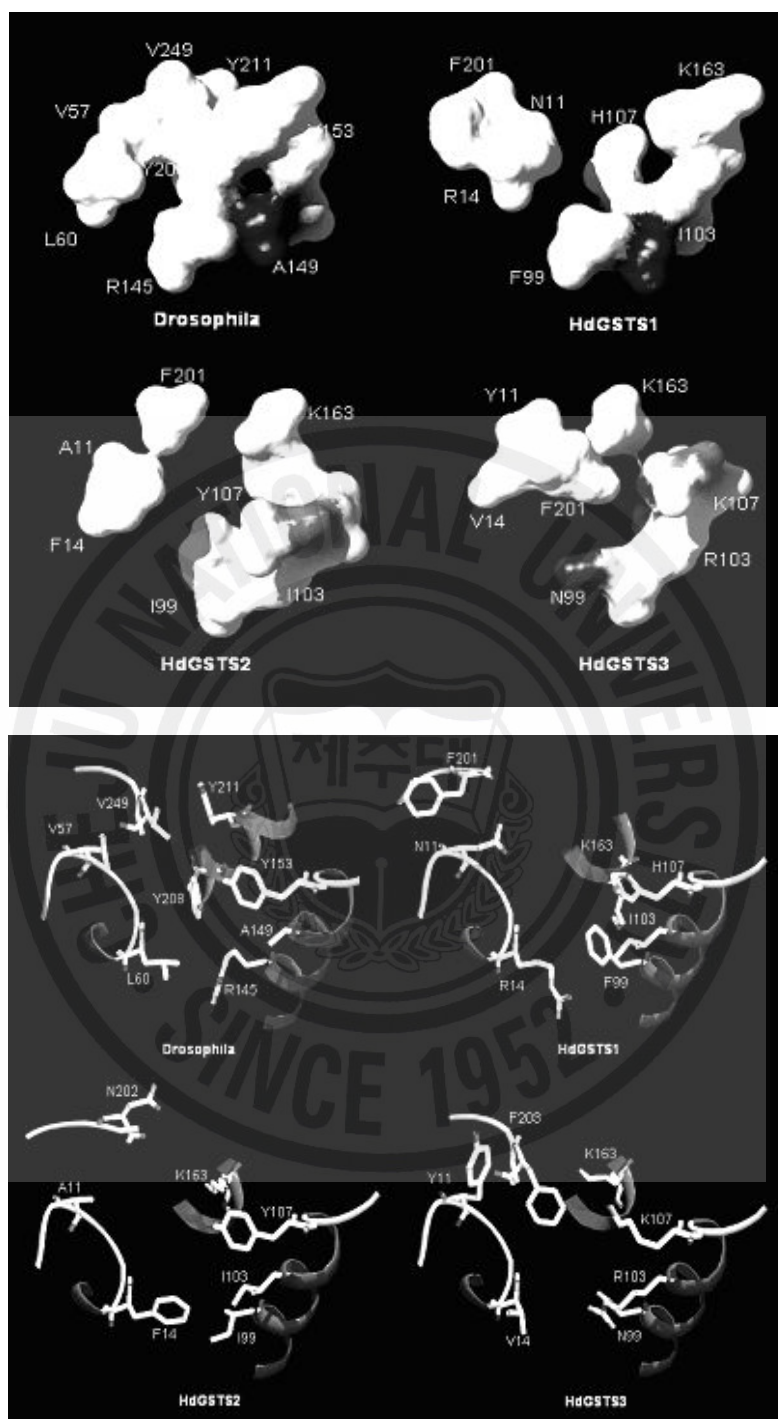
Fig.6-5: Comparison of component and potential electrostatic surfaces of hydrophobic pockets in three abalone sigma GSTs and drosophila GST-2.

Fig.6-6: Homology modeling structure of HdGSTR1.

2.5 Tissue distribution of GST transcripts in disk abalone

Five tissues included both outer (gills, mantle and foot) and inner (gonad and digestive tract) organ origins were examined by semi-quantitative RT-PCR. The intensity of the amplified products was normalized using β-actin cDNA as internal control. The comparison of relative values were showed as bar graphic (Fig.7). The mRNA of HdGSTM1, HdGSTO1 and HdGSTS1 were detected in all above tissues (Fig.7-1, 7-2 and 7-3), revealing the housekeeping-like roles in disk abalone. Among all the examined tissues, HdGSTM1 showed highest transcription level in the tissue of gills and gonad. On the contrary, there were much fewer transcripts in mantle and foot. And the tissue of digestive tract (comprised of both stomach and intestine) displayed a moderate abundance among all tissues examined. HdGSTO1 mRNA distributed in all tested tissues averagely (Fig.7-2). However, high level HdGSTO2 transcripts were only found in gonad and gills, with much lower level in digestive tract and foot, and no signal in mantle.Three sigma GSTs exhibited significantly different tissue specificities of expression (Fig.7-3). HdGSTS1was ubiquitously distributed in tissues of disk abalone in low expression levels, which is only approximately 3% of β-actin abundance. The highest abundance of HdGSTS1 transcripts were found in three tissues of gonad, foot and eye/eyestalk, without significant difference. Expression of HdGSTS2 was very high in the gills and moderatein the tissue of digestive tract but relatively low in the mantle, gonad, foot and eye/eyestalk. HdGSTS3 performed a high expression level in foot and digestive tract, showing approximately 4 times higher than those ofthe other two sigma GSTs. In the tissue of eye/eyestalk of disk abalone, there was only HdGSTS1 showing observable expression.

Interesting, rho GST HdGSTR1 showed a very similar expression pattern as HdGSTM1, specifically expressed in gill, gonad and digestive tract (Fig.7-4).
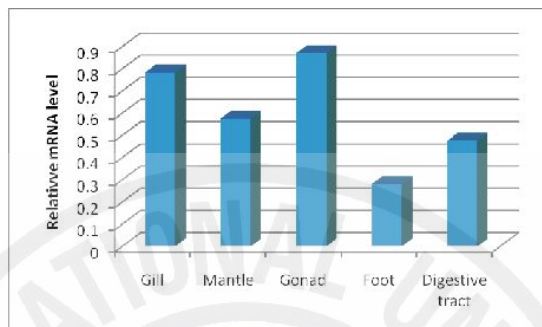
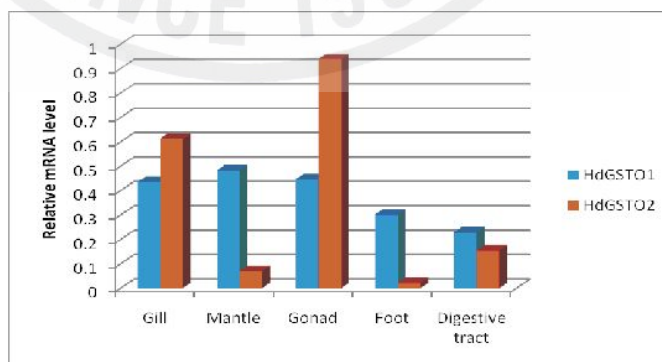Fig.7-1: Distribution of HdGSTM1 mRNA transcripts in disk abalone tissues

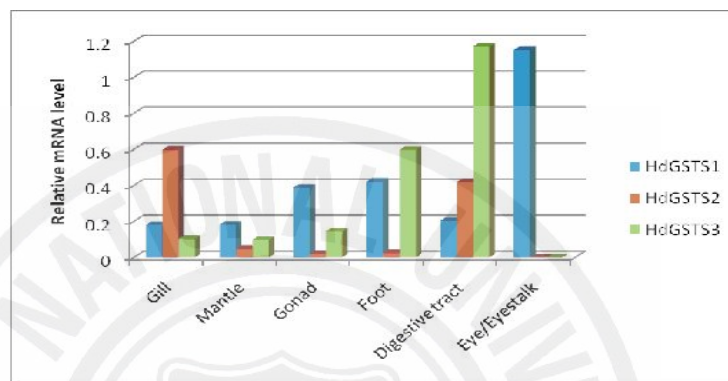**Fig.7-2:** Distribution of two omega GSTs mRNA in various disk abalone tissue

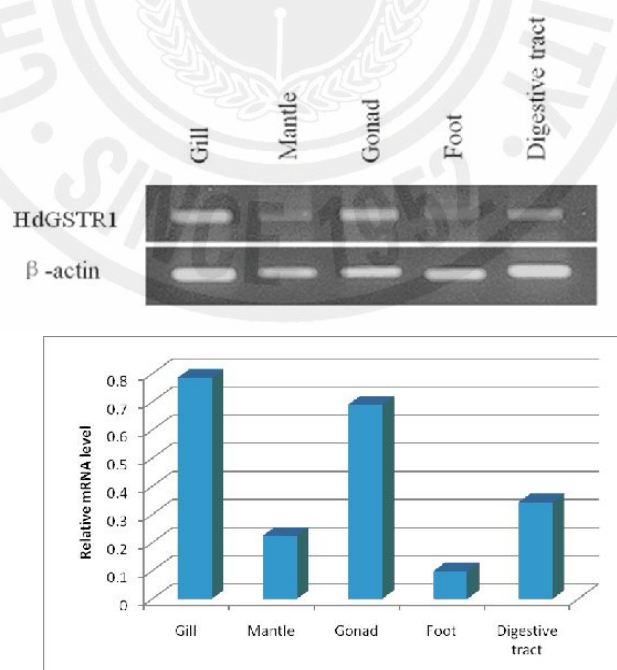Fig.7-3: Semi-quantitative analysis of three abalone sigma GSTs expression in various tissues.

Fig. 7-4: Tissue expression profiles of rho class GST HdSGSTR1.

**2.6 Semi-quantitative analysis of inducible expression of seven GSTs after EDCs exposure**

In orther to apply seven GSTs as a biomarker of marine pollution, mRNA levels of seven GSTs from abalone gills and digestive tract were investigated after exposure of three endocrine-disrupting chemicals at two different concentrations using semi-quantitative RT-PCR (Fig.8-1~8-4). The ribosomal protein gene was used as the internal control to normalize the quantity of each GST transcripts, since the mRNA levels of β-actin, one of the most usually used housekeeping gene, were also significantly regulated during treatment (data was not shown). After 48 hrs incubation with two concentrations of a PAH-type chemical β-naphthoflavone (0.1 and 1 μM), a PCB-type chemical aroclor-1254 (5 and 50 ppb) and a TBT-type chemical tributyltin chloride (0.1 ppb and 1 ppb), respectively, mRNA levels of HdGSTM1 were significantly higher in both gills and digestive tract than that in vehicle-exposed controls. In gills of abalones exposed to the low dose chemical, normalized mRNA levels of HdGSTM1 showed stronger induction, which were more than 2.5 folds. Following the dose increase of β-naphthoflavone and tributyltin chloride, induction level of HdGSTM1 showed a significant reduction, which might be caused by severe tissue burden under the exposure of highly concentrated toxicants. In digestive tract, the induction profiles showed a little different that it exhibited a dose dependent increase when exposed to β-naphthoflavone. Additionally, approximate 0.5 fold lower induction level was investigated in the treatment of aroclor-1254 compared with that in gills. The response of Rho GST HdGSTR1 to EDCs exposure was different from HdGSTM1. β-naphthoflavon was a poor inducer for HdGSTR1 with two doses. However, it was very sensitive to TBT treatment with about 2 folds induction in both gill and digestive tract. The inducible ability of aroclor-1254 is stronger in digestive tract than in gill for rho GST. Two omgea GSTs exhibited two distinctive

expression profiles. HdGSTO1 was dramatically induced by all three EDCs for higher than 10 folds. However, HdGSTO2 was induced only for no more two folds. For three sigma GSTs, most of the inductions were happened in HdGSTS1 in digestive tract, indicating the key role of HdGSTS1 in protecting digestive system of abalone. However, as the member with highest activity, HdGSTS2 was poorly induced by any treatment. The non-active sigma GST showed a only significant induction in gill when exposed to 1.0 μM β-naphthoflavone. None of three sigma GSTs showed significant induction by either TBT dose exposure.Generally, in the treatment of β-naphthoflavone, a dose-dependent response was found in almost all the GSTs that higher dose β-naphthoflavone would reduced the induction levels.
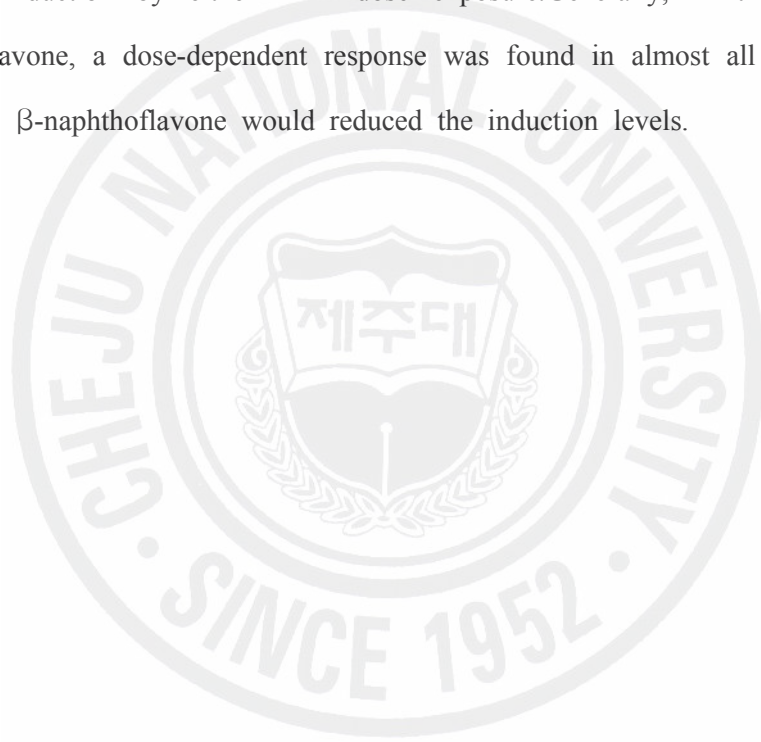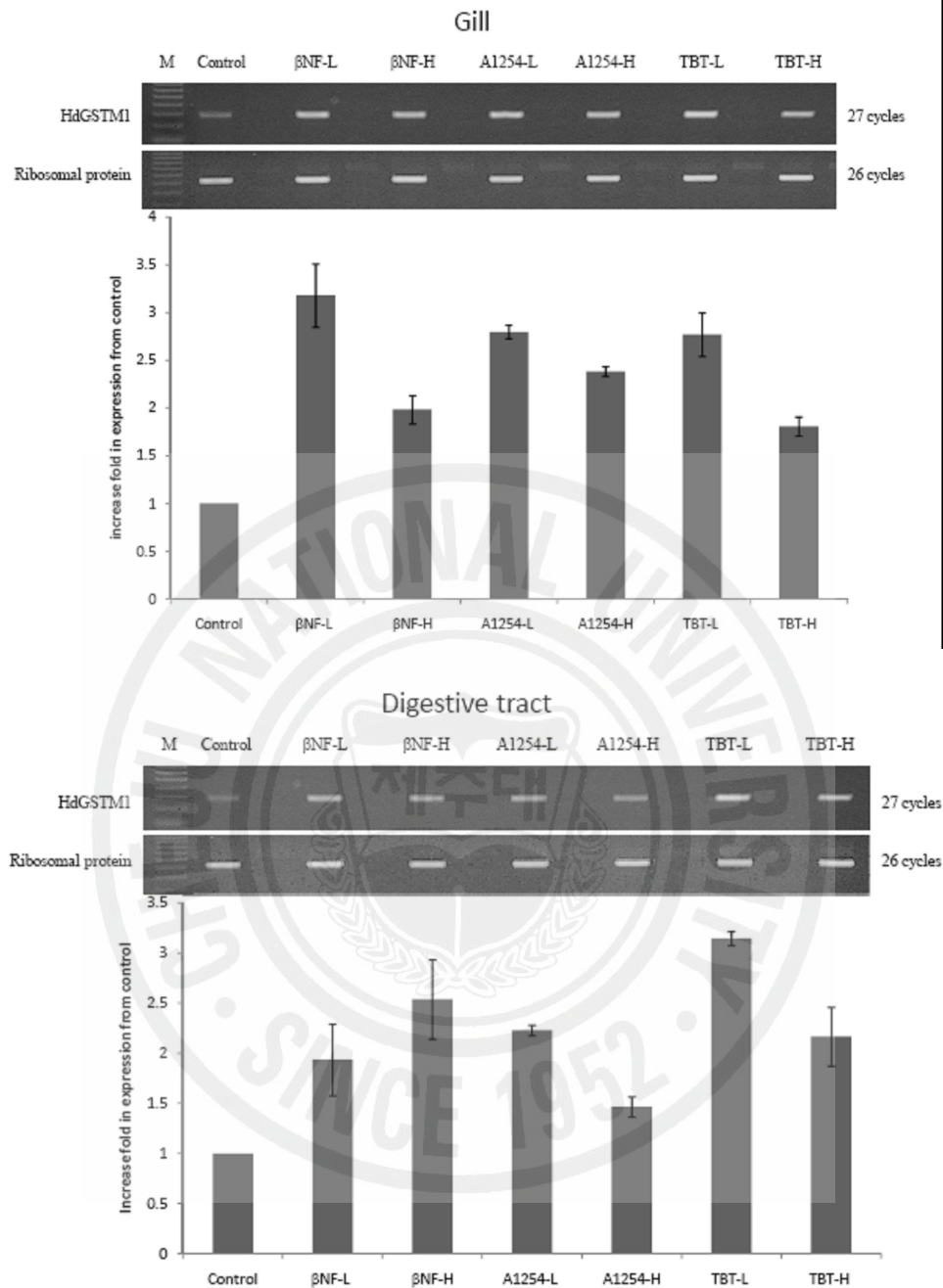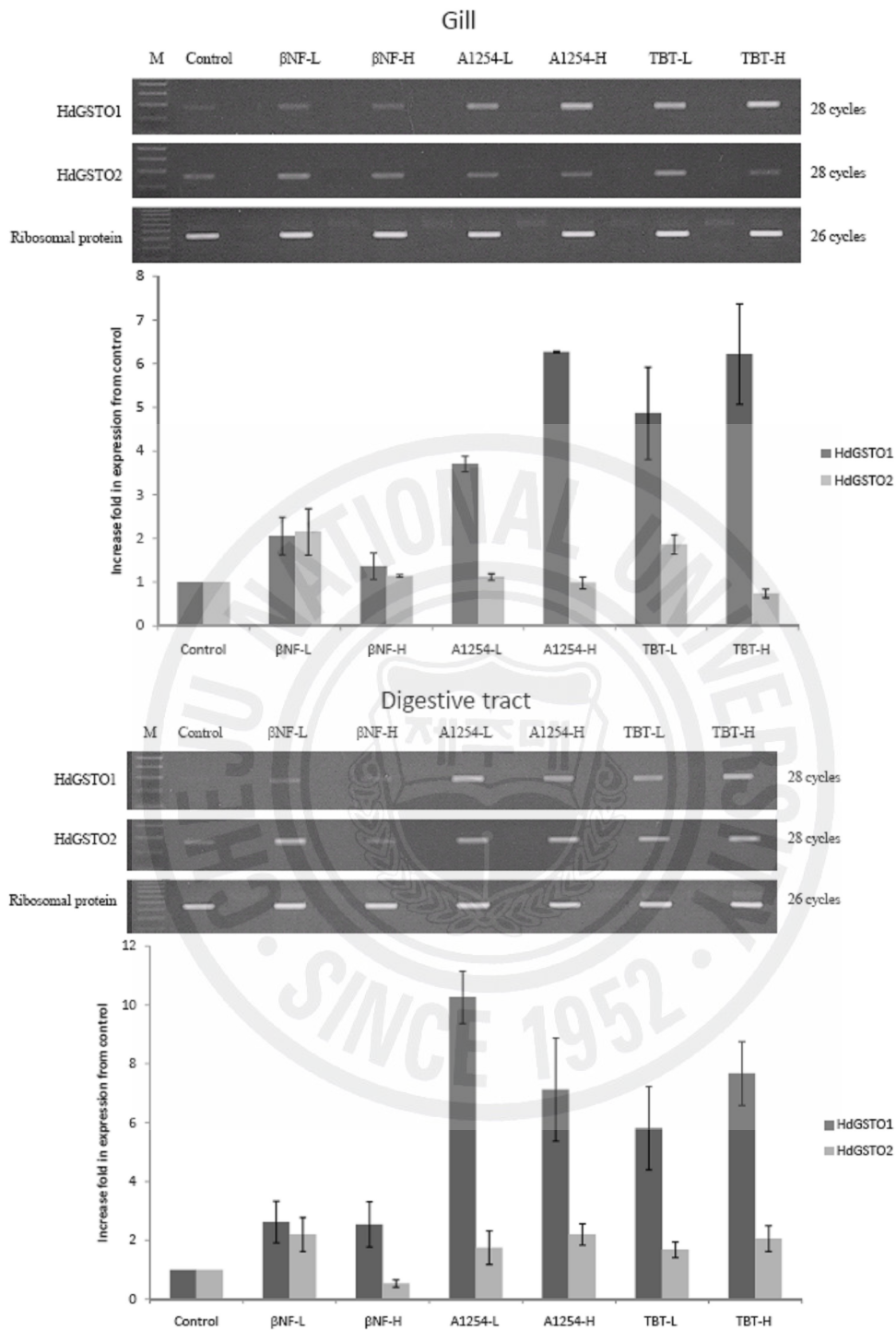
Fig.8-1: Relative HdGSTM1 expression in abalones from control and after 48 hrs exposure to two different doses of three endocrine-disrupting chemicals individually. (βNF-L, βNF-H, A1254-L, A1254-H, TBT-L and TBT-H are β-naphthoflavone 0.1 and 1 μM, aroclor-1254 5 and 50 ppb, and tributyltin chloride 0.1 and 1.0 ppb, respectively. Values are expressed as the mean ± standard deviation of 3 abalones.).
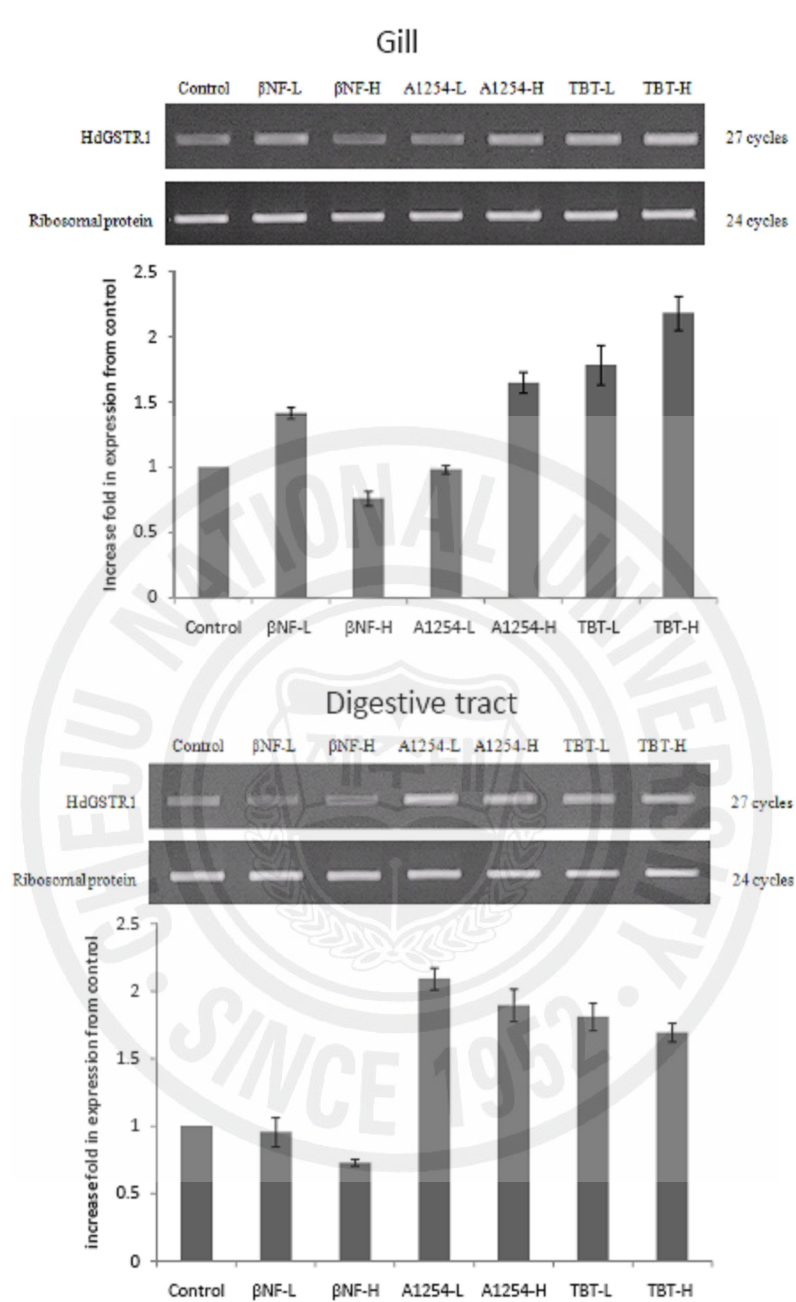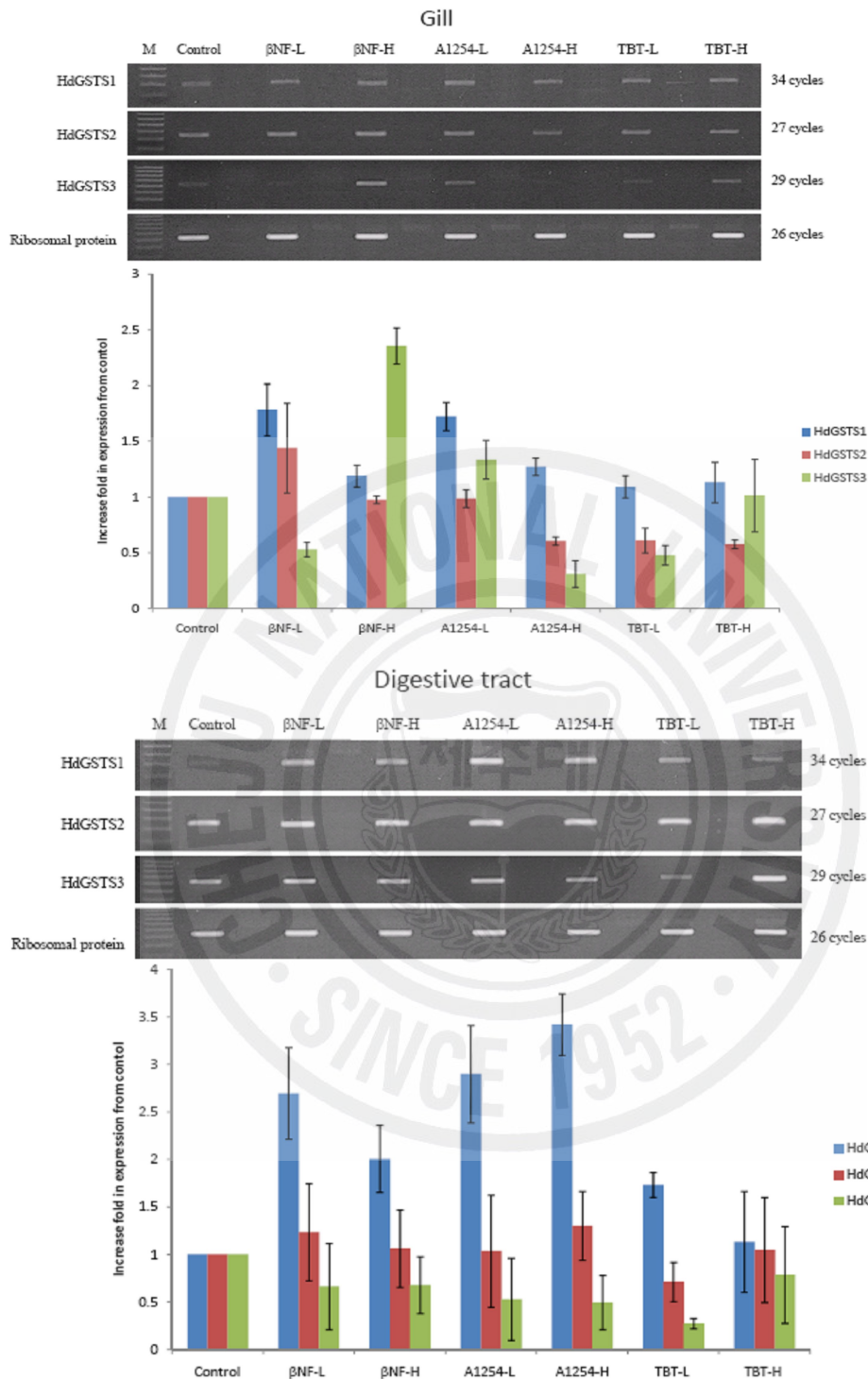
Fig.8-2: Relative HdGSTR1 expression in abalones from control and after 48 hrs exposure to two different doses of three endocrine-disrupting chemicals individually.

Fig.8-3: Relative HdGSTO1 and HdGSTO2 expression in abalones from control and after 48 hrs exposure to two different doses of three endocrine-disrupting chemicals individually.

Fig.8-4: Relative three sigma GST expression in abalones from control and after 48 hrs exposure to two different doses of three endocrine-disrupting chemicals individually.

Ⅳ. DISCUSSION

4.1 Catalytic activity of abalone GSTs

*Haliotis discus discus*is a major species in abalone aquaculture of South Korea, Japan, Taiwan and China. In this study, we cloned, expressed and purified the recombinant protein of seven cDNA clones from *Haliotis discus discus* cDNA library. According to the primary structure analysis of seven GSTs, it was recognized that they are one mu class GST, two omega GSTs, three sigma GSTs and one rho class GST. Among them, mu class GST supposed to have high catalytic activity towards CDNB, a common GST substrate, according to studies in other animals. However, the recombinant abalone HdGSTM1, fused with a 42.5 kDa maltose binding protein (MBP) tag at N-terminal, however, showed much lower activity towards CDNB than other characterized mu class GSTs (Table. 5). In order to ascertain our observation and to exclude the influence of large MBP tag, which might interfere correct folding of protein and formation of catalytic dimmer, we adopted a second expression and purify system. pET-21 plasmid was used to construct the expression vector and express recombinant GST with a six-His-tag. Thereafter, the enzyme assay was carried out in the same condition as previous test, however, showing no significant improvement of activity that the activity towards CDNB increased from 0.17 μmol/min/mg to 0.30 μmol/min/mg at pH 6.5. Consequently, we could conclude that this low catalytic activity is the native feature of HdGSTM1, and it might be an explanation that *Hiliotis discus discus*showed higher mortality than the other mollusks when exposed to tributyltin (TBT) and triphenyltin (Horiguchi 1998). Furthermore, all the species of abalones are sensitive towards heavy metal and organic compounds in the water (Ronald S. Tjeerdema 1996; Horiguchi 1998; Shofer and Tjeerdema 1998; Chou 2005; Jeng-Wei Tsai 2006). Even if there is only trace amount of pollutant in

environment, it will threaten the growth and survival of abalones, indicating that abalones may have a correspondingly poor detoxification system. So far, very few reports concerning the abalone GST genes have been published. However, this present study could draw a conclusion that the lowly active mu class GST, which is a recognized key detoxification enzyme in other organisms, should take a responsibility to the deficient detoxification ability in abalone species.

Besides the activities tested in our study, human omega GSTs have also been reported to have a monomethylarsonate (MMA^V) reductase activity (Zakharyan, Sampayo-Reyes et al. 2001; Schmuck, Board et al. 2005; Chowdhury, Zakharyan et al. 2006). Arsenic is a common contaminant in drinking water, showing both genotoxicity and cytotoxicity, and also is a recognized human carcinogen. Human and other mammalians metabolize arsenic mainly through the biomethylation pathway, in which arsenate will be transformed into Methylarsonate (MMA) and Dimethylarsinous acid (DMA).Human omega GSTs performed to mediate this biotransformation and play a key role in the rate-limiting enzymatic reaction (Zakharyan, Sampayo-Reyes et al. 2001). In contrast to the hazardous role in mammalians, for most marine animals, which are at lower trophic level in food chains, arsenic seems innoxious and can be accumulated to a high concentration lethal for mammalians. The explanation might be that the principal arsenical species accumulated in those organisms are arsenobetaine and arsenocholine, which are highly methyl substitutes and considered non-toxic, rather than MMA and DMA in mammalians, revealing the different pathways to metabolize arsenicals (Kubota, Kunito et al. 2002; Katano, Matsuo et al. 2003; Hirata and Toshimitsu 2005; Yeh and Jiang 2005). Consequently, we can deduce that omega GSTs in abalones and mammalians should have some functional polymorphism to detoxicate arsenicals. Therefore, though we have not carried out the monomethylarsonate (MMA^V) reductase assay, we could predict the negative activity

on the basis of the above information. However, further study on arsenical detoxification in abalone needs to be carried out in future.

Sigma class is one of the largest GST classes. Whenas, unlike mu and alpha GSTs, which share more than 80% homology within class generally, it always shows identity of less 40% between different members. The variable primary structures would determine the variable enzymatic properties and multiple functions of sigma GSTs. Drosophila GST-2 was reported to be lowly active towards the most commonGST substrate 1-chloro-2,4-dinitrobenzene (CDNB), but showed relatively high glutathione-conjugating activity for 4-hydroxynoenal (4-HNE), one of the major products of lipid peroxidation (Singh, Coronella et al. 2001). 4-HNE has been suggested to be a key mediator of oxidative stress-induced cell death, responsible to mutation, carcinoma and other oxidative stress-related degenerative diseases (Poli and Schaur 2000; Soh, Jeong et al. 2000; Laurora, Tamagno et al. 2005). The main scavenger of 4-HNE in mammalian are a specialized group of alpha class GSTs (Zimniak, Eckles et al. 1992; Prabhu, Reddy et al. 2004), however, sigma GST-2 plays a similar role in drosophila. Additionally, the activity of GSH-dependent prostaglandin D2 synthase were found specifically in sigma GSTs of vertebrates (Meyer and Thomas 1995; Thomson, Meyer et al. 1998; Kanaoka, Fujimori et al. 2000; Jowsey, Thomson et al. 2001), responsible for the specific isomerization of PGH_2 to PGD_2 in the peripheral immune organ and mast cells (Urade, Watanabe et al. 1995). Besides the catalytic GSTs, there are several members in sigma subfamily with minor or no enzymatic activities, performing as structural protein. Lens specific protein S-crystallins from cephalopod failed to bind to the *S*-hexylglutathione affinity column and shows little GST activity in the nucleophilic aromatic substitution reaction between GSH and CDNB (Tomarev, Zinovieva et al. 1992). S-crystallins of cephalopod have been considered as natural mutation of highly active GST from

digestive gland during evolutional process (Tomarev, Zinovieva et al. 1993). In the comparison with other sigma GSTs, the *S*-crystallin has an 11-amino acid residues insertion between the conserved α4 and α5 helices. In the previous homology modeling study of *S*-crystallin, the diminished enzymatic activity had been ascribed to the changing of the hydrophobic phenylalanine to a hydrophilic His108 residue that may hamper the binding of hydrophobic substrate (Chuang, Wu et al. 1999). It was also thought that the replacement of asparagine by Asp101 in *S*-crystallin would result in a decrease in the positive charge environment at the active center, thus might diminish the important function of arginine residue in stabilizing the negatively charged Meisenheimer complex. It is noteworthy that all three abalone sigma GSTs display similar changing of hydrophobic phenylalanine to hydrophilic residues. Correspondingly, the activities of three GSTs have been diminished much in comparison with sigma GST from squid digestive gland.

4.2 Active sites of abalone GSTs

The mechanism of GST detoxification is clear that GST can catalyze the covalent conjugation between GSH and electrophilic xenobiotics by binding these two substrates on their separated domains (Xiao, Singh et al. 1999). Therefore, the strength of interaction between GST and substrates will directly determine the efficiency of enzymatic detoxification.

HdGSTM1 shows only three obvious active sites (Met-104, Val-111and Leu-12) binding to hydrophobic substrate CDNB (Fig.2-1), revealing that it has a weak affinity towards CDNB, which is coincident to the low activity and high K_m value in enzyme assay. Based on the study of crystal structures and site-directive mutation, the hydrophilic binding sites of mu class GST appear to locate mainly on two regions which form a hydrophobic pocket: the C-terminus of α4 and the last C-tail

(Ji, Johnson et al. 1994). To investigate the relationship between enzyme activity and H-sites composition, a sequence comparison of these two H-site regions in different GSTs was done (Table.5). According to the activity towards CDNB, the GSTs in table.5 were divided into four groups: "I" (activity is less than 1 U/mg), "II" (activity is between 10 and 1 U/mg), "III" (activity is between 10 and 100 U/mg) and "IV"(activity is more than 100 U/mg). Except for the residues Asp-105 and Cys-114, which are conserved among all four groups, the profiles of H-site are various among different groups. As the highest activity GSTs, human GSTM2, mouse GSTM1 and rat GSTM1 in group IV are considered as the criteria of optimum hydrophobic pocket to bind CDNB. Fig.6-2 shows the differences between abalone HdGSTM1 and human GSTM2 in hydrophobic binding region. In the position 106 of group IV, there is a hydrophilic prevalent, which is important to stabilize the H-site through forming a hydrogen bond with vicinal residues on helix 6 (Ji, von Rosenvinge et al. 1996; Agianian, Tucker et al. 2003; Contreras-Vergara, Harris-Valle et al. 2004; Schuller, Liu et al. 2005), however, hydrophobic residues (valine or phenylalanine) has taken the place in HdGSTM1 and other lower activity GSTs. Additionally,we found a variety in the position 108 among different groups. It shows a conserved methionine in group IV, whereas hydrophilic residues in other low activity groups mostly. The residue Met108 of group IV appears to contact with CDNB by Van der Waals interaction, performing as a hydrophobic binding site. In table 5, it is noteworthy that the increase of polarity of residues in the position of 108 is accompanied with a reduction of enzyme activity. Thus, we proposed that the absence of Met108 would contribute to the low activity of recombinant HdGSTM1. Moreover, HdGSTM1 also appears different composition from other highly active GSTs in the position of 208, 209 and 214 in C-terminal loop (table.4). The residue 208 of HdGSTM1 is asparagine instead of phenylalanine that appears in other GSTs

whose activities are higher than 20 U/mg.The serine or threonine in 209 position of highly active GSTs has been proved to interact with Tyr-115 or Cys-115 by hydrogen bond, to decrease motion of hydrophobic pocket and inhibit the release of substrate (Liu, Zhang et al. 1992; Johnson, Liu et al. 1993; Chelvanayagam, Wilce et al. 1997; Cheng, Tchaikovskaya et al. 2001; Perbandt, Burmeister et al. 2004). We have compared the three-dimension structures of HdGSTM1 and human GSTM2, showing that the side chain of Asn-209 in HdGSTM1 appears a larger distance to Tyr-115 and forms a weaker hydrogen bond OH⋯O=C than O-H⋯O-R in human GSTM2. Consequently, HdGSTM1 has more flexible H-site and lower substrate affinity. In both cattle tick GST and HdGSTM1, Phe-214 has taken the place of Trp-214, which is conserved in most mu class GSTs. The function of Trp-214 is still unclear currently, however, it is interesting that the GSTs without it show activity towards CDNB of less than 1 μmol/min/mg, suggesting it could be another key site potentially.

Table.5: Comparison of active sites and correlated activity between HdGSTM1 and other known mu class GSTs.

Group	Gene name	Specific activity (μmol/min/mg protein)				C-domain active sites		References
		CDNB	DCNB	ECA	4-NBC	Residues 104-115	Residues 207-214	
I	Abalone GSTM1	0.172±0.01	ND	0.114±0.001	ND	MDFRNGIVGLCY	INNKSALFK	This study
I	Cattle tick GST	0.3	——	——	——	ADFRMNWVRLCY	LNGDMASFG	(Rosa de Lima, Sanchez Ferreira et al. 2002)
II	Human GSTM4	1.25	ND	0.04	——	MDVSNQLARVCY	LYTRVAVWG	(Guo, Zimniak et al. 2002)
II	Mouse GSTM7	3.0±0.4	ND	0.14±0.006	ND	MDVSNQLARVCY	LYTKVATWG	(Guo, Zimniak et al. 2002)
II	Human GSTM3	7.5	0.029	0.2	——	MDFRTQLIRLCY	INNKMAQWG	(Campbell, Takahashi et al. 1990)
II	Clonorchis sinensis GST	9.17±1.69	ND	0.3±0.1	——	ADFRMNWVRLCY	LFMKLAVWG	(Hong, Lee et al. 2001)
III	Bovine GST	11±3	——	——	——	MDVRLAMARICY	LNGDMASFG	(Jimenez-Asensio and Garland 2000)
III	Rat GSTM4-4	13.8±0.06	0.11±0.03	ND	ND	MDTRIHLMIVCC	VFTKIPQWG	(Cheng, Tchaikovskaya et al. 2001)
III	Mouse GSTM3	22.2	0.08	0.012	0.50	MDTRIQLMIVCC	VFTKIAQWG	(Guo, Zimniak et al. 2002)
III	Chicken GSTM1	23.6±0.5	ND	0.29±0.01	——	MDLRMAFARLCY	IFWYTALWN	(Sun, Kuan et al. 1998)
IV	Rat GSTM1-1	121.2±0.21	1.83±0.08	0.09	——	MDNRMQLIMLCY	IFSKLAQWS	(Cheng, Tchaikovskaya et al. 2001)
IV	Mouse GSTM1	148	4.4	0.12	——	MDTRMQLIMLCY	IFSKMAHWS	(Guo, Zimniak et al. 2002)
IV	Human GSTM2	196	1.60	0.22	——	MDSRMQLAKLCY	VFTKMAVWG	(Vorachek, Pearson et al. 1991)

Despite the variable homology in omega class, all the members of this subfamily share a conserved active residue: a cystine residue at the end of α₁ helix. Compared with the tyrosine or serine residue in other classes, which bind glutathione by forming a hydrogen bond between thiol group of glutathione and hydroxyl group of amino acid side chains, the cysteine of omega class shows a different manner that the thiol group of cysteine will form a mixed disulfide with glutathione, indicating the closer molecular distance and stronger interaction force (Board, Coggan et al. 2000). The conserved cysteine of omega class GST is equivalent to the first cysteine in the C-X-X-C motif of glutaredoxins, performing a same function as a redox active residue capable to reduce GSH mixed disulfides, as well. Consequently omega GSTs were also proposed to be grouped as a subclass of glutaredoxin which catalyze in a monothiol mechanism (Fernandes and Holmgren 2004; Sun, Su et al. 2005). However, the cysteine-containing tetramers of glutaredoxins and omega GTSs are sequence divergent as C-P-Y-C, C-P-F-A, C-P-Y-A, C-P-Y-S, C-P-W-A, etc. These divergences correspond to the variable catalytic ability as dehydroascorbate reductase (DHAR) and thioltransferase (TTase), appearing a prevalent increasing of DHAR activity when tyrosine replaces phenylalanine or tryptophan in the third residue (Table.6). HdGSTO1 showed one novel structure of C-P-Y-A, displaying high DHAR and TTase activities. HdGSTO2 shared the same active tetramer of C-P-F-A with human GSTO1 and pig omega GST, showing a similar enzyme property with low DHAR activity. Additionally, Leu56, Lys59, Leu71, Val72, Glu85 and Ser86 of human GSTO1 also showed close interactions with glutathione molecule, playing the same role of G-sites (Board, Coggan et al. 2000). These residues are conserved in two abalone omega GSTs, except tryptorphan replaced leucine in the residue 60 of HdGSTO1.

Table.6: Comparison of cysteine-containing tetramer structures and correlated activities.

GSTs	Motif component	DHAR[a]	TTase[b]	Reference
Abalone HdGSTO1	C-P-Y-A	1.18	2.59	This study
Abalone HdGSTO2	C-P-F-A	0.05	0.18	This study
Pig GSTO	C-P-F-A	0.17	—	(Rouimi, Anglade et al. 2001)
Human GSTO1-1	C-P-F-A	0.13	2.0	(Board, Coggan et al. 2000)
Yeast GSTO1	C-P-F-T	0.23	1.93	(Garcera, Barreto et al. 2006)
Human GSTO2-2	C-P-Y-S	13.8	1.5	(Wang, Xu et al. 2005)
Schistosoma GSTO	C-P-Y-V	0.20	0.11	(Girardini, Amirante et al. 2002)
Human glutaredoxin 1	C-P-Y-C	3.0	—	(Levine 1996)
Yeast GSTO2	C-P-W-A	0.11	3.27	(Garcera, Barreto et al. 2006)
Yeast GSTO3	C-P-W-A	0.16	1.18	(Garcera, Barreto et al. 2006)

In our study, there is a non-activity sigma GST isform, HdGSTS3. Interestingly, there are also several members in sigma subfamily with minor or no enzymatic activities, performing as structural protein. Lens specific protein S-crystallins from cephalopod failed to bind to the *S*-hexylglutathione affinity column and shows little GST activity in the nucleophilic aromatic substitution reaction between GSH and CDNB (Tomarev, Zinovieva et al. 1992). S-crystallins of cephalopod have been considered as natural mutation of highly active GST from digestive gland during evolutional process (Tomarev, Zinovieva et al. 1993). In the comparison with other sigma GSTs, the *S*-crystallin has an 11-amino acid residues insertion between the conserved α4 and α5 helices. In the previous homology modeling study of *S*-crystallin, the diminished enzymatic activity had been ascribed to the changing of the hydrophobic phenylalanine to a hydrophilic His108 residue that may hamper the binding of hydrophobic substrate (Chuang, Wu et al. 1999). It was also thought that the replacement of asparagine by Asp101 in *S*-crystallin would result in a decrease in the positive charge environment at the active center, thus might diminish the important function of arginine residue in stabilizing the negatively charged Meisenheimer complex. It is noteworthy that all three abalone sigma GSTs display similar changing of hydrophobic phenylalanine to hydrophilic residues. Correspondingly, the activities of three GSTs have been diminished much in comparison with sigma GST from squid digestive gland.

4.3 Tissue specific expression of abalone GSTs

In glutathione-s-tranferases family, there have been reported more than ten subclass members exhibiting different primary structures, enzyme features and physiological functions (Ivarsson, Mackey et al. 2003). Moreover, more than one GST isoform would exist in single organism, playing different roles, such as detoxification enzyme,

antioxidant enzyme or structural protein. According to the different functions, GST genes would express differently in tissues. Mu class GSTs, as one of the most important components of mammalian GST system, displayed ubiquitous expression in all inner organs of human and rat with high levels, revealing the pivotal role of defending xenobiotics and endogenetic oxidative stress (Vorachek, Pearson et al. 1991; Lee, Lee et al. 1995). In contrast to the wide distribution in mammals, however, mu GSTs of aquatic invertebrate had few report and exhibited much different expression patterns. Shrimp mu GST transcripts, for example, distributed primarily in hepatopancreas and gills, which is major enzymic production organ and respiration organ, respectively (Contreras-Vergara, Harris-Valle et al. 2004). In our study, mu GST of disk abalone showed high transcripts level in gills, where are most potential to be exposed to xenobiotics. Gonad of disk abalone also showed high abundance of HdGSTM1 transcripts, perhaps in order to protect germ cells against toxic and oxidative stress, which would cause fatal mutagenesis. This expression pattern was similar with that of some GSTs in bivalves, shrimp and some fish GSTs (Doi, Pham et al. 2004; Lee, Chang et al. 2005).

HdGSTO1 mRNA was found distributed in all tested tissues with high abundances, indicating important roles in disk abalone. On the contrary, HdGSTO2 showed a significantly different expression profiles. The different tissue distribution of two omega GSTs would reveal their different functions. HdGSTO1, which showed high activity and wide tissue distribution, would play a role of regular intracellular detoxification to defend both xenobiotics and endogenetic oxidative stress. Similar as bivalves, Gill is the major organ of abalone that filters large amount of seawater to cope with breath so that it would suffers xenobiotics in ocean most seriously. Therefore, more detoxification or antioxidant enzymes would be required in the cells of gill to prevent toxic effect. Similarly, gonad, as the location of reproductive cells

which are sensitive to toxicant and oxidative stress, also need more detoxification enzymes. HdGSTO2, which showed abundance only in gonad and gill, would play a role as a detoxification enzyme specifically in these two organs. The studies on two human omega GSTs also showed different expression profiles of two genes. Human GSTO1 showed a wide tissue distribution, exhibiting high expression level in most examined organs, similar to HdGSTO1. However, human GSTO2 showed predominant expression in ovary, testis, liver and small intestine, similar to HdGSTO2. Northern blot analysis of pig omega GST showed a widespread expression of GSTO transcripts in various tissues with especially high level in liver and muscle. Lung is the major respiration organ of all terraneous animals, hence it is also the organ exposing to highest atmospheric oxygen, air pollutant and ROS. Numerous antioxidant and detoxification enzyme express in lung with high level to prevent oxidative injury. Nevertheless, neither human nor pig showed high expression of omega GSTs in lung. Similarly, abalone omega GST HdGSTO2 showed very few transcripts in gills, which is respiration organ of mollusks. HdGSTO1, a housekeeping like gene, also showed least expression in gills. It suggested that different class GSTs would have different *in vivo* functions. Omega GSTs might be lack of protection roles in respiration organs, or their expression might be triggered only when exposing to specific stressors.

Due to the different functions, the tissue distribution of sigma GSTs are distinctly different. Drosophila GST-2 shows a specific expression in asynchronous indirect fight muscles (IFMs) and mediates in muscle repeated cycles of contraction, though the precise mechanism is still not clear. Similar to indirect flight muscles of drosophila, which stretch and contract in frequency, the foot muscle of abalone would keep contraction for a long time to attach to the rock. Consequently, a number of genes might express largely to cope with the potential oxidative stress and signal

transmission in cells of foot muscle. HdGSTS3, a non-activity GST in our study, showed specifically high expression in foot muscle (Fig.10), suggesting a similar function as GST-2 of drosophila. Not like the specific expression of S-crystallin in lens, the transcripts of PGDS distribute variously in different organisms. Rat PGDS shows exclusive expression in spleen (Kanaoka, Ago et al. 1997), however, chicken PGDS expresses in most inner organs (Thomson, Meyer et al. 1998). In our study, HdGSTS1 showed a universal expression in tissues including eye/eyestalk. The reason that we chose the tissue of eye/eyestalk was to elucidatethe relationship between abalone sigma GSTs and cephalopod S-crystallins. Abalones have two lowly developed eyes comprised with only photoreceptor membranes (Kataoka and Yamamoto 1981). Whereas, the vision organs of cephalopod are thought to be most highly developed in invertebrates. As gradually evolution of vision system, S-crystallin cannot directly evolve directly from GST in digestive gland. Therefore, there must exist some intergradation genes between ancestral GST and advanced S-crystallin. Among all three sigma GSTs, only HdGSTS1 was observed in eye/eyestalk tissue. Admittedly, the transcripts of HdGSTS1 might be derived from tissue of only eyestalk rather than eyes. The further evolutional study of abalone sigma GSTs need be conducted in future.

4.4 Biomarker of marine endocrine-disrupting chemicals

In the past 40 years, owing to the intensive industrial and agricultural activities of human, pollution of marine environment has already become a global concernment. And in order to assess the marine pollution, several biomarkers, such as cytochrome P4501A induction, metallothionein induction, vitellogenin induction, DNA integrity and acetylcholinesterase inhibition, have been developed and widely used in environment monitoring programs. PAHs, PCBs and TBT are three most ubiquitous

and the most widely studied organic pollutants that are threatening the health of the marine ecosystem, due to their high persistence and endocrine disrupting effect (Peachey 2003; Devier, Augagneur et al. 2005; Perez-Carrera, Leon et al. 2007). PAHs, as one of the most important marine contaminants, are known as functionally oestrogenic or antioestrogenic chemicals (Fertuck, Kumar et al. 2001). Most PAHs are introduced into the marine environment through dumping of oil and combustion of fossil fuels.Differently, PCBs are mainly from the dielectric fluids of capacitors and transformers, performing as mimics of thyroid hormone to decrease thyroid hormone levels in contaminated animals (Zoeller 2005). Both these two groups of chemicals have been proved to mediate in aryl hydrocarbon receptor (AhR) pathway to regulate the expression of cytochrome P450 family genes, the phase I detoxification enzymes (Chaty, Rodius et al. 2004). Fish cytochrome P4501A is one widely accepted biomarker for PAHs and PCBs pollution due to its broad-spectrum utility and dramatic induction response. Its transcriptional levels and related enzyme (ethoxyresorufin-O-deethylase) activities have been investigated in both laboratory studies and field monitoring programs (Rees, McCormick et al. 2005; Roberts, Oris et al. 2006; Abrahamson, Brandt et al. 2007).

It is noteworthy that most of the metabolites from phase I detoxification are still toxic or become even more toxic in many cases, therefore the phase II enzymes, particularly GSTs, are supposed to be involved to cope with the crisis as well. Moreover, theoretically speaking,a number of cis-acting regulatory sequences, such as xenobiotic response elements (XREs) and antioxidant response elements (AREs), have been found in the promoter regions of most GSTs. These elements could be activated bythe xenobiotics, electrophilic metabolites or consequential oxidative stress to enhance the expression of relative GST isoforms (Wasserman and Fahl 1997; Lindros, Oinonen et al. 1998). So far, the study of GST induction and its biomarker

application are mostly based on the simple activity tests, which could represent the response of integral GSTs. The GST activities could be significantly induced by exposure of heavy metals (Ferrat, Bingert et al. 2002; Ognjanovic, Markovic et al. 2007), PAHs (Pegram and Chou 1989; Shailaja and D'Silva 2003), PCBs (Blanchette and Singh 2002; Perez Lopez, Novoa Valinas et al. 2002), and insecticides (Gowlan, Moffat et al. 2002; Monteiro, de Almeida et al. 2006; Rao 2006). In the current studies of GST induction, we could findthat different GST isoforms in one organism could exhibit reverse response to the same treatment transcriptionally or translationally. In our study, abalone GST HdGSTM1, HdGSTO1 and HdGSTS1 was significantly induced by two model chemicals of PAHs and PCBs,revealing the probable existence of XREs in the promoter region of them. However, the expression of HdGSTR1, HdGSTO2 and HdGSTS3 were inhibited by high dose of PAH chemicals. As for the induction mechanism, it needs more further study to clarify.

TBT is probably the most toxic pollutant for mollusks in marine environment. It has been widely used as antifouling additive in paints of fish nets, mariculture cages, ship hulls and marine platforms for more than 40 years. TBT could cause several adverse effect to heath of mollusk, such as shell deformation of oysters (Ebdon, Evans et al. 1989) and famous imposex of gastropods, resulting in severe decline of population or even extinction of species (Horiguchi, Kojima et al. 2006). However the mechanism of TBT effecting mollusk endocrine system is still not elucidated clearly. TBT has been reported to act as a neurotoxin to abnormally release the peptide hormone, and also inhibit aromatase activity to influent the steroid hormone metabolism leading to change of androgen and estrogen levels. Some recent research also suggested that TBT would mediate in retinoid x receptor (RXR) signal pathway to induce masculinization (Castro, Lima et al. 2007). In spite of being important detoxification enzymes, GSTs activity and expression level were rarely investigated in

the studies of TBT exposure. According to these limited studies, there established a hypothesis that there might be a threshold concentration of TBT and other organotin compounds exposure for specific organisms. Only a dose lower than this threshold concentration would induce GST expression, otherwise, GST activity could be inhibited (Al-Ghais and Ali 1999; Schmidt, Steinberg et al. 2004; Wang, Chen et al. 2005; Wang, Zhao et al. 2006). It was said that TBT can interact directly with the SH group of glutathione molecule, making it less available to the GST reactions. TBT has also been shown to inhibit GST by depletion of GSH on murine epidermal cell lines, and indirectly by inhibiting cytochrome P450 1A1 activity. In our study, it showed a similar result that the higher dose (1.0 ppb) TBT exposed abalones exhibited significantly lower induction level of HdGSTM1 in both gill and digestive tract tissues than those under lower dose (0.1 ppb) exposure.
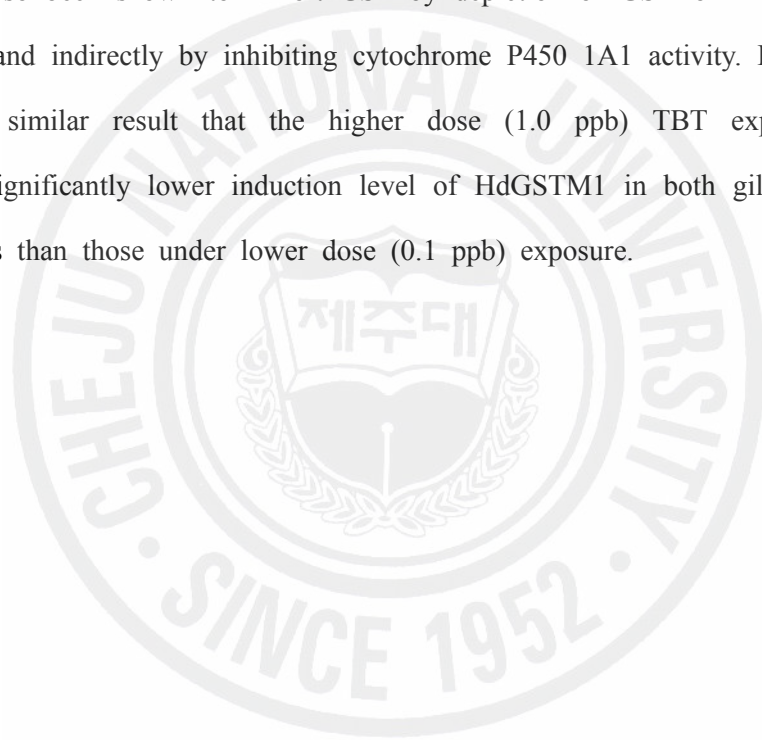
Ⅴ. REFERENCES

Abrahamson, A., I. Brandt, et al. (2007). "Monitoring contaminants from oil production at sea by measuring gill EROD activity in Atlantic cod (Gadus morhua)." Environ Pollut.

Agianian, B., P. A. Tucker, et al. (2003). "Structure of a Drosophila sigma class glutathione S-transferase reveals a novel active site topography suited for lipid peroxidation products." J Mol Biol **326**(1): 151-65.

Al-Ghais, S. M. and B. Ali (1999). "Inhibition of glutathione S-transferase catalyzed xenobiotic detoxication by organotin compounds in tropical marine fish tissues." Bull Environ Contam Toxicol **62**(2): 207-13.

Beeghly, A., D. Katsaros, et al. (2006). "Glutathione S-transferase polymorphisms and ovarian cancer treatment and survival." Gynecol Oncol **100**(2): 330-7.

Blanchette, B. N. and B. R. Singh (2002). "Induction of glutathione-S-transferase in the Northern quahog Mercenaria mercenaria after exposure to the polychlorinated biphenyl (PCB) mixture Aroclor 1248." J Protein Chem **21**(8): 489-94.

Board, P. G., M. Coggan, et al. (2000). "Identification, characterization, and crystal structure of the Omega class glutathione transferases." J Biol Chem **275**(32): 24798-806.

Bondgaard, M. and P. Bjerregaard (2005). "Association between cadmium and calcium uptake and distribution during the moult cycle of female shore crabs, Carcinus maenas: an in vivo study." Aquat Toxicol **72**(1-2): 17-28.

Boutet, I., A. L. Meistertzheim, et al. (2005). "Molecular characterization and expression of the gene encoding aspartate aminotransferase from the Pacific oyster Crassostrea gigas exposed to environmental stressors." Comp Biochem Physiol C Toxicol Pharmacol **140**(1): 69-78.

Bradford, M. M. (1976). "A rapid and sensitive method for the quantitation of microgram quantities of protein utilizing the principle of protein-dye binding." Anal Biochem **72**: 248-54.

Castro, L. F., D. Lima, et al. (2007). "Imposex induction is mediated through the Retinoid X Receptor signalling pathway in the neogastropod Nucella lapillus." Aquat Toxicol **85**(1): 57-66.

Chaty, S., F. Rodius, et al. (2004). "A comparative study of the expression of CYP1A and CYP4 genes in aquatic invertebrate (freshwater mussel, Unio tumidus) and vertebrate (rainbow trout, Oncorhynchus mykiss)." Aquat Toxicol **69**(1): 81-94.

Chelvanayagam, G., M. C. Wilce, et al. (1997). "Homology model for the human GSTT2 Theta class glutathione transferase." Proteins **27**(1): 118-30.

Cheng, H., T. Tchaikovskaya, et al. (2001). "Rat glutathione S-transferase M4-4: an isoenzyme with unique structural features including a redox-reactive cysteine-115 residue that forms mixed disulphides with glutathione." Biochem J **356**(Pt 2): 403-14.

Chou, C.-M. L. a. B. Y.-H. (2005). "Site-specific environmental quality criteria for survival and growth of farmed abalone exposed to zinc." Aquaculture**249**(1-4): 159-173.

Chowdhury, U. K., R. A. Zakharyan, et al. (2006). "Glutathione-S-transferase-omega [MMA(V) reductase] knockout mice: Enzyme and arsenic species concentrations in tissues after arsenate administration." Toxicol Appl Pharmacol **216**(3): 446-57.

Chuang, C. C., S. H. Wu, et al. (1999). "Homology modeling of cephalopod lens S-crystallin: a natural mutant of sigma-class glutathione transferase with diminished endogenous activity." Biophys J **76**(2): 679-90.

Clayton, J. D., R. M. Cripps, et al. (1998). "Interaction of troponin-H and glutathione S-transferase-2 in the indirect flight muscles of Drosophila melanogaster." J Muscle Res Cell Motil **19**(2): 117-27.

Colborn, T., F. S. vom Saal, et al. (1993). "Developmental effects of endocrine-disrupting chemicals in wildlife and humans." Environ Health Perspect **101**(5): 378-84.

Contreras-Vergara, C. A., C. Harris-Valle, et al. (2004). "A mu-class glutathione S-transferase from the marine shrimp Litopenaeus vannamei: molecular cloning and active-site structural modeling." J Biochem Mol Toxicol **18**(5): 245-52.

Czeczot, H., D. Scibior, et al. (2006). "Glutathione and GSH-dependent enzymes in patients with liver cirrhosis and hepatocellular carcinoma." Acta Biochim Pol **53**(1): 237-42.

Daglish, C. (1951). "The spectrophotometic determination of ascorbic acid in tissue extracts, particularly those of the walnut (Juglans regia)." Biochem J **49**(5): 635-9.

Damiens, G., E. His, et al. (2004). "Evaluation of biomarkers in oyster larvae in natural and polluted conditions." Comp Biochem Physiol C Toxicol Pharmacol **138**(2): 121-8.

Devier, M. H., S. Augagneur, et al. (2005). "One-year monitoring survey of organic compounds (PAHs, PCBs, TBT), heavy metals and biomarkers in blue mussels from the Arcachon Bay, France." J Environ Monit **7**(3): 224-40.

Dirr, H., P. Reinemer, et al. (1994). "X-ray crystal structures of cytosolic glutathione S-transferases. Implications for protein architecture, substrate recognition and catalytic function." Eur J Biochem **220**(3): 645-61.

Doi, A. M., R. T. Pham, et al. (2004). "Molecular cloning and characterization of a glutathione S-transferase from largemouth bass (Micropterus salmoides) liver that is involved in the detoxification of 4-hydroxynonenal." Biochem Pharmacol **67**(11): 2129-39.

Ebdon, L., K. Evans, et al. (1989). "The accumulation of organotins in adult and seed oysters from selected estuaries prior to the introduction of U.K. regulations governing the use of tributyltin-based antifouling paints." Sci Total Environ **83**(1-2): 63-84.

Fernandes, A. P. and A. Holmgren (2004). "Glutaredoxins: glutathione-dependent redox enzymes with functions far beyond a simple thioredoxin backup system." Antioxid Redox Signal **6**(1): 63-74.

Ferrat, L., A. Bingert, et al. (2002). "Mercury uptake and enzymatic response of Posidonia

oceanica after an experimental exposure to organic and inorganic forms." Environ Toxicol Chem **21**(11): 2365-71.

Fertuck, K. C., S. Kumar, et al. (2001). "Interaction of PAH-related compounds with the alpha and beta isoforms of the estrogen receptor." Toxicol Lett **121**(3): 167-77.

Gao, Q., L. Song, et al. (2007). "cDNA cloning and mRNA expression of heat shock protein 90 gene in the haemocytes of Zhikong scallop Chlamys farreri." Comp Biochem Physiol B Biochem Mol Biol **147**(4): 704-15.

Garcera, A., L. Barreto, et al. (2006). "Saccharomyces cerevisiae cells have three Omega class glutathione S-transferases acting as 1-Cys thiol transferases." Biochem J **398**(2): 187-96.

Girardini, J., A. Amirante, et al. (2002). "Characterization of an omega-class glutathione S-transferase from Schistosoma mansoni with glutaredoxin-like dehydroascorbate reductase and thiol transferase activities." Eur J Biochem **269**(22): 5512-21.

Gowlan, B. T., C. F. Moffat, et al. (2002). "Cypermethrin induces glutathione S-transferase activity in the shore crab, Carcinus maenas." Mar Environ Res **54**(2): 169-77.

Habig, W. H., M. J. Pabst, et al. (1974). "Glutathione S-transferases. The first enzymatic step in mercapturic acid formation." J Biol Chem **249**(22): 7130-9.

Harris, J., B. Coles, et al. (1991). "The isolation and characterization of the major glutathione S-transferase from the squid Loligo vulgaris." Comp Biochem Physiol B **98**(4): 511-5.

Hayes, J. D., J. U. Flanagan, et al. (2005). "Glutathione transferases." Annu Rev Pharmacol Toxicol **45**: 51-88.

Hayes JD, P. D. (1995). "The glutathione S-transferase supergene family: regulation of GST and the contribution of the isoenzymes to cancer chemoprotection and drug resistance." Crit Rev Biochem Mol Biol. **30**(6): 445-600.

Hirata, S. and H. Toshimitsu (2005). "Determination of arsenic species and arsenosugars in marine samples by HPLC-ICP-MS." Anal Bioanal Chem **383**(3): 454-60.

Hoarau, P., G. Damiens, et al. (2006). "Cloning and expression of a GST-pi gene in Mytilus galloprovincialis. Attempt to use the GST-pi transcript as a biomarker of pollution." Comp Biochem Physiol C Toxicol Pharmacol **143**(2): 196-203.

Holmgren, A. and F. Aslund (1995). "Glutaredoxin." Methods Enzymol **252**: 283-92.

Horiguchi, T., Imai, T., Cho, H. S., Shiraishi, H., Shibata, Y., Morita, M., Shimizu,M. (1998). "Acute Toxicity of Organotin Compounds to the Larvae of the Rock Shell, Thais clavigera, the Disk Abalone, Haliotis discus discus and the Giant Abalone, Haliotis madaka,." Marine Environmental Research **46**(1-5): 469-473

Horiguchi, T., M. Kojima, et al. (2006). "Impact of tributyltin and triphenyltin on ivory shell (Babylonia japonica) populations." Environ Health Perspect **114 Suppl 1**: 13-9.

Ishikawa, T., A. F. Casini, et al. (1998). "Molecular cloning and functional expression of rat liver glutathione-dependent dehydroascorbate reductase." J Biol Chem **273**(44): 28708-12.

Ivarsson, Y., A. J. Mackey, et al. (2003). "Identification of residues in glutathione transferase capable of driving functional diversification in evolution. A novel approach to protein redesign." J Biol Chem **278**(10): 8733-8.

Jeng-Wei Tsai, C.-M. L., Vivian Hsiu-Chuan Liao (2006). "A biologically based damage assessment model to enhance aquacultural water quality management." Aquaculture **251**: 280-294.

Ji, X., W. W. Johnson, et al. (1994). "Structure and function of the xenobiotic substrate binding site of a glutathione S-transferase as revealed by X-ray crystallographic analysis of product complexes with the diastereomers of 9-(S-glutathionyl)-10-hydroxy-9,10-dihydrophenanthrene." Biochemistry **33**(5): 1043-52.

Ji, X., M. Tordova, et al. (1997). "Structure and function of the xenobiotic substrate-binding site and location of a potential non-substrate-binding site in a class pi glutathione S-transferase." Biochemistry **36**(32): 9690-702.

Ji, X., E. C. von Rosenvinge, et al. (1996). "Location of a potential transport binding site in a sigma class glutathione transferase by x-ray crystallography." Proc Natl Acad Sci U S A **93**(16): 8208-13.

Ji, X., P. Zhang, et al. (1992). "The three-dimensional structure of a glutathione S-transferase from the mu gene class. Structural analysis of the binary complex of isoenzyme 3-3 and glutathione at 2.2-A resolution." Biochemistry **31**(42): 10169-84.

Johnson, W. W., S. Liu, et al. (1993). "Tyrosine 115 participates both in chemical and physical steps of the catalytic mechanism of a glutathione S-transferase." J Biol Chem **268**(16): 11508-11.

Jowsey, I. R., A. M. Thomson, et al. (2001). "Mammalian class Sigma glutathione S-transferases: catalytic properties and tissue-specific expression of human and rat GSH-dependent prostaglandin D2 synthases." Biochem J **359**(Pt 3): 507-16.

Kanaoka, Y., H. Ago, et al. (1997). "Cloning and crystal structure of hematopoietic prostaglandin D synthase." Cell **90**(6): 1085-95.

Kanaoka, Y., K. Fujimori, et al. (2000). "Structure and chromosomal localization of human and mouse genes for hematopoietic prostaglandin D synthase. Conservation of the ancestral genomic structure of sigma-class glutathione S-transferase." Eur J Biochem **267**(11): 3315-22.

Katano, S., Y. Matsuo, et al. (2003). "Arsenic compounds accumulated in pearl oyster Pinctada fucata." Chemosphere **53**(3): 245-51.

Kataoka, S. and T. Y. Yamamoto (1981). "Diurnal changes in the fine structure of photoreceptors in an abalone, Nordotis discus." Cell Tissue Res **218**(1): 181-9.

Kirchin, M. A., Wiseman, A., Livingstone, D.R. (1992). "Seasonal and sex variation in the mixed-function oxygenase system of digestive gland microsomes of the common mussel, Mytilus edulis L." Comp. Biochem. Physiol **101C**: 81-91.

Konishi, T., K. Kato, et al. (2005). "A new class of glutathione S-transferase from the

hepatopancreas of the red sea bream Pagrus major." Biochem J **388**(Pt 1): 299-307.

Kubota, R., T. Kunito, et al. (2002). "Chemical speciation of arsenic in the livers of higher trophic marine animals." Mar Pollut Bull **45**(1-12): 218-23.

Kuhajek, J. M. and D. Schlenk (2003). "Effects of the brominated phenol, lanosol, on cytochrome P-450 and glutathione transferase activities in Haliotis rufescens and Katharina tunicata." Comp Biochem Physiol C Toxicol Pharmacol **134**(4): 473-9.

Laurora, S., E. Tamagno, et al. (2005). "4-Hydroxynonenal modulation of p53 family gene expression in the SK-N-BE neuroblastoma cell line." Free Radic Biol Med **38**(2): 215-25.

Lee, R. F. (1988). "Glutathione S-transferase in marine invertebrates from Langesundfjord." Mar. Ecol. Prog. Ser **46**: 33-36.

Lee, S. H., S. H. Lee, et al. (1995). "Cloning and expression of a cDNA for mu-class glutathione S-transferase from rabbit liver." Arch Biochem Biophys **318**(2): 424-9.

Lee, Y. M., S. Y. Chang, et al. (2005). "Cloning and expression of alpha class glutathione S-transferase gene from the small hermaphroditic fish Rivulus marmoratus (Cyprinodontiformes, Rivulidae)." Mar Pollut Bull **51**(8-12): 776-83.

Li, Y. J., S. A. Oliveira, et al. (2003). "Glutathione S-transferase omega-1 modifies age-at-onset of Alzheimer disease and Parkinson disease." Hum Mol Genet **12**(24): 3259-67.

Liebau, E., R. D. Walter, et al. (1994). "Isolation, sequence and expression of an Onchocerca volvulus glutathione S-transferase cDNA." Mol Biochem Parasitol **63**(2): 305-9.

Lindros, K. O., T. Oinonen, et al. (1998). "Aryl hydrocarbon receptor-associated genes in rat liver: regional coinduction of aldehyde dehydrogenase 3 and glutathione transferase Ya." Biochem Pharmacol **55**(4): 413-21.

Liu, S., P. Zhang, et al. (1992). "Contribution of tyrosine 6 to the catalytic mechanism of isoenzyme 3-3 of glutathione S-transferase." J Biol Chem **267**(7): 4296-9.

Maina, C. V., P. D. Riggs, et al. (1988). "An Escherichia coli vector to express and purify foreign proteins by fusion to and separation from maltose-binding protein." Gene **74**(2): 365-73.

Mattson, M. P. (2004). "Pathways towards and away from Alzheimer's disease." Nature **430**(7000): 631-9.

McIlwain, C. C., D. M. Townsend, et al. (2006). "Glutathione S-transferase polymorphisms: cancer incidence and therapy." Oncogene **25**(11): 1639-48.

Meyer, D. J., R. Muimo, et al. (1996). "Purification and characterization of prostaglandin-H E-isomerase, a sigma-class glutathione S-transferase, from Ascaridia galli." Biochem J **313 (Pt 1)**: 223-7.

Meyer, D. J. and M. Thomas (1995). "Characterization of rat spleen prostaglandin H D-isomerase as a sigma-class GSH transferase." Biochem J **311 (Pt 3)**: 739-42.

Monteiro, D. A., J. A. de Almeida, et al. (2006). "Oxidative stress biomarkers in the

freshwater characid fish, Brycon cephalus, exposed to organophosphorus insecticide Folisuper 600 (methyl parathion)." Comp Biochem Physiol C Toxicol Pharmacol **143**(2): 141-9.

Ognjanovic, B. I., S. D. Markovic, et al. (2007). "Effect of chronic cadmium exposure on antioxidant defense system in some tissues of rats: protective effect of selenium." Physiol Res.

Peachey, R. B. (2003). "Tributyltin and polycyclic aromatic hydrocarbon levels in Mobile Bay, Alabama: a review." Mar Pollut Bull **46**(11): 1365-71.

Pegram, R. A. and M. W. Chou (1989). "Effect of nitro-substitution of environmental polycyclic aromatic hydrocarbons on activities of hepatic phase II enzymes in rats." Drug Chem Toxicol **12**(3-4): 313-26.

Perbandt, M., C. Burmeister, et al. (2004). "Native and inhibited structure of a Mu class-related glutathione S-transferase from Plasmodium falciparum." J Biol Chem **279**(2): 1336-42.

Perez-Carrera, E., V. M. Leon, et al. (2007). "Simultaneous determination of pesticides, polycyclic aromatic hydrocarbons and polychlorinated biphenyls in seawater and interstitial marine water samples, using stir bar sorptive extraction-thermal desorption-gas chromatography-mass spectrometry." J Chromatogr A.

Perez, E., J. Blasco, et al. (2004). "Biomarker responses to pollution in two invertebrate species: Scrobicularia plana and Nereis diversicolor from the Cadiz bay (SW Spain)." Mar Environ Res **58**(2-5): 275-9.

Perez Lopez, M., M. C. Novoa Valinas, et al. (2002). "Induction of cytosolic glutathione S-transferases from Atlantic eel (Anguilla Anguilla) after intraperitoneal treatment with polychlorinated biphenyls." Sci Total Environ **297**(1-3): 141-51.

Poli, G. and R. J. Schaur (2000). "4-Hydroxynonenal in the pathomechanisms of oxidative stress." IUBMB Life **50**(4-5): 315-21.

Prabhu, K. S., P. V. Reddy, et al. (2004). "Characterization of a class alpha glutathione-S-transferase with glutathione peroxidase activity in human liver microsomes." Arch Biochem Biophys **424**(1): 72-80.

Rao, J. V. (2006). "Biochemical alterations in euryhaline fish, Oreochromis mossambicus exposed to sub-lethal concentrations of an organophosphorus insecticide, monocrotophos." Chemosphere **65**(10): 1814-20.

Rees, C. B., S. D. McCormick, et al. (2005). "A non-lethal method to estimate CYP1A expression in laboratory and wild Atlantic salmon (Salmo salar)." Comp Biochem Physiol C Toxicol Pharmacol **141**(3): 217-24.

Reinemer, P., H. W. Dirr, et al. (1991). "The three-dimensional structure of class pi glutathione S-transferase in complex with glutathione sulfonate at 2.3 A resolution." Embo J **10**(8): 1997-2005.

Rice, M. E. (2000). "Ascorbate regulation and its neuroprotective role in the brain." Trends

Neurosci **23**(5): 209-16.

Roberts, A. P., J. T. Oris, et al. (2006). "Gene expression in caged juvenile Coho Salmon (Oncorhynchys kisutch) exposed to the waters of Prince William Sound, Alaska." Mar Pollut Bull **52**(11): 1527-32.

Ronald S. Tjeerdema, W. S. S., Linda B. Martello, Robert J. Kauten and Donald G. Crosby. (1996). "Interactions of chemical and natural stresses in the abalone (Haliotis rufescens) as measured by surface-Probe localized 31P NMR." Marine Environmental Research **42**(1-4): 369-374.

Rouimi, P., P. Anglade, et al. (2001). "Purification and characterization of a glutathione S-transferase Omega in pig: evidence for two distinct organ-specific transcripts." Biochem J **358**(Pt 1): 257-62.

Schmidt, K., C. E. Steinberg, et al. (2004). "Xenobiotic substances such as PCB mixtures (Aroclor 1254) and TBT can influence swimming behavior and biotransformation activity (GST) of carp (Cyprinus carpio)." Environ Toxicol **19**(5): 460-70.

Schmuck, E. M., P. G. Board, et al. (2005). "Characterization of the monomethylarsonate reductase and dehydroascorbate reductase activities of Omega class glutathione transferase variants: implications for arsenic metabolism and the age-at-onset of Alzheimer's and Parkinson's diseases." Pharmacogenet Genomics **15**(7): 493-501.

Schuller, D. J., Q. Liu, et al. (2005). "Crystal structure of a new class of glutathione transferase from the model human hookworm nematode Heligmosomoides polygyrus." Proteins **61**(4): 1024-31.

Schwede, T., J. Kopp, et al. (2003). "SWISS-MODEL: An automated protein homology-modeling server." Nucleic Acids Res **31**(13): 3381-5.

Shailaja, M. S. and C. D'Silva (2003). "Evaluation of impact of PAH on a tropical fish, Oreochromis mossambicus using multiple biomarkers." Chemosphere **53**(8): 835-41.

Shofer, S. L. and R. S. Tjeerdema (1998). "Effects of hypoxia and toxicant exposure on adenylate energy charge and cytosolic ADP concentrations in abalone." Comp Biochem Physiol C Pharmacol Toxicol Endocrinol **119**(1): 51-7.

Singh, S. P., J. A. Coronella, et al. (2001). "Catalytic function of Drosophila melanogaster glutathione S-transferase DmGSTS1-1 (GST-2) in conjugation of lipid peroxidation end products." Eur J Biochem **268**(10): 2912-23.

Soh, Y., K. S. Jeong, et al. (2000). "Selective activation of the c-Jun N-terminal protein kinase pathway during 4-hydroxynonenal-induced apoptosis of PC12 cells." Mol Pharmacol **58**(3): 535-41.

Sole′, M., Porte, C., Biosca, X., et al. (1996). "Effects of the 'Aegan Sea' oil spill on biotransformation enzymes, oxidative stress and DNA-adducts in digestive gland of the mussel (Mytilus edulis L.)." Comp. Biochem. Physiol **113C**: 257-265.

Sun, Q. A., D. Su, et al. (2005). "Reaction mechanism and regulation of mammalian thioredoxin/glutathione reductase." Biochemistry **44**(44): 14528-37.

Sun, Y. J., I. C. Kuan, et al. (1998). "The three-dimensional structure of an avian class-mu glutathione S-transferase, cGSTM1-1 at 1.94 A resolution." J Mol Biol **278**(1): 239-52.

Thomson, A. M., D. J. Meyer, et al. (1998). "Sequence, catalytic properties and expression of chicken glutathione-dependent prostaglandin D2 synthase, a novel class Sigma glutathione S-transferase." Biochem J **333 (Pt 2)**: 317-25.

Tomarev, S. I. and R. D. Zinovieva (1988). "Squid major lens polypeptides are homologous to glutathione S-transferases subunits." Nature **336**(6194): 86-8.

Tomarev, S. I., R. D. Zinovieva, et al. (1993). "Squid glutathione S-transferase. Relationships with other glutathione S-transferases and S-crystallins of cephalopods." J Biol Chem **268**(6): 4534-42.

Tomarev, S. I., R. D. Zinovieva, et al. (1992). "Characterization of squid crystallin genes. Comparison with mammalian glutathione S-transferase genes." J Biol Chem **267**(12): 8604-12.

Townsend, D. M., V. L. Findlay, et al. (2005). "Glutathione S-transferases as regulators of kinase pathways and anticancer drug targets." Methods Enzymol **401**: 287-307.

Urade, Y., K. Watanabe, et al. (1995). "Prostaglandin D, E, and F synthases." J Lipid Mediat Cell Signal **12**(2-3): 257-73.

Van der Oost, R., Goksbyr, A., Celander, M., Heida, H., Vermeulen, N.P.E. (1996). "Biomonitoring of aquatic pollution with feral eel (Anguilla anguilla): II. Biomarkers: pollution-induced biochemical responses." Aquat. Toxicol **36**(189-222): 189.

Vorachek, W. R., W. R. Pearson, et al. (1991). "Cloning, expression, and characterization of a class-mu glutathione transferase from human muscle, the product of the GST4 locus." Proc Natl Acad Sci U S A **88**(10): 4443-7.

Wang, C., Y. Zhao, et al. (2006). "Effects of tributyltin, benzo[a]pyrene, and their mixture on antioxidant defense systems in Sebastiscus marmoratus." Ecotoxicol Environ Saf **65**(3): 381-7.

Wang, C. G., Y. X. Chen, et al. (2005). "Effects of low dose tributyltin on activities of hepatic antioxidant and phase II enzymes in Sebastiscus marmoratus." Bull Environ Contam Toxicol **74**(1): 114-9.

Wasserman, W. W. and W. E. Fahl (1997). "Functional antioxidant responsive elements." Proc Natl Acad Sci U S A **94**(10): 5361-6.

Wells, W. W., D. P. Xu, et al. (1995). "Glutathione: dehydroascorbate oxidoreductases." Methods Enzymol **252**: 30-8.

Whitbread, A. K., A. Masoumi, et al. (2005). "Characterization of the omega class of glutathione transferases." Methods Enzymol **401**: 78-99.

Whitbread, A. K., N. Tetlow, et al. (2003). "Characterization of the human Omega class glutathione transferase genes and associated polymorphisms." Pharmacogenetics **13**(3): 131-44.

Willett, K. L., Wilson, C., Thomsen, J., Porter, W. (1999). "Evidence for and against the presence of polynuclear aromatic hydrocarbon and 2,3,7,8-tetrachloro-p-dioxin binding proteins in the marine mussels,." Aquat. Toxicol **48**: 51-64.

Wilson, R., R. Ainscough, et al. (1994). "2.2 Mb of contiguous nucleotide sequence from chromosome III of C. elegans." Nature **368**(6466): 32-8.

Xiao, B., S. P. Singh, et al. (1999). "Crystal structure of a murine glutathione S-transferase in complex with a glutathione conjugate of 4-hydroxynon-2-enal in one subunit and glutathione in the other: evidence of signaling across the dimer interface." Biochemistry **38**(37): 11887-94.

Yeh, C. F. and S. J. Jiang (2005). "Speciation of arsenic compounds in fish and oyster tissues by capillary electrophoresis-inductively coupled plasma-mass spectrometry." Electrophoresis **26**(7-8): 1615-21.

Zakharyan, R. A., A. Sampayo-Reyes, et al. (2001). "Human monomethylarsonic acid (MMA(V)) reductase is a member of the glutathione-S-transferase superfamily." Chem Res Toxicol **14**(8): 1051-7.

Zimniak, P., M. A. Eckles, et al. (1992). "A subgroup of class alpha glutathione S-transferases. Cloning of cDNA for mouse lung glutathione S-transferase GST 5.7." FEBS Lett **313**(2): 173-6.

Zinov'eva, R. D., S. I. Tomarev, et al. (1994). "[The evolutionary kinship of the crystallins of cephalopods and vertebrates with heat-shock proteins and stress-induced proteins]." Izv Akad Nauk Ser Biol(4): 566-76.

Zoeller, R. T. (2005). "Environmental chemicals as thyroid hormone analogues: new studies indicate that thyroid hormone receptors are targets of industrial chemicals?" Mol Cell Endocrinol **242**(1-2): 10-5.

Ⅵ. ACKNOWLEDGEMENT

I am deeply indebted to my direct supervisor Prof. Jehee Lee to offer me the opportunity to commence my postgraduate studies in Cheju National University. His wide knowledge and logical way to thinking have been of great valuable for me. His teaching, encouraging and personal guidance have provide a good basis for my research.

I would like to express my great gratitude to Prof. Moon-Soo Heo, Prof. In-Kyo Yeo, College of Ocean Science in Cheju National University, who gave me the instructions to complete this thesis. And all professors who have instructed me in college are also greatly appreciated.

I particularly appreciate all my lab members for their valuable advice and kindly assistance. I'm thankful to Wang, Ning and all other Chinese friends in Cheju National University. At the same time I make this opportunity to thank all other Korean and international friends who supported me in many ways.

Last but not least, I would like to give my special thanks to my parents who formed part of my vision and taught me the good things that really matter in life. Their patient love enable me to complete my research work in Korea.